uOttawa

L'Université canadienne
Canada's university

FACULTÉ DES ÉTUDES SUPÉRIEURES ET POSTOCTORALES

uOttawa

L'Université canadienne
Canada's university

FACULTY OF GRADUATE AND POSDOCTORAL STUDIES

Julie S. O'Brien
AUTEUR DE LA THÈSE / AUTHOR OF THESIS

M.Sc. (Chemistry)
GRADE / DEGREE

Department of Chemistry
FACULTÉ, ÉCOLE, DÉPARTEMENT / FACULTY, SCHOOL, DEPARTMENT

Main Group Compounds with π-Conjugated Nitrogen Support: Carbenes, Boranes, and Guanidines

TITRE DE LA THÈSE / TITLE OF THESIS

Dr. D. Richeson
DIRECTEUR (DIRECTRICE) DE LA THÈSE / THESIS SUPERVISOR

CO-DIRECTEUR (CO-DIRECTRICE) DE LA THÈSE / THESIS CO-SUPERVISOR

EXAMINATEURS (EXAMINATRICES) DE LA THÈSE / THESIS EXAMINERS

Dr. K. Fagnou

Dr. S. Gambarotta

Gary W. Slater
Le Doyen de la Faculté des études supérieures et postdoctorales / Dean of the Faculty of Graduate and Postdoctoral Studies

Main Group Compounds with π-Conjugated Nitrogen Support: Carbenes, Boranes, and Guanidines

Julie S. O'Brien

Thesis submitted to the
Faculty of Graduate and Postdoctoral Studies
in partial fulfillment of the requirements for the degree of

Master's of Science
in
Chemistry

Ottawa-Carleton Chemistry Institute
University of Ottawa

Candidate
Julie S. O'Brien

Supervisor
Professor Darrin Richeson

Your file Votre référence
ISBN: 978-0-494-34097-4
Our file Notre référence
ISBN: 978-0-494-34097-4

Acknowledgements

I would like to thank Professor Darrin S. Richeson, my research supervisor, for his direction, guidance and support throughout the course of my work. Doctors Gan Ong and Patrick Bazinet deserve my thanks as well for their endless knowledge in the field of synthetic inorganic chemistry. Glenn Facey for his help with both sequence selection and interpretation of NMR spectra as well as Ilia Korobkov for his help with the single crystal X-ray structures also need to be acknowledged.

Finally, I would like to thank my mother for her endless support throughout the ongoing course of my work.

Prelude —

Abstract

This work focuses on the coordination and stabilization of unusual compounds and their chemistry, namely that of 1,8-diaminonaphthalene (1,8-DAN) and guanidines. Although both are bidentate ligands, 1,8-DAN is dianionic, whereas guanidines are monoanionic. As both ligands are nitrogen-based, they participate in strong interactions with their target element. The strength of chelation is enhanced by the unique π-systems that both ligands possess. This work deals with the design of 1,8-DAN-based ligands as dianionic systems for the stabilization of main group (B, C, Ge) metals. The catalytic synthesis of guanidines, a class molecules with strong biological relevance, is presented, which is catalysed by lithium.

Chapter 1 presents the background and motivation to investigate 1,8-DAN as a versatile ligand as well as the drive to synthesize guanidines by a catalytic method.

Chapter 2 discusses the general design of different 1,8-DAN-based ligands by varying their pendant groups. Both symmetric and asymmetric ligands are presented.

The transformation from ligands through perimidinium salts to carbenes will then be reviewed. The reason behind the existence of free carbenes versus enetetraamines for other ligands will be explained. Two interesting reactions of free carbenes will be presented and elaborated. Two different types of chelating carbenes, as well as their reactivity will follow. Finally, a metal complex of one of the free carbenes is discussed.

Chapter 3 investigates the possible construction of heavier metal carbene analogues. Reasons for the illusiveness of the 1,8-DAN stabilized silylene are discussed, as well as those for the germylene. A stable borane compound is presented with two different ligand systems.

Chapter 4 presents the lithium-catalyzed construction of a wide variety of guanidines from amines and carbodiimides. Reasons for their varying yields and reaction conditions are discussed. The scope of the amine substrates is expanded to heterocyclic amines and amides. Finally, the construction of propiolamidines from terminal alkynes and carbodiimides by the same catalytic route is investigated. Crystal structures which support the proposed mechanism are presented.

Chapter 5 summarizes the work presented in this document and presents its final conclusions.

Table of Contents

List of Figures

List of Tables

Chapter 1 — Introduction

Ligand design, for the purpose of stabilizing transition metal complexes or unusual valencies of main group elements is the focus of many research projects. Consequently, a great deal of thought has been invested in the design of organic molecules specifically tailored for this purpose. In general, the role of the ligand is to modify the electronic properties and structure of the topology around the metal atom in a predictable and desirable manner. These electronic and structural properties dictate the modifications that will be necessary for the metal centre. This in turn creates a set of features a ligand will need to impart. Since these features are different for each chemical route to a desired product, unique ligands for each process are necessary.

Methods for generating unique ligands are rooted in the fundamental aspects of structure and bonding in chemistry. The first aspect to consider is the type of atom which will be bonding, and thus interacting, directly with the metal. The number of these attachment atoms will indicate the strength of a ligand's clasp on a metal atom. A second design feature to consider is the overall geometrical shape of the ligand, both of the

structural components which affect more strongly the space immediately around the metal, as well as those which take a more passive role in protecting the metal. A crucial design feature this statement considers is the proximity, and thus physical placement on the ligand, of groups which can act as pendant arms to reach into the immediate space of one face of a metal atom and act to protect it from collisions with ambient, or even like, molecules. The third feature which will be considered is the overall rigidity or flexibility of the organic structure. Depending on the function, the ligand will likely favour one or the other. For example, an enzyme is a flexible molecule, capable of changing its shape to effectuate a desired chemical reaction. On the other hand, a rigid structure which holds a specific, desired shape in space to protect an element is otherwise desired. Finally, the choice of elements themselves, which are used to construct the structure, must be considered to give it maximum chemical stability. The ligand is meant, in the case of steric protection or electronic modification, to be an observer to the chemistry taking place on the metal centre. Bonds between elements such as C-C and C-N are highly stable, a motif which is repeatedly confirmed by their prevalence in nature.

Understanding the key design features previously discussed, two ligands, which satisfy these design criteria, will be presented. The 1,8-diaminonaphthalene-based (1,8-DAN) ligand displays many desirable design characteristics ideally suited for the chemistry which will be proposed, Scheme 1.1. First is the tunability of the groups closest to the metal. A nitrogen-based attachment site was chosen over its neighbour of higher atomic number, oxygen, due to its lacking of steric tunability due to the inability to generate a secondary anion. Nitrogen is also more suitable than its neighbour of lower atomic number, carbon due to its lacking π-conjugation through the absence of lone pairs. Nitrogen is also both a better σ- and π-donor than oxygen. Constructing the remainder of the ligand from carbon gives chemical stability, high steric tunability by ease of reaction during preparation, as well as a wide choice of starting materials for use as pendant (R) groups. Carbon also generates very stable π-conjugated systems which can also participate in electronic stabilization of the anionic charge on the nitrogen sites.

Scheme 1.1

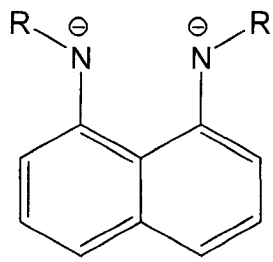

The presence of two anionic charges presents a set of chemistry beyond that of single anionic ligands: the ability to electronically stabilize an oxidation state of two with one ligand framework. For example, this possibility opens up the chemistry of the unusual oxidation state of two for carbon, producing carbenes. Its neighbour, boron, can also take advantage of the dianionic stabilization of the 1,8-DAN ligand, generating a borane with a protonated boron site.

A second class of ligands which displays similar desirable characteristics is guanidines and amidines. Despite their simplicity, they carry many advantageous design characteristics in common with the 1,8-DAN ligand. In their deprotonated form, Scheme 1.2, they are monoanionic ligands, although they can be doubly deprotonated to form a dianionic ligand. Their attachment sites to metal centres are at nitrogen atoms, a desirable choice as described previously. Through a conjugated π-system, the anionic charge can be delocalized, as well as making π-donation to the metal centre possible through both N-attachment sites. A rigid, stable structure is another result of this extended π-system. The highly stable C-N bonds create a chemically inert, CN_3, core. The pendant groups (R), though not pointing towards the metal site, are still in a position to impart steric protection for the metal centre.

Scheme 1.2

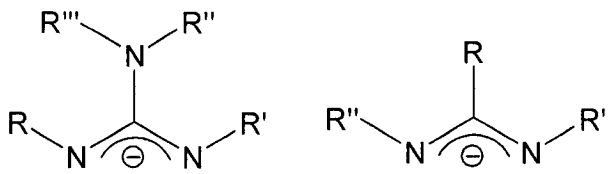

Guanidinate Amidinate

Synthesis of these biologically relevant molecules proceeds from a carbodiimide and amine or terminal alkyne. Variability of the pendant groups is dictated by the availability or ability to synthesize a variety of these organic molecules. Since reaction between these moieties does not occur to any measurable amount when simply combined, a catalyst is required. A simple alkali metal amide base, when added in a catalytic amount, can generate quantitative yields of the desired products.

The following thesis can be divided into two project goals. The first was to synthesize several group 13 and 14 1,8-DAN-stabilized complexes. The second was to develop a novel route to catalytic guanylation.

Chapter 1 presents the background and motivation to investigate 1,8-DAN as a versatile ligand as well as the drive to synthesize guanidines by a catalytic method.

Chapter 2, employing the 1,8-DAN array as a starting point, outlines the routes developed in the synthesis of symmetric and asymmetric versions of this ligand, and their conversion to carbenes through their corresponding perimidinium salts. A metal carbene complex is also presented.

Chapter 3 pushes the related main group chemistry of the 1,8-DAN ligand forward, exploring the further applicability of this ligand to stabilize divalent and trivalent main group element centres such as Ge(II) and B(III).

Chapter 4 presents the development of alkali metal catalysis of guanidines and propiolamidines from their substituent carbodiimides, amines, or terminal alkynes. A wide variety of amines are employed including primary and heterocyclic, as well as amides, as substrates for catalysis.

Chapter 5 summarizes the work presented in this document and presents its final conclusions.

Chapter 2 — 1,8-Diaminonaphthalene-Based Ligand and Carbene Design

I. Introduction

Carbenes are defined as divalent carbon atoms surrounded by six, rather than the expected eight, electrons.[1] Due to this unique electronic structure, the geometry and hybridization are different from the more commonly known, traditional organic compounds. The carbene atom can adopt either a linear or bent geometry; the linear geometry shows an sp-hybridization with two degenerate nonbonding *p*-orbitals at the carbene. The bent geometry enforces a different hybridization at the carbene centre, an sp^2-model, and breaks the degeneracy of the nonbonding orbitals. In this case, one orbital remains unchanged as a nonbonding orbital, denoted as p_π, whereas the second orbital gains some *s* character and is denoted as σ. A noteworthy effect of this difference is that there is a net stabilization of the orbitals of the bent, singlet state.

As will be described in detail below, carbenes can possess four electronic configurations, Scheme 2.1. In the first two states, the electrons are in a $\sigma^1\pi^1$-triplet state configuration. This configuration can exist in two different energy states, one exists in a

Scheme 2.1

$^3B_1$ $^1A_1$ $^1A_1$ $^1B_1$

ground state with parallel electron spins and is denoted as the $^3B_1$ state, whereas the other exists in an excited states with antiparallel electron spins, denoted as the $^1B_1$ state. The remaining two states are singlet state with both electrons of the carbene in the same orbital. The first of these is the ground state with an electronic configuration of σ^2, the second, an excited state, has an electronic configuration of p_π^2; both of these states are described as $^1A_1$.

Given this information, whether the carbene will exist as a singlet or triplet is related to the relative energy of the σ- and p_π-orbitals and the pairing energy for the two electrons. A large separation between these orbitals will favour the singlet state while a smaller one will favour a triplet state. The values that define the qualitative terms "large" and "smaller" were experimentally determined by Hoffmann[2] to be approximately 2 eV and 1.5 eV respectively. The relative energy of the σ- and p_π-orbitals is directly related to the inductive σ-electron polarity of the two atoms *alpha* to the carbene centre. Elements that are σ-electron withdrawing favour the singlet state, whereas neutral or donating elements favour the triplet one. This is better visualized by a molecular orbital diagram, Scheme 2.2. A σ-electron withdrawing heteroatom (X) will have the effect of stabilizing the σ-orbital of the nonbonding pair. This results from the inductive withdrawal of electron density from the carbene carbon, which in turn increases the *s*-character on this centre, and favours the singlet state. In this case, the p_π-orbital is unchanged since it is orthogonal to this effect, and does not participate in hybridization.

In the opposite case, where the heteroatom is electron donating or has a neutral effect, the σ-p_π-gap becomes much smaller (or in the extreme case, these two orbitals become degenerate p_x and p_y) as the triplet state is approached. In this case, all of the molecular orbitals are destabilized with respect to the previous case with an electron withdrawing heteroatom. This can also be related to ring size and N-C-N angle in

controlling the resultant diaminocarbene behaviour, namely with a larger angle, a more reactive nucleophile is synthesized, though a stronger base is needed during deprotonation.

Scheme 2.2

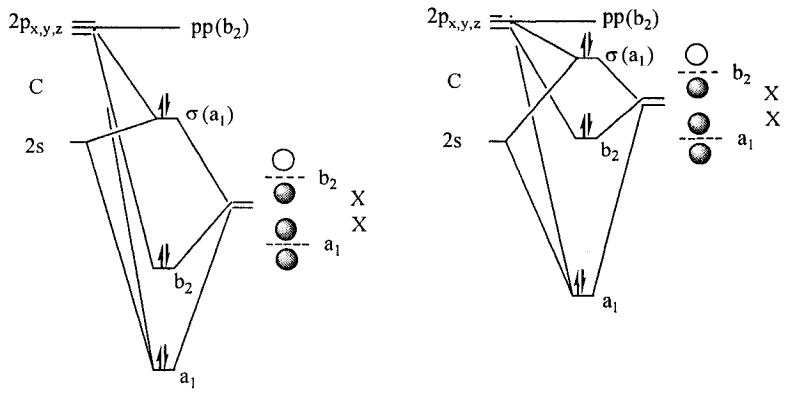

The reactivity of a carbene can be directly related to its ground-state spin multiplicity. Triplet carbenes can be viewed as diradicals since they have two singly occupied orbitals. On the other hand, singlet carbenes are viewed as 2-electron sigma donors in their reactivity; however, since they also possess an empty *p*-orbital, they hold some ambiphilic characteristics.

When considering the ability of any ligand to modify a metal centre for the purpose of catalysis, its relative field strength and *trans*-effect should be measured. NHCs are considered in the literature to be both higher field and have a higher *trans*-effect than phosphines.[3]

Since the first N-heterocyclic carbene (NHC) was isolated and structurally characterized in 1991 by Arduengo,[4, 5] many different architectures have been proposed and realized. An NHC is defined as a carbene where this carbon atom is a member of a cyclic ring, where the two sites *alpha* to the carbene are nitrogen atoms. This forces the carbene into a bent, singlet state. NHCs are developing their own set of chemistry, finding original or much more useful roles for these species than their phosphine counterparts. However, their chemistry is turning out to be much more complex than originally thought in comparison to the similar class of phosphine ligands.

Characteristic to NHCs, the divalent carbon adjacent to two tertiary nitrogen centres, is stabilized by an electron withdrawing-electron donating model, Scheme 2.3. As mentioned above, there is a strong sigma polarity towards the nitrogen centres (away

from the carbene), creating an advantageous sigma site for a singlet carbene. To stabilize this extreme deficiency, two lone pairs *alpha* to the carbene can provide stabilization to the empty p_π-orbital through hyperconjugation, specifically donation from the filled *p*-nonbonding orbitals of nitrogen to the empty *p*-nonbonding orbital of the carbene.

Scheme 2.3

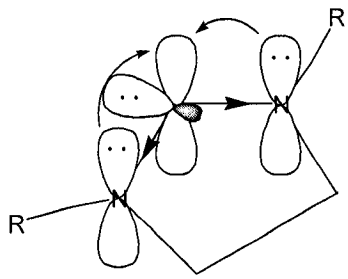

NHCs are emerging and proving to be highly effective ligands for many catalytic reactions such as the Heck reaction, Suzuki and Sonogashira couplings, aryl amination, amide α-arylation, hydrosilylation, Kumada coupling, hydrogenation, hydroformylation, alkyne coupling, olefin cyclopropanation, arylation of aldehydes, and olefin metathesis.[6] In some cases these ligands are replacing phosphine ligands due to the fact that NHCs improve upon some of the basic desired characteristics of these ligands. Whereas NHCs are more tightly bound, directing ligands; phosphines are more labile bound, stabilizing ligands.[7] This fundamental difference provides a foothold when using these ligands in the same complex for organometallic catalysis: the tightly bound NHC is used as the resting ligand whereas the phosphine dissociates from a pre-catalyst complex to form an active catalyst species. Another point to consider is that with phosphines, the thermodynamic product is favoured due to the reversible binding nature of the ligand; due to their more stable bonding mode, the kinetic product is obtained for carbenes, the resulting complex is the initial product. This can be seen as an advantage when considering the possibility of attaching a carbene to a solid support.[3] However, both phosphines and carbenes act as spectator, rather than actor ligands, since they do not directly participate in most catalytic reactions.

Carbenes act as neutral, nucleophilic, 2-electron-donor ligands, similar to amine, ether, and phosphine ligands. Although carbenes are strong σ-donors, along with amines and ethers, they do not have significant π-acceptor abilities.[8] This distinguishes them from phosphine ligands which have π-acceptor character.

The strength of carbene σ-donation to a metal centre can be measured by several different techniques. Infrared CO stretching measurements of a carbonyl in a metal complex *trans* to the carbene is the most commonly used technique, also known as the Tolman method.[9, 10, 11] These measurements can be done either experimentally or theoretically. The basis of this technique is rooted in the effect of molecular orbital interactions *trans* to each other in a metal complex, Scheme 2.4. A strong carbene σ-donor will increase electron localization on the metal centre; this will cause the metal to donate (in this case, to a carbonyl) in the *trans* position through a symmetry-appropriate *d*-orbital to interact with the σ^*-orbital of the carbonyl. This donation weakens the internal carbonyl bond, lowering its stretching frequency along with its wavenumber measurement in the infrared spectrum.

Scheme 2.4

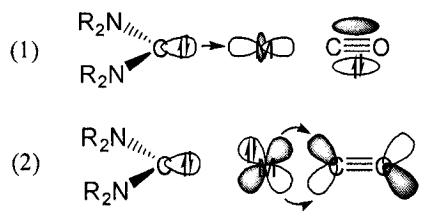

Although phosphines have larger variability in these measurements,[12] NHCs indicate stronger net electron-donating capabilities. The power of σ-donation of NHCs is stronger than phosphines due to their larger susceptibility, among other arguments, towards protonation.

Among the less common methods of measuring carbene donor strength is the determination of pK_a values of the salt precursor to the carbene.[13, 14] A salt precursor with a higher pK_a value will require a stronger base for deprotonation, but will yield a stronger σ-donating carbene. Electrochemical measurements of carbene-metal complexes are also used to determine Lever's electrochemical parameter (E_L).[15] In essence, when determining this parameter, a more strongly donating ligand is expected to stabilize the higher oxidation state of a metal better than a weakly donating ligand. The common, exclusive conclusion from each of these studies is that carbenes have stronger σ-donor abilities than their strongest phosphine cousins (such as PCy_3).

Recently, there has been a small number of papers suggesting the existence of a π-acceptor character in NHCs.[3, 15] Mercs, *et al*, in a recent publication, found "indications for π-acceptor ability" in NHCs involved in bonding with electron-rich metal centres. It

was proposed that the π-acceptor ability of NHCs should be comparable to pyridine, an established π-acceptor ligand, since NHCs possess a stronger σ-donation than pyridine. Through electrochemical measurements and the study of solid state structures of the type [Fe(cp)(CO)(NHC)(L)]X, Scheme 2.5, the following conclusion was reached: π-back-bonding should be comparable to or stronger than that in pyridines to account for the observed net charge transfer. The accepted trend in σ-donation, that carbenes are

Scheme 2.5

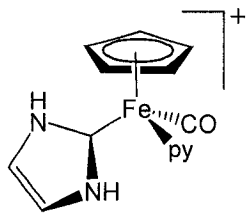

stronger than pyridines, and the stronger calculated bond dissociation energy (BDE) of carbenes in comparison to pyridine and CO, reinforces this argument.

Theoretical studies of the molecular orbitals involved in this bonding mode revealed that the π-contribution to the Fe-L bond strength is comparable for similar complexes of pyridine and NHCs. Electron donation from the HOMO of the $[Fe(cp)(CO)_2]^+$ fragment is highly energetically favourable into the LUMO+1 for the NHC (the LUMO for pyridine), both of which represent the ligand's aromatic π^*-orbitals. Considering the NHC system and the sp^2-hybridization of the carbene carbon, this is preferential to allow π-back-donation from the adjacent nitrogen orbitals, as well as symmetry-appropriate orbitals of the metal.

When designing an NHC carbene ligand, there are generally two methods for tuning the electronics: the backbone of the ring, and the R-groups of the nitrogen centres. The carbon-containing backbones of all known NHC ligands contain either sp^2- or sp^3-hybridized carbons. Those with sp^3-carbon backbones should carry more possible σ-electron-induction towards the carbene centre due to their known, stronger electron donating capacity, whereas those with available π-electrons have the ability to donate into the empty p_π-orbital of singlet carbenes. Modifying the backbone ring is found to be the best strategy for tuning the electronic properties of a carbene.

The electronic interaction of the R-groups on the nitrogen centres should be relatively small for several reasons. Due to steric arguments, phenyl rings are more often oriented orthogonally relative to the NHC ring, meaning π-interaction with the carbene

carbon is negligible. Alkyl groups are relatively neutral in terms of their ability to cause sigma induction. The strong electronegativity of the nitrogen centres adjacent to the carbene carbon reduces any σ-induction imparted towards the carbene by the pendant groups. Another factor is the distance any induction must travel from these groups; any donating or withdrawing trend will be reduced by the number of bonds through which it must travel. For phosphine ligands, changing the R-substituents causes a noticeable change in the electronic effect of the ligand since the group is attached directly to the donor atom. For NHC ligands however, the donor atom environment is not as easily changed, since the electronic effect of R-substituents is further removed.

Steric factors have been found to contribute much more to the stability of the carbene centre than electronic ones. Pendant groups spanning the full range from primary to tertiary have been explored with different carbene frameworks. Methyl groups offer the smallest steric impact of the carbon-containing pendant groups, the earliest of which among stable NHCs is that synthesized by Arduengo.[5] Other primary alkyl groups such as neopentyl or benzyl impart slightly more steric protection through their ability to rotate towards the carbene centre, though they are likely to prefer to be directed away. Secondary groups follow in the continuum of increasing steric protection, though alkyl groups such as iso-propyl are proving to have larger steric bulk than phenyl in protecting the carbene centre from dimerization.[16,17] Finally, tertiary groups such as adamantyl provide the largest possible steric bulk[4] due to their large three-dimensional shape, and their inability to rotate to provide a configuration with reduced steric bulk near the carbene centre.

Since phosphines have a conical shape, with R-groups that point away from the metal, there is little consequence to a change in sterics when rotating around the M-L bond, Scheme 2.6. NHCs have been described as fan-shaped[3] with their R groups pointing towards the metal, so rotation around the same bond has a much larger effect.

Scheme 2.6

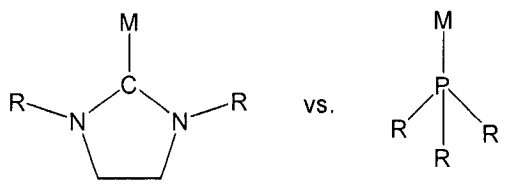

This can be a productive interaction when designing a ligand for a specific catalytic reaction. This difference is seen most acutely when a monodentate NHC rotates to minimize steric interaction with its surrounding ligands. The sterics of chelating carbenes are more complex, *vide infra*.

Asymmetric NHCs are also possible, through a structural design with different R-groups on each nitrogen centre, through the backbone, or through a combination of each.[18] Constructing a carbene with R-groups of different size provides the possibility of designing a metal complex with two very different faces. This feature, with the proper sterics, can direct incoming substrate molecules to a preferred orientation, providing the possibility of a chiral catalyst and racemically pure products.

The stability of the carbene bonded to a metal complex can be further increased after tuning the steric bulk of the N-pendant groups by introducing one or more chelating groups. A second possibility is to link two carbene complexes by an arm with variable length, or containing a chelating heteroatom of its own. Organometallic complexes designed for catalysis are more stable with a chelating ligand due to the thermodynamic "chelate effect" and because such an arrangement often puts the carbene in an orientation that prevents it from reacting with any incoming or existent alkyl/aryl groups.[8]

Carbene complexes which have a chelating arm with a heteroatom (X) capable of chelation such as O or S are classified as [L,X]-type chelating complexes, Scheme 2.7. This ligand class frequently has a pendent group comprising a phenyl ring with a heteroatom ortho-substitution.[8] Deprotonation of the precursor salt is usually

Scheme 2.7

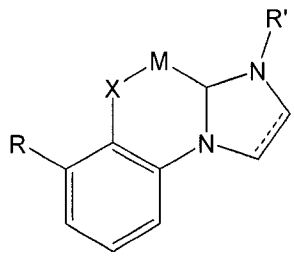

accomplished with two equivalents of a strong base such as potassium hexamethyldisilazide (KHMDS) or potassium hydride (KH) in a polar solvent. Those which have a chelating arm with a coordinating atom such as P, N, or another carbene are classified as [L,L]-type chelating complexes. Deprotonation requires only one equivalent

of base, since the chelating arm does not require deprotonation to become active towards complexation.

Two independent, sterically hindered carbenes will arrange themselves *trans* to each other when chelating to a metal centre. The strategy behind the development of creating two carbenes linked together is that they will be forced to adopt a *cis*-orientation; this feature is proposed to stimulate the reductive elimination step common to catalytic cycles.

Among the type of chelating ligands comprised of two linked carbenes, the length and type of the chelating linker can vary their expected coordination behaviour, Scheme 2.8. Among short alkyl linkers (one atom), the NHCs are generally coplanar after complexation. During preparation of such chelating complexes, each carbene usually coordinates to a separate metal centre. In contrast, longer alkyl linkers (3 or more atoms)

Scheme 2.8

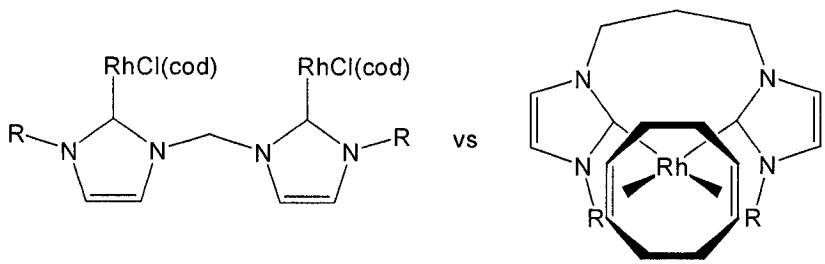

generally result in complexes with mutually parallel NHCs. This case produces complexes with the expected chelation behaviour: both carbene centres coordinate to the same metal.

At the present time, cyclic five-membered ylidenes dominate the known, stable, monomeric singlet carbenes. Given the geometric and steric constraints (of the R-groups on the nitrogen centres *alpha* to the carbene centre) imposed by the rings size, the steric impact of R-groups is extremely dependent on the ring size. The positioning of functional groups in ideal geometries illustrates the importance of this design feature, Scheme 2.9.

The dimerization of tetraaminoethane derivatives, although not well understood, has had several recent insights. The dimerization mechanism between two singlet carbenes is unknown experimentally; the closest known example is a singlet dimerization between a carbene and germylene.[19] In this model, two filled sp^2-orbitals on opposite

Scheme 2.9

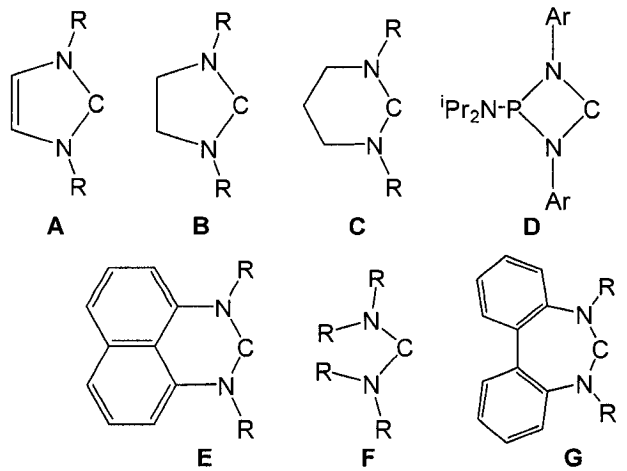

carbene centres each interact with an empty *p*-orbital, Scheme 2.10. Transition state calculations show that the energy barrier for this mechanism is prohibitively high, verifying the experimental results.

Scheme 2.10

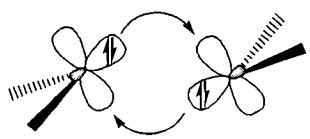

Most dimerizations are proposed to proceed through a proton-catalyzed mechanism. The method of preparation is important in proton-catalyzed dimerization mechanisms, the most common of which is deprotonation of formamidinium cations with a sterically hindered, alkali metal amide base, Scheme 2.11. Over the timescale of deprotonation, while both free carbene and precursor salt are present in solution, the reaction shown can occur to produce tetraaminoolefins (dimers). This proposed mechanism is lower energy than that proposed above between two singlet carbenes.

Scheme 2.11

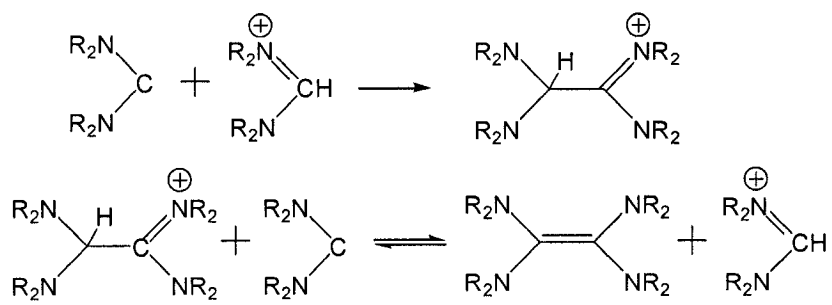

The unique framework offered by the perimidine core has many advantages in design over the five membered NHCs. The diaminonaphthalene base creates the smallest α-angle of the ones without chirality, Scheme 2.12, by creating a six-membered, heterocyclic ring containing the carbene carbon. This maximizes the steric impact of the N-substituents. Another feature of the presented carbene is the extended aromatic system of the perimidine core. This should increase the ability of the adjacent nitrogen centres to stabilize the electron-deficient divalent carbon through its empty p-orbital. Furthermore, the entire diaminonaphthalene backbone offers a total of 14-π-electrons, an aromatic

Scheme 2.12

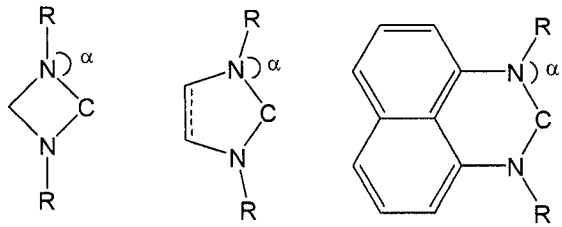

system satisfying Hückel's rule, comprising a stable system to offer stabilization of the divalent carbon. These features together could increase the nucleophilic character of the carbene, the result of these effects being a ligand with a stronger electron donating capacity (stronger nucleophilic character).

II. Results and Discussion

A. Ligand Synthesis

The N,N'-diisopropyl-1,8-diaminonaphthalene was prepared by a four-step procedure that was developed previously in the lab.[17] From the 1,8-diaminonaphthalene (DAN) starting material, addition of acetone across the nitrogen centres, also a condensation reaction, produces intermediate **2.1**, Scheme 2.13, which is reduced with a large excess of $LiAlH_4$ to the monoisopropyl-1,8-DAN product **2.2**. Reaction with acetone and excess $LiAlH_4$ proceeds through an intermediate similar to aminal **2.1** to produce the symmetric N,N'-diisopropyl-1,8-DAN product **2.3**.

The alternative asymmetric product, N,N-diisopropyl-1,8-DAN, is not observed, likely due to steric and thermodynamic arguments. It has been proposed that the aminal is in equilibrium with its corresponding imine, which would further support the exclusive formation of the symmetric product, Scheme 2.14. Furthermore, although the procedure

Scheme 2.13

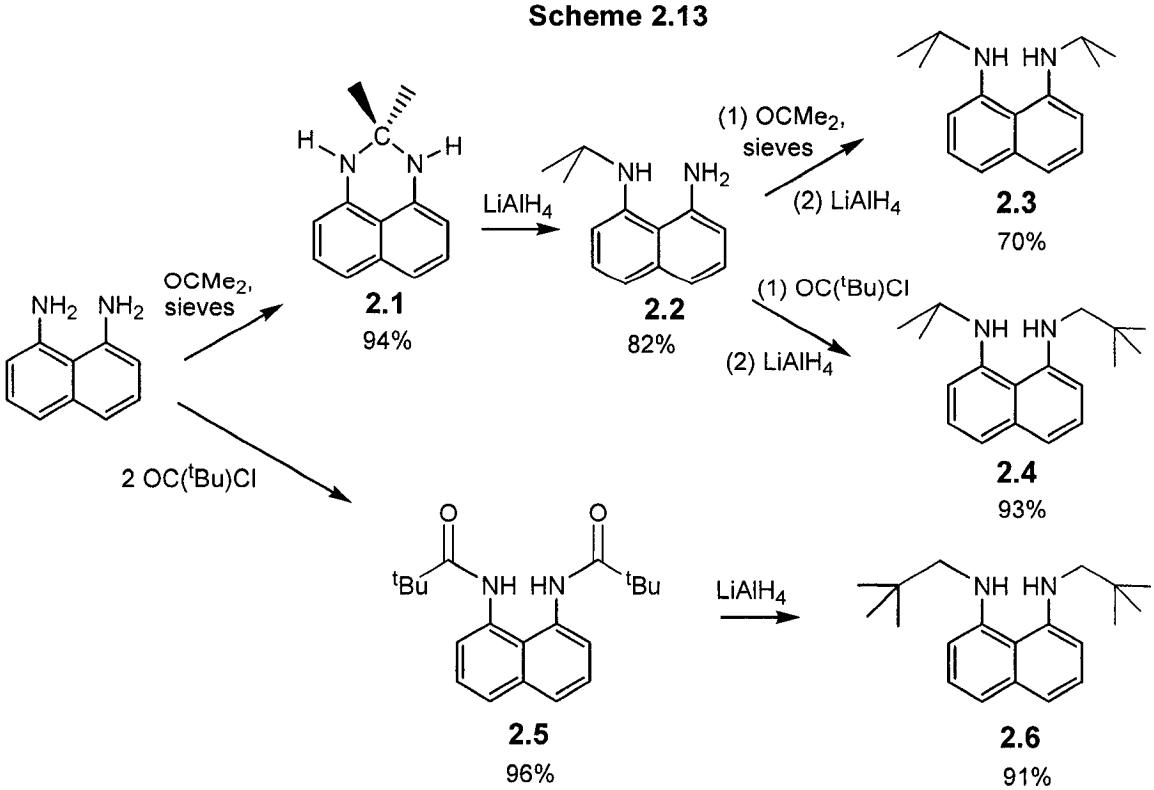

to produce ligand **2.3** is extensive, it is necessary since the double condensation reaction to form the diimine **2.I** does not occur when 1,8-DAN is first treated with acetone.

Due to the sequential nature of synthesis of product **2.3**, it is possible to introduce two different substituents with high specificity of the desired product and no need for lengthy purification. Introducing a small excess of trimethylacyl chloride to **2.2** in a

Scheme 2.14

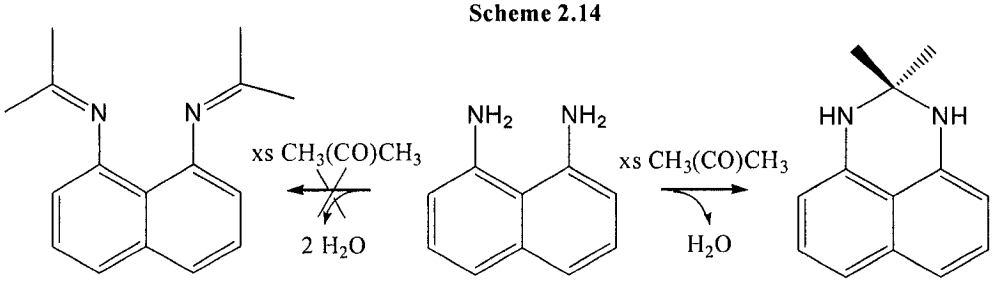

2.I **2.1**

polar solvent, followed by reduction with excess $LiAlH_4$ produces exclusively the asymmetric product N-isopropyl-N'-neopentyl-1,8-DAN ligand **2.4**. The sterics of this product are unique since these two alkyl groups, one primary the other secondary, possess drastically different steric bulk, as will be discussed later in the section on carbene synthesis.

Following a literature preparation,[20] the corresponding N,N'-dineopentyl-1,8-DAN ligand **2.6** was synthesized through intermediate **2.5** by reaction with a slight excess of trimethylacyl chloride followed by reduction with a large excess of $LiAlH_4$. Crystal structures of both **2.5** and **2.6** were obtained and show no deviation from their expected geometries, Figures 2.1 and 2.2. Selected bond lengths and angles are listed in Tables 2.2 and 2.3

B. Perimidinium Salts

From the three ligands described previously, **2.3**, **2.4**, and **2.6**, addition of a C-H moiety across the two nitrogens of the DAN ligand for the purpose of subsequent preparation of carbenes by deprotonation was relatively simple. For the N,N'-diisopropyl-1,8-DAN diamine ligand **2.3**, reaction with a large excess of triethyl orthoformate with a catalytic amount of formic acid forms the perimidinium salt **2.7a**, Scheme 2.15. In this case, the anion can be exchanged by washing a solution of perimidinium salt **2.7a** in methylene chloride with a concentrated solution of sodium chloride. This produces the perimidinium salt **2.7b** with chlorine as the anion.

Addition of the C-H moiety to close the six-membered ring of the remaining two ligands, N-isopropyl-N'-neopentyl-1,8-DAN, **2.4,** and N,N'-dineopentyl-1,8-DAN, **2.6**, proceeds through addition of one equivalent of *p*-toluenesulfonic acid in an excess of triethyl orthoformate. A characteristic feature in the NMR spectrum of these

Scheme 2.15

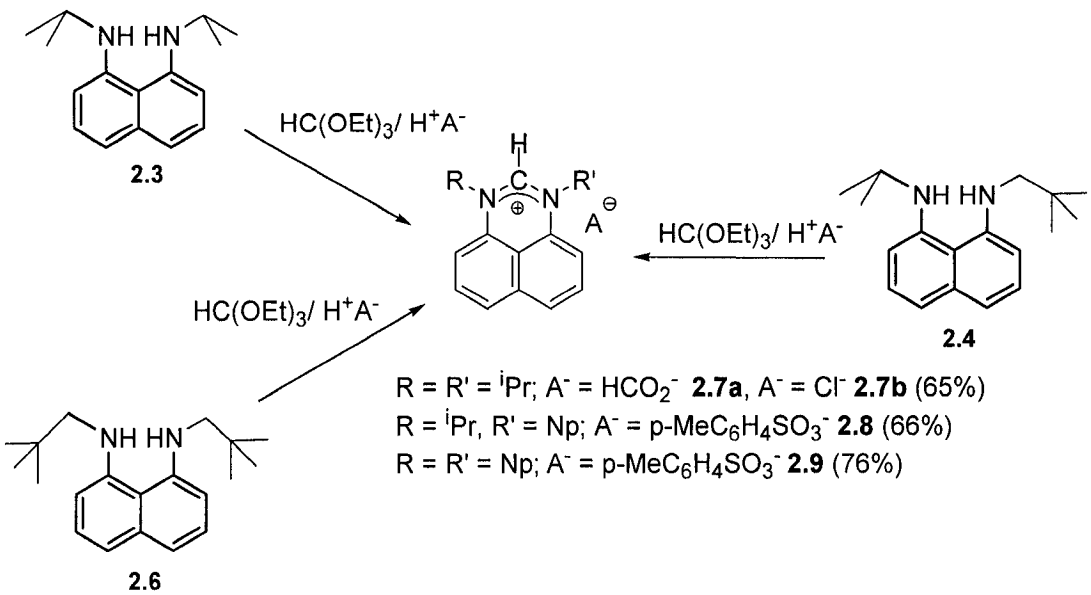

R = R' = ^{i}Pr; A^- = HCO_2^- **2.7a**, A^- = Cl^- **2.7b** (65%)
R = ^{i}Pr, R' = Np; A^- = p-$MeC_6H_4SO_3^-$ **2.8** (66%)
R = R' = Np; A^- = p-$MeC_6H_4SO_3^-$ **2.9** (76%)

perimidinium salts is the strongly downfield shifted signal produced by the central N(*CH*)N species. The proton NMR signals for compounds **2.7a** to **2.9** range from 8.7 - 9.9 ppm and integrate for one proton, paired with a ^{13}C NMR signal in the range 148 - 157 ppm, a notable downfield shift for both of these signals. The structure of compound **2.8** was also characterized by single crystal X-ray analysis after crystallizing from methylene chloride, Figure 2.3. Selected bond lengths and angles are listed in Table 2.4.

C. Free Carbenes and Enetetraamines

Preliminary methods used for the purpose of deprotonation of the imidazolium precursor to yield a free carbene employed sodium *tert*-butoxide as the base, Scheme 2.16. Rather than deprotonating the salt, **2.7b**, to yield the free carbene, nucleophilic addition of the butoxide base was observed instead, which produces the α-diamino ether, **2.II**.

Scheme 2.16

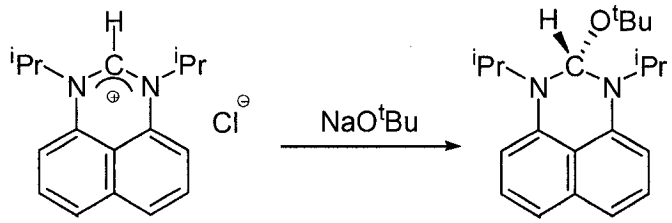

2.7b **2.II**

A less nucleophilic, more sterically encumbered base is needed to achieve successful deprotonation of the imidazolium precursor to yield the free carbene. Reacting the diisopropyl perimidinium salt **2.7b** with one equivalent of lithium hexamethyldisilazide [$LiN(Si(CH_3)_3)_2$], yields the desired free carbene product **2.10**, Scheme 2.17. A parallel reaction occurs with the mixed isopropyl-neopentyl imidazolium **2.8** to yield the free carbene product **2.11**.

Scheme 2.17

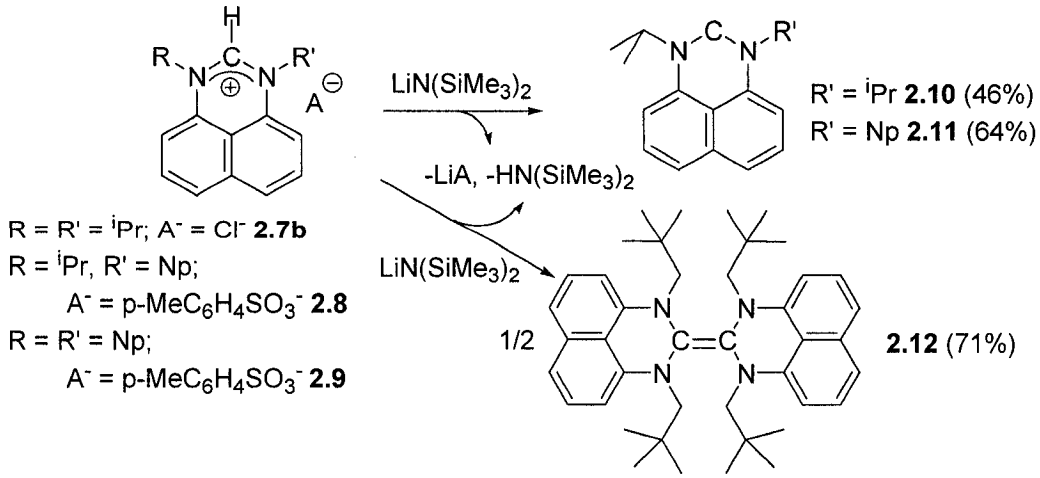

For these two products, **2.10** and **2.11**, two spectroscopically diagnostic features were observed. The first was the disappearance of the strongly downfield signal of the imidazolium proton in the ^{1}H NMR; this indicates deprotonation specifically at the desired site. The second was the observation of a peak characteristic to free carbenes in the ^{13}C NMR at 241.7 and 247.9 ppm for carbenes **2.10** and **2.11** respectively, a strongly deshielded signal compared to those originating from tetravalent carbon. This observation is due to the deficiency of electron density on the formally 6-electron, divalent carbene carbon centre. All other NMR signals were present in the expected regions for these two free carbene products, notably one doublet for the isopropyl groups of carbene **2.10** indicating a symmetric product with free rotation around the N-C_{ipso} bond, as well as confirming the free carbene structure for product **2.11** by the lack of diastereotopic signals.

Single crystal X-ray diffraction analysis was performed for carbene **2.11**, Figure 2.4, to confirm the existence of the free carbene in the solid state as well as in solution, *vide supra*. Selected bond lengths and angles are listed in Table 2.5. The divalent carbene carbon is confirmed and shows an N-C-N angle of 115.5°, which agrees well with the previously published carbene angle for carbene **2.10** of 115.3°.[17] The geometries of both nitrogen centres are completely planar (with angle sums of 359.9 and 360.0°), and the N-$C_{carbene}$ bond lengths show an average of 1.356(3) Å, both features consistent with a carbene centre. This value is slightly longer than that for the corresponding perimidinium salt **2.8** which shows an average N-$C_{carbene}$ bond length of 1.325(4) Å due to partial π-

conjugation of a delocalized double bond. The asymmetric carbene **2.11** displays an average α-angle of 115.8°, the smallest of all angles measured around these centres. This design feature ensures the largest steric protection possible by the alkyl groups adjacent to the carbene centre. This average angle is smaller than that of the perimidinium precursor **2.8** of 118.2°, which is likely related to the larger relative angle of the central perimidinium carbon (the carbene precursor carbon) of 124.3(3)°, and its π-conjugation. Finally, the average N-$C_{naphthalene}$ bond lengths are slightly shorter for the perimidinium precursor, 1.432(4) Å, compared to the carbene product, 1.419(3) Å, likely due to increased π-conjugation from the naphthalene ring.

Deprotonation of the dineopentyl perimidinium salt **2.9** by the same method as **2.7b** and **2.8**, namely with $LiN(Si(CH_3)_3)_2$, yielded the enetetraamine product **2.12** rather than the free carbene, Scheme 2.17. Spectroscopic evidence to support the enetetraamine form is threefold. The disappearance of the characteristic perimidinium signal at 9.39 ppm in the ^1H NMR spectrum indicates successful deprotonation at that site. The existence of diastereotopic methylene signals as a downfield shifted set of doublets at 7.10 and 6.89 ppm, each integrating for two protons relative to the rest of the molecule, support the dimerization of two perimidinium molecules, rather than the formation of a free carbene. Finally, the absense of any signal in the ^{13}C NMR spectrum diagnostic to free carbenes and the addition of an extra signal in the region characteristic to aromatic carbons supports the dimerized form. This is in agreement with a previously published article which assigns a quaternary carbon signal at 125.9 ppm to the dimerized carbene carbon. [21]

From these observations a strong conclusion can be drawn: in order to produce a six-membered, free carbene with the DAN backbone, the steric protection of a minimum of one isopropyl pendant group is required. As presented, those with one, **2.11**, or two, **2.10**, isopropyl groups alpha to the carbene centre exist in their free form; however when none are present, **2.12**, the free carbene does not exist. This demonstrates the large steric impact of the secondary isopropyl group with free rotation possible around the N-C_{ipso} bond in solution in agreement with the spectroscopic evidence presented above.

When designing and synthesizing unstable compounds, undesired side-reactions often occur. The following is an interesting side reaction observed while purifying the asymmetric carbene **2.11** and the enetetraamine **2.12**. Relatively small amounts of methylene chloride remain coordinated to the perimidinium salts despite efforts to dry the product thoroughly, resulting in complexes **2.8.CH_2Cl_2** and **2.9.CH_2Cl_2**, Scheme 2.18.

Scheme 2.18

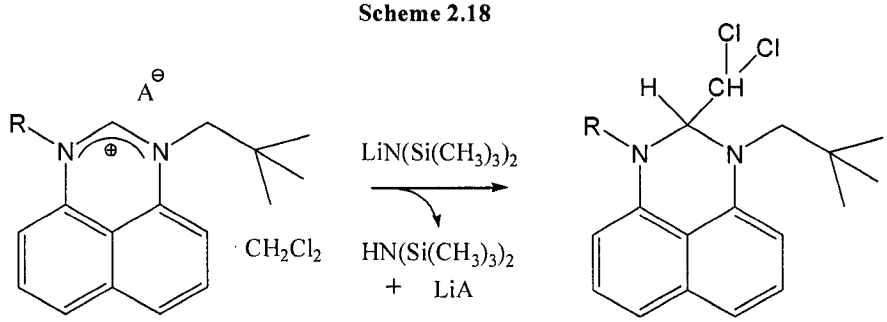

R=^{i}Pr, A$^-$= p-$MeC_6H_4SO_3^-$ **2.8.CH_2Cl_2**
R=Np, A$^-$= p-$MeC_6H_4SO_3^-$ **2.9.CH_2Cl_2**

R=^{i}Pr **2.13**
R=Np **2.14**

Proceeding with the same deprotonation process described above, the compounds **2.13** and **2.14** are produced, Figures 2.5 and 2.6. Selected bond lengths and angles are listed in Tables 2.6 and 2.7. These two compounds, which appear to be the result of nucleophilic addition across the carbene centre, crystallize out of a solution of cold hexane preferentially over the desired carbene products. The nucleophile, trace methylene chloride in this case, effectively undergoes C-H activation across the electrophilic carbene centre to produce these side-products. Single crystal X-ray studies of both side-products show many similarities. Both central carbons, which underwent C-H activation, show strong pyramidalization by their average angle sum of 330.2°. The C-C bond distances from the central carbon to that of the activated methylene chloride show a notable difference in length. That of side-product **2.13** is 1.549(7) Å whereas that of **2.14** is 1.7811(7) Å. The nitrogen centres of both structures are slightly pyramidalized, showing an overall average angle sum of 357.0°. With average bond lengths of 1.403(6) Å and 1.389(3) Å for **2.13** and **2.14** respectively, they are shorter than both of their perimidinium salts and carbenes. This is likely due to the greater ease with which the slightly pyramidalized nitrogen centres can interact with the naphthalene ring. These two compounds were not characterized spectroscopically, as they were not the desired products.

Deprotonation of the perimidinium salt **2.8** followed by reaction with half an equivalent of water produces the ether-bridged product **2.15**, Scheme 2.19, Figure 2.7. Selected bond lengths and angles are listed in Table 2.8. The product of this reaction, though undesirable, shows the nucleophilic addition of water across two carbene centres to link them through an ether bridge. Characterized by a single crystal X-ray study after

Scheme 2.19

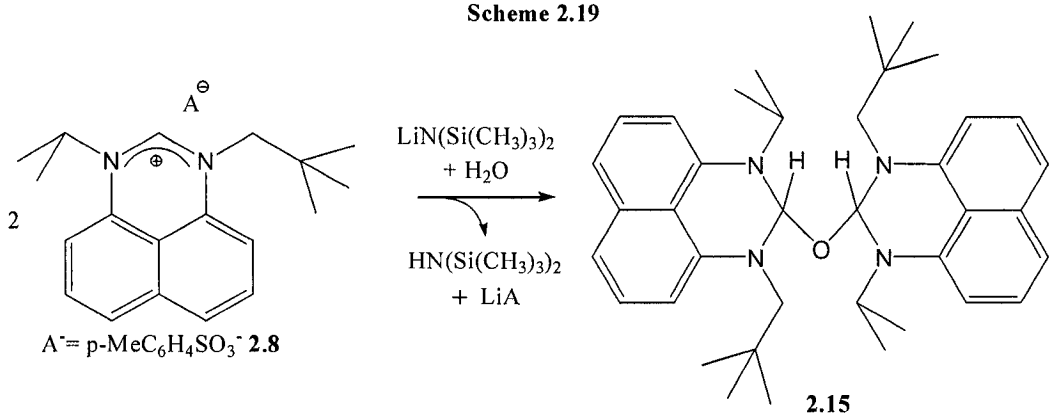

crystallizing from hexane, the structure does not show any unusual deviations in bond lengths or angles from what would be expected. The average angle sum of the four nitrogen centres is 349.0°, which shows moderate pyramidalization. The C-O-C angle of the ether bridge is 118.5°, slightly larger than the expected 109.5° of an ideal tetrahedral geometry, but understandable given the steric bulk of the two moieties it holds together. The central carbon atoms show an average pyramidalization with an average angle sum of 335.4°.

D. Chelating Carbenes and their Perimidinium Salt Precursors

Chelating carbenes take advantage of the thermodynamic chelate effect and can be generated by the same deprotonation method as those described in the previous section. The only difference in the deprotonation step is that two equivalents of base are required, rather than a single one, since there are two sites which require deprotonation. The N-isopropyl-1,8-DAN ligand **2.2** developed is an ideal precursor for designing chelating ligands, since it has one pendant group with a well developed steric background, and one site for attachment of a chelating arm or linker. An example of each will be described in this section.

Closing the six-membered ring can be accomplished by reacting precursor **2.2** with excess triethyl orthoformate and a catalytic amount of formic acid, producing the perimidine intermediate **2.16**, Scheme 2.20. This product is specifically identified by the

appearance of a new peak in the ^{13}C NMR spectrum at 144.5 ppm, the most strongly downfield shifted signal in this spectrum. Following a literature preparation,[22] the double electrophile, 1,8-bis-bromomethyl-naphthalene, synthesized for the purpose of linking two perimidine molecules together, creates the precursor for a chelating carbene with a

Scheme 2.20

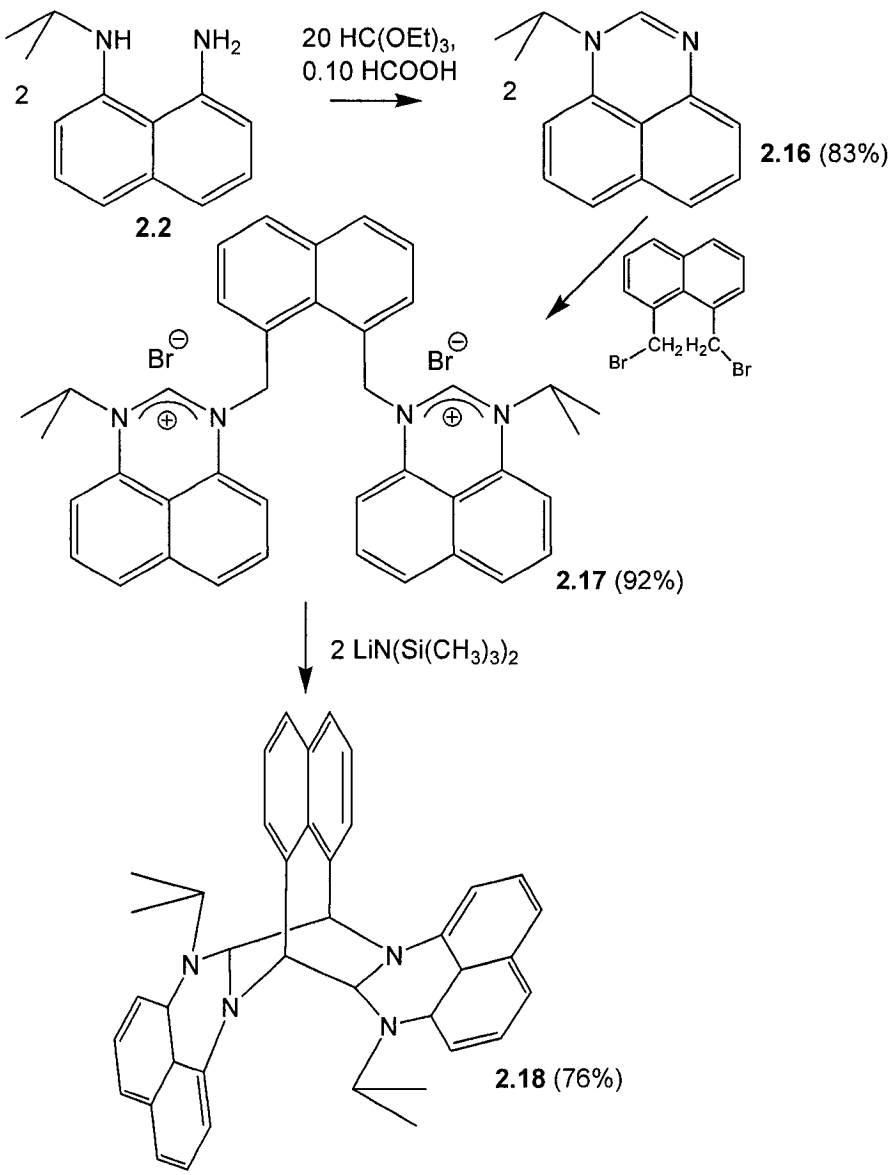

naphthalene bridge. The product from this reaction, **2.17**, displays the characteristic peak in the ^{1}H NMR spectrum for a perimidinium salt at 9.37 ppm, integrating for two protons, consistent with the formation of two electrophilic deprotonation sites at the desired locations. The methylene protons of the naphthalene bridge are shifted from 5.29 to 6.83 ppm and integrate for four protons, indicating an overall deshielding effect, consistent

with the new proton environment of the perimidinium salt and successful attachment to the perimidine at the desired site.

Based on previous results indicating successful deprotonation of perimidinium salts to yield the corresponding free carbenes or enetetraamines, two equivalents of $LiN(Si(CH_3)_3)_2$ are used to deprotonate perimidinium salt **2.17**. However, the ^{13}C NMR spectrum of the resulting product does not possess the peaks characteristic of a free carbene. Single crystal X-ray analysis of the product reveals that an unintentional intramolecular reaction occurs to produce a product with an internal bicyclic ring structure, **2.18**, Figure 2.8. Selected bond lengths and angles are listed in Table 2.9. It is hypothesized that, rather than undergoing the deprotonation as predicted at the perimidinium site, the compound **2.17** proceeds through the zwitterionic intermediate **2.17.int**, Scheme 2.21. Deprotonation at the methylene likely occurs because this site possesses a proton with a higher pK_a value than the proton at the perimidinium site. Due to the creation of opposite charges within the molecule, and the thermodynamic favourability of creating a six membered ring within the product, this intramolecular reaction happens very rapidly without the formation of the desired free carbene product.

Scheme 2.21

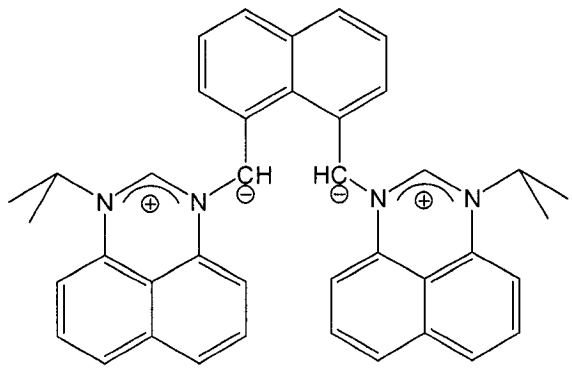

2.17.int

The second method to generate a chelating carbene is to include a pendant arm with a site capable of chelating to a metal centre. A strong nucleophile, such as an alkyl bromide, is needed to achieve addition at the weakly nucleophilic nitrogen centre of the perimidine **2.16**. This addition, shown in Scheme 2.22, was successful, creating perimidinium salt **2.19**. The characteristic peak seen from perimidinium salts is observed at 9.84 ppm, which integrates for one proton, as well as a shift of the methylene protons from 4.56 to 3.85 ppm, which integrate for two protons.

Scheme 2.22

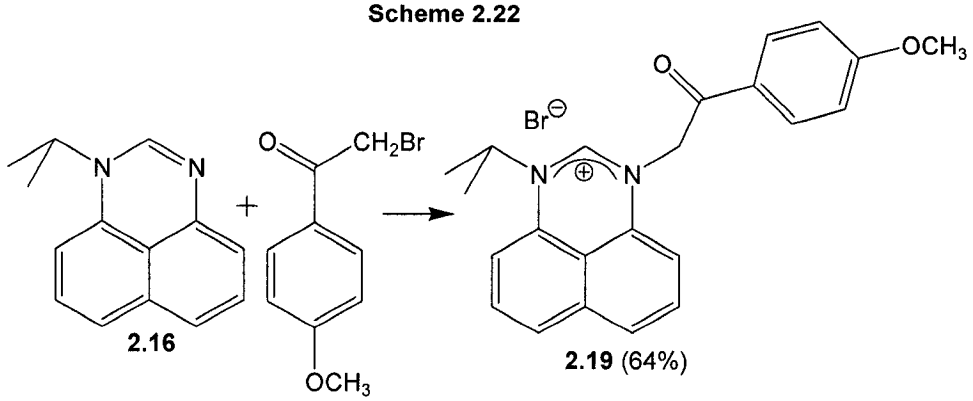

Deprotonation by the same route, applying one equivalent of $LiN(Si(CH_3)_3)_2$, stimulates deprotonation at the methylene site, producing the enolate. Based on values from the Bordwell pK_a tables, this observation is supported by the lower value for the enolate site, ~19-20, as compared to the value for imidazoliums, ~24. Applying two equivalents of base produce an irresolvable result by ^1H NMR. Reaction with a basic metal complex such as $Zr(N(CH_3)_2)_4$ produces a very similar result as application of one equivalent of base: deprotonation and coordination of the perimidinium salt proceeds only at the enol-site, leaving the perimidinium site dangling and uncoordinated. Deprotonation with one and two equivalents of the similar base $KN(Si(CH_3)_3)_2$ mirrors the results with the lithium salt.

E. Metal Complex of a Carbene

Direct addition of the asymmetric free carbene **2.11** to $Pd(OAc)_2$ produces the palladium dicarbene complex **2.20** with no change in metal oxidation state, Scheme 2.23,

Scheme 2.23

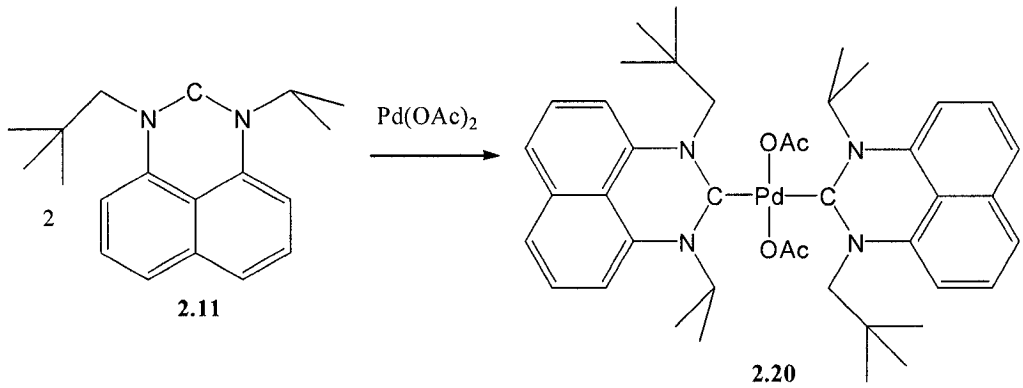

Figure 2.9. Selected bond lengths and angles are listed in Table 2.10. This structure was elucidated by single crystal X-ray study. The $N\text{-}C_{carbene}\text{-}N$ angle has opened up slightly from 115.5° in the free carbene to 117.9°. The structure is distorted from the ideal square

planar geometry expected from palladium complexes; the plane of the DAN ligands is rotated out of plane from the acetate groups by 50.7°. This is likely to minimize the steric impact between the pendant groups of the carbene with the acetate groups of the palladium. All four nitrogen atoms are still planar with an average angle sum of 359.8°. The carbene centres are, therefore, the exclusive donors to the metal centre.

III. Experimental Section

General: Unless otherwise noted, all manipulations were carried out in either a nitrogen filled glovebox or under nitrogen using standard Schlenk techniques. Reaction solvents were sparged with nitrogen then dried by passage through column of activated alumina using an apparatus purchased from Anhydrous Engineering. Deuterated benzene, and dichloromethane were purchased from Aldrich Chemical Company. Deuterated benzene and dichloromethane were dried over activated molecular sieves for 3 days. $LiN(SiMe_3)_2$ was purchased from Aldrich Chemical Company and purified by crystallization from cold hexane. The following chemicals were purchased from Aldrich Chemical Company and used without further purification: 1,8-diaminonaphthalene, $LiAlH_4$, triethylamine, pivaloyl chloride, sodium sulfate, triethyl orthoformate, formic acid, NaOH, NaCl, p-toluenesulfonic acid, anhydrous chlorobenzene, 1,8-naphthalic anhydride, lithium bromide, and phosphorous (III) bromide. Celite 545 was purchased from Aldrich Chemical Company and dried at 110°C for 3 days. Molecular sieves (4Å, beads, 4-8 mesh) were purchased from Aldrich Chemical Company and activated by drying under vacuum at 120°C for 5-6 hours. ^{1}H and ^{13}C NMR spectra were run on either a Varian Gemini 200 MHz, a Bruker Advance 300 MHz, a Varian Inova 500 MHz or a Bruker Advance 500 MHz spectrometer using the residual protons of the deuterated solvent for reference. Elemental analyses were performed by Guelph Chemical Laboratories Ltd., Guelph, ON or in the Department of Chemistry at the University of Ottawa on a Perkin-Elmer PE CHN 4000 elemental analysis system.

Preparation of 2,2-dimethyl-2,3-dihydroperimidine, Compound **2.1:**

To a Teflon screw cap-sealed flask was added 1,8-diaminonaphthalene (5.0g, 31.6 mmol), activated molecular sieves (5.0g) and acetone (18.5g, 319 mmol). The reaction was heated to 80°C overnight. The reaction mixture was filtered and the solids were washed with diethyl ether. The ether solutions were combined and all volatiles were removed under vacuum to give 5.87g (94%) of a red/purple solid that we have identified as the aminal, 2,2-dimethyl-2,3-dihydroperimidine.

^{1}H NMR ($CDCl_3$, 200 MHz): δ 7.17-7.32 (m, 4H, C*H*), 6.45 (d, 2H, C*H*), 4.18 (br, 2H, N*H*), 1.40 (s, 6H, CH_3).

^{13}C NMR ($CDCl_3$, 200 MHz): δ 140.3, 134.4, 126.9, 116.6, 112.6, 105.6 (C_{arom}), 64.3 ($CHMe_2$), 28.4 ($CH(CH_3)_2$).

Analysis Calcd $C_{13}H_{14}N_2$ C, 78.75; H, 7.12; N, 14.13; Found C, 78.79; H, 7.23; N, 13.98.

Preparation of N-(isopropyl)-1,8-diaminonaphthalene, (^{i}PrNH)(NH_2)$C_{10}H_6$, Compound **2.2:**

A sample of compound **1** (5.0g, 25.2 mmol) was dissolved in diethyl ether and added dropwise to a suspension of $LiAlH_4$ (2.9g, 76 mmol) in 100 ml of diethyl ether that was maintained at 0°C. After addition, the reaction was allowed to warm to room temperature and stirred for an additional 12 hrs. The reaction was then quenched, at 0°C, with isopropanol followed by water. This mixture was extracted with diethyl ether and dried under vacuum to give **2a** as a purple oil (4.12g, 82%).

^{1}H NMR ($CDCl_3$, 300 MHz): δ 7.12-7.26 (m, 4H, C*H*), 6.55-6.59 (m, 2H, C*H*), 4.89 (br, 3H, N*H*), 3.60 (sept, 1H, $CHMe_2$), 1.26 (d, 6H, CH_3).

^{13}C NMR ($CDCl_3$, 300 MHz): δ 145.3, 144.1, 137.1, 126.2, 125.9, 119.9, 118.7, 117.3, 112.1, 108.5 (C_{arom}), 45.8 ($CHMe_2$), 22.7(CH_3).

Analysis Calcd $C_{13}H_{16}N_2$ C, 77.96; H, 8.05; N, 13.99; Found C, 78.21; H, 8.35; N, 14.32.

Preparation of N,N'-diisopropyl-1,8-diaminonaphthalene, (^{i}PrNH)$_2C_{10}H_6$, Compound **2.3:**

Compound **2.2** (1.0g, 5 mmol) was mixed with acetone (5.8g, 100 mmol) and activated molecular sieves (2g) in a Teflon screw cap-sealed flask. The reaction was heated to

reflux overnight. The product was isolated as a purple oil. A sample of the resulting aminal (3.0g, 12.5 mmol) was allowed to react with $LiAlH_4$ (1.2g, 32 mmol) and stirred overnight. The reaction was then quenched, at 0°C, with isopropanol followed by water. The resulting mixture was extracted with diethyl ether, dried and the solvent evaporated to yield **IVa** as a purple oil (2.1g, 70%). This product can be further purified by silica gel column chromatography using hexanes as the eluent.

^{1}H NMR ($CDCl_3$, 500 MHz): δ 7.19-7.24 (m, 4H, C*H*), 6.58 (m, 2H, C*H*), 5.63, (br, 2H, N*H*), 3.58 (sept, 2H, C*H*Me_2), 1.24 (d, 12H, CH_3).

^{13}C NMR ($CDCl_3$, 500 MHz): δ 145.0, 137.3, 125.9, 119.3, 117.9, 110.3 (C_{arom}), 46.4 (*C*HMe_2), 22.6 (*C*H_3).

Analysis Calcd $C_{16}H_{22}N_2$ C, 79.29; H, 9.15; N, 11.56; Found C, 79.53; H, 9.35; N, 11.19.

Synthesis of N-(isopropyl)-N'-(neopentyl) -1,8-diaminonaphthalene, (^{i}PrNH)(NpNH)$C_{10}H_6$, Compound **2.4:**

Reaction of pivaloylchloride with **2.2** in the presence of excess base generated the trimethylacetamide intermediate, (^{i}PrNH)(^{t}BuCONH)$C_{10}H_6$, which was used without further purification. In a Schlenk flask, lithium aluminum hydride (1.46 g, 38.4 mmol) was dissolved in 50 mL of dry ether, cooled in an ice bath and stirred for 1 h. The trimethylacetamide intermediate (4.37 g, 15.3 mmol) was added slowly as a solid to this solution under nitrogen and allowed to stir for 2 h. The reaction was stirred for 18 h at room temperature, and quenched with wet ether. The organic layer was extracted with water, dried with sodium sulfate, by vacuum, and purified by flash chromatography to yield a purple solid (3.85 g, 93%).

^{1}H NMR (200MHz, 298 K, $CDCl_3$): δ 7.19(m, 4H), 6.60 (m, 2H), 5.23 (br, 2H), 3.65 (sept, 1H, J_{HH}=6.4 Hz), 2.91 (s, 2H), 1.29 (d, 6H, J_{HH}=6.4 Hz), 1.12 (s, 9H).

^{13}C NMR (500MHz, 298 K, $CDCl_3$): δ 147.2, 144.8, 136.8, 126.1, 125.6, 117.8, 117.3, 109.3, 105.4 (C_{arom}), 57.2 (*C*$H_2$$Me_3$), 45.2 (*C*H$Me_2$), 31.2 (*C*$Me_3$), 27.9 (*C*$H_3$), 22.7 (*C*$H_3$).

Analysis Calcd $C_{18}H_{26}N_2$ C, 79.95; H, 9.69; N, 10.36; Found C, 79.63; H, 10.01; N, 10.39.

Preparation of 1,3-diisopropylperimidinium formate, $\{C_{10}H_6(^{i}PrN)_2CH\}\{O_2CH\}\cdot(HCOOH)_2$, Compound 2.7a:

Under nitrogen in a teflon screw-top Schlenk flask equipped with a stir bar was added the diamine **2.3** (1.452g, 6 mmol) and approximately 50 ml of dry, deoxygenated toluene. To this solution was added triethyl orthoformate (8.00 g, 54 mmol) followed by formic acid (4.08 g, 77 mmol). The solution was then degassed (freeze/pump/thaw) and stirred at 80°C overnight. All volatiles were removed under vacuum and the yellow solid was dissolved in THF and cooled to 4°C. The crystallized product was then filtered and washed with diethyl ether which was removed under vacuum (2.25 g). ^{1}H NMR revealed that the salt had co-crystallized with two equivalents of formic acid (FW = 390 g/mol, yield 96 %).

^{1}H NMR (300 MHz, $CDCl_3$): δ 14.67 (s, 2H, CO_2H), 8.72 (s, 1H, HCN_2), 8.37 (s, 3H, HCO_2), 7.49 (d, 2H, CH_{Ar}), 7.41 (t, 2H, CH_{Ar}), 6.93 (d, 2H, CH_{Ar}), 4.60 (sept, 2H, $HCMe_2$), 1.65 (d, 12H, CH_3).

^{13}C NMR (300 MHz, $CDCl_3$): δ 166.0 (HCO_2), 148.2 (N_2CH), 135.4, 131.2, 128.0, 124.6, 122.2, 108.1 (C_{arom}), 55.1 (s, $CHMe_2$), 19.8 (s, CH_3).

Analysis Calcd $(C_{17}H_{21}N_2)(HCO_2)(HCO_2H)_2$ C, 61.53; H, 6.71; N, 7.18. Found C, 61.23; H, 6.57; N, 7.49.

Preparation of 1,3-diisopropylperimidinium chloride, $\{C_{10}H_6(^{i}PrN)_2CH\}Cl$, Compound 2.7b:

Compound **2.7a** (1.0 g, 2.6 mmol) was added to 10 ml of a NaOH/NaCl solution (0.51 M and 5.0 M respectively) in a separatory funnel. The aqueous layer was extracted repeatedly with 10 ml aliquots of CH_2Cl_2 until the organic layer showed very little yellow color. The crude product obtained by removal of solvent under vacuum was purified by crystallization from a CH_2Cl_2 solution layered with diethyl ether (0.50 g, 65 % yield).

^{1}H NMR (300 MHz, $CDCl_3$): δ 9.89 (s, 1H, HCN_2), 7.46 (dd, 2H, CH), 7.38 (t, 2H, CH), 6. 92 (dd, 2H, CH), 4.81 (sept, 2H, $HCMe_2$), 1.82 (d, 12H, CH_3).

^{13}C NMR (300 MHz, $CDCl_3$): δ 149.9 (s, N_2CH), 135.0, 132.3, 128.0, 124.3, 122.5, 108.0 (C_{arom}), 55.7 (s, $CHMe_2$), 19.8 (s, CH_3).

Analysis Calcd $C_{17}H_{21}ClN_2$ C, 70.70; H, 7.33; N, 9.70. Found C, 70.47; H, 6.99; N, 9.89.

Synthesis of 1-isopropyl-3-neopentylperimidinium tosylate, $\{C_{10}H_6(^iPrN)(NpN)CH\}\{O_3SC_6H_4CH_3\}$, Compound **2.8:**

In a round bottom flask, **2.4** (3.87 g, 14.3 mmol), p-toluenesulfonic acid (monohydrate) (2.72 g, 14.3 mmol), and triethylorthoformate (21.2 g, 0.143 mol) were combined and stirred for 18 h at 45°C. The solvent was dried, and the product recrystallized from methylene chloride was a yellow solid (3.85 g, 66%).

^{1}H NMR (200MHz, 298 K, $CDCl_3$): δ 9.15 (s, 1H, N_2CH), 7.78 (d, 2H, C*H*), 7.38 (m, 4H, C*H*), 7.09 (d, 2H,C*H*), 6.90 (m, 2H, C*H*), 4.45 (sept, 1H, $CHMe_2$), 4.27 (s, 2H, CH_2), 2.30 (s, 3H, CH_3), 1.72 (d, 6H, CH_3), 1.08 (s, 9H, CH_3).

^{13}C NMR (500MHz, 298 K, $CDCl_3$): δ 152.0 (N_2CH), 143.7, 138.7, 135.0, 132.7, 131.4, 138.2, 128.1, 127.6, 125.8, 124.2, 124.0, 121.6, 108.4, 107.6 (C_{arom}), 59.4 (CH_2CCH_3), 53.5 ($CHCH_3$), 33.6 (tosylate CH_3), 27.7 (CH_2CCH_3), 21.1 (CH_2CCH_3), 19.8 ($CHCH_3$).

Analysis Calcd $C_{26}H_{32}N_2O_3S$ C, 69.00; H, 7.13; N, 6.19. Found C, 68.88; H, 7.16; N, 6.24.

Synthesis of 1,3-dineopentylperimidinium tosylate, $\{C_{10}H_6(NpN)_2CH\}\{O_3SC_6H_4CH_3\}$, Compound **2.9:**

In a round bottom flask, **2.6** (2.83 g, 9.48 mmol), p-toluenesulfonic acid (monohydrate) (1.80 g, 9.48 mmol), and triethylorthoformate (12.6 g, 85.3 mmol) were combined and stirred for 18 h at 45°C. The solvent was removed under vacuum and the product recrystallized from methylene chloride was a green solid (3.48 g, 76%).

^{1}H NMR (200MHz, 298 K, $CDCl_3$): δ 9.39 (s, 1H, N_2CH), 7.78 (d, 2H, C*H*), 7.36 (m, 4H, C*H*), 7.10 (d, 2H, C*H*), 6.89 (d, 2H, C*H*), 4.13 (s, 4H, CH_2), 2.29 (s, 3H, CH_3), 1.13 (s, 18H ,CH_3).

^{13}C NMR (500MHz, 298 K, $CDCl_3$): δ 156.5 (N_2CH), 143.5, 139.2, 135.1, 133.4, 128.5, 127.7, 126.0, 124.4, 121.9, 108.7 (C_{arom}), 60.6 (CH_2), 33.8 (CH_3), 28.4 (CH_3), 21.3 (CCH_3).

Analysis Calcd $C_{28}H_{36}N_2O_3S$ C, 69.97; H, 7.55; N, 5.83. Found C, 69.40; H, 7.86; N, 5.83.

Preparation of 1,3-(^{i}Pr)$_2$-perimidin-2-ylidene, $C_{10}H_6(^iPrN)_2C$, Compound 2.10:
Compound **2.7b** (0.40 g, 1.4 mmol) in 20 mL of 1:1 chlorobenzene/THF was added to a solution of $LiN(SiMe_3)_2$ (0.232 g, 1.4 mmol) in 4 mL of 1:1 chlorobenzene/THF at room temperature. The reaction was stirred overnight and the volatiles were removed under vacuum. This solid was extracted with 15 mL toluene followed by filtration. The filtrate was evaporated under vacuum to afford a white powder which was purified by crystallizing from an ether solution at –25°C (0.160 g, 46 % yield).
^{1}H NMR (300 MHz, C_6D_6): δ 7.12 (m, 4H, *CH*), 6.29 (dd, 2H, *CH*), 4.08 (sept, 2H, *H*CMe$_2$), 1.41 (d, 12H, C*H*$_3$).
^{13}C NMR (300 MHz, C_6D_6): δ 241.7 (N*C*N), 136.0, 133.7, 128.0, 122.7, 119.4, 102.9 (C_{arom}), 51.5 (*C*HMe$_2$), 22.3 (*C*H$_3$).
Analysis Calcd $C_{17}H_{20}N_2$ C, 80.91; H, 7.99; N, 11.10. Found C, 80.55; H, 8.01; N, 10.84.

Synthesis of 1-isopropyl-3-neopentylperimidin-2-ylidene, $C_{10}H_6(^iPrN)(NpN)C$, Compound **2.11:**.
Compound **2.8** (0.185 g, 1.10 mmol) in 15 mL of anhydrous chlorobenzene was added to a solution of $LiN(SiMe_3)_2$ (0.500 g, 1.10mmol) in 10 mL of anhydrous chlorobenzene. The reaction was stirred for 2 days and the volatiles were removed under vacuum. The solid was extracted with 15 mL toluene followed by filtration. The filtrate was evaporated under vacuum to afford a pale orange, sticky solid which was purified by crystallizing from hexane to give a pale beige solid (0.20 g, 64%).
^{1}H NMR (200MHz, 298 K, C_6D_6): δ 7.12 (m, 4H, C*H*), 6.51 (m, 1H, C*H*), 6.40 (m, 1H, C*H*), 4.10 (sept, 1H, C*H*Me$_2$), 3.96 (s, 2H, C*H*$_2$), 1.46 (d, 6H, *C*H$_3$), 1.04 (s, 9H, *C*H$_3$).
^{13}C NMR (200MHz, 298 K, C_6D_6): δ 247.9 (NCN), 136.0, 135.0, 133.7, 128.3, 127.6, 119.7, 119.4, 104.9, 102.9 (C_{arom}), 64.2 (*C*H$_2$C(CH$_3$)$_3$), 51.1 (*C*H(CH$_3$)$_2$), 29.0 (CH$_2$*C*(CH$_3$)$_3$), 22.3 (CH(*C*H$_3$)$_2$).
Analysis Calcd $C_{19}H_{24}N_2$ C, 81.38; H, 8.63; N, 9.99; Found C, 80.94; H, 8.97; N, 9.61.

Preparation of enetetramine, (C[N{[CH$_2$C(CH$_3$)$_3$]}$_2$C$_{10}$H$_6$)$_2$, Compound **2.12:**
Compound **2.9** (0.500 g, 1.10 mmol) in 20 mL of anhydrous chlorobenzene was added to a solution of $LiN(SiMe_3)_2$ (0.185 g, 1.10 mmol) in 10 mL of anhydrous chlorobenzene.

The reaction was stirred 18 h and the volatiles were removed under vacuum. This solid was extracted with 15 mL toluene followed by filtration. The filtrate was evaporated under vacuum to afford a green, sticky solid which was purified by crystallizing from an hexane to give a pale beige solid (0.120g, 71%).

^{1}H NMR (200MHz, 298 K, C_6D_6): δ 7.27 (m, 4H, C*H*), 6.86 (m, 2H, C*H*), 6.87 (d, 2H, CH_2), 6.84 (d, 2H, CH_2), 0.866 (s, 18H, CH_3).

^{13}C NMR (200MHz, 298 K, C_6D_6): δ 145.7, 136.2, 132.0, 128.3, 126.7, 119.2, 107.3, 61.3 ($CH_2C(CH_3)_3$), 34.0 ($CH_2C(CH_3)_3$), 29.2 ($CH_2C(CH_3)_3$).

Analysis Calcd $C_{21}H_{28}N_2$ C, 81.77; H, 9.15; N, 9.08. Found C, 82.15; H, 9.42; N, 9.09.

Preparation of 1-isopropylperimidine, $C_{10}H_6N(^iPrN)CH$, Compound **2.16:**

In a 250ml round bottom flask was added N-isopropyl-1,8-diaminonaphthalene **2.2** (4.0g, 20 mmol), triethyl orthoformate (29.6g, 200 mmol) and formic acid (0.04 ml, 1 mmol). The reaction was heated to 100°C under nitrogen for 4 hours and monitored by TLC. The product was purified by column chromatography using silica gel and a 1:1 ether:dichloromethane elution solvent mixture. Product **2.16** was isolated as a brown solid 3.5g (83%).

^{1}H NMR ($CDCl_3$, 300 MHz): *δ* 7.40 (s, 1H, C*H*), 7.21 (t, 1H, C*H*), 7.04-7.13 (m, 3H, C*H*), 6.80 (d, 1H, C*H*), 6.21 (d, 1H, C*H*), 4.02 (sept, 1H, C*H*Me_2), 1.42 (d, 6H, CH_3).

^{13}C NMR ($CDCl_3$, 300 MHz): *δ* 144.5 (*C*H), 143.3, 137.7, 135.6, 128.7, 127.3, 123.2, 120.2, 119.1, 114.8, 100.2 (C_{arom}), 47.8 (*C*HMe_2), 20.8 (*C*H_3).

Analysis Calcd $C_{14}H_{14}N_2$ C, 79.97; H, 6.71; N, 13.32; Found C, 79.60; H, 6.51; N, 13.00.

Preparation of 1,8-bis(bromomethyl)naphthalene, $C_{12}H_{10}Br_2$:

Prepared according to the literature preparation from *The Journal of Organic Chemistry*, **1984**, 49(22), 4128-32, from 1,8-naphthalic anhydride, lithium aluminum hydride, lithium bromide, and phosphorous (III) bromide.

Preparation of $\{[C_{10}H_6N(^iPrN)CH]_2(CH_2)_2C_{10}H_8\}\{Br\}_2$, Compound **2.17:**

In a 150 ml round bottom flask was added 1-isopropylperimidine (1.00 g, 4.76 mmol), 1,8-bis(bromomethyl)naphthalene (0.75 g, 2.38 mmol), and 40 ml of toluene. The

reaction was heated to 105°C for 40 hours under a reflux set-up. The solvent was removed by vacuum, and the solid left was washed with 50 ml of diethyl ether, followed by 20 ml of hexane (to wash away any coordinated ether). Product **2.17** was isolated as a bright yellow powder (3.22 g, 92%) that is insoluble in $CHCl_3$, and DMSO.
^{1}H NMR ($CDCl_3$, 500 MHz): δ 9.37 (s, 2H, NC*H*N), 8.00 (d, 2H, ar), 7.71 (d, 2H, ar), 7.63 (m, 8H, ar), 7.46 (m, 2H, ar), 7.40 (m, 4H, ar), 6.83 (s, 4H, NCH_2), 4.78 (m, 2H, $CH(CH_3)_2$), 1.61 (d, 12H, $CH(CH_3)_2$).
^{13}C NMR ($CDCl_3$, 500 MHz): δ 151.2 (NC*H*N), 134.5 (ar), 132.1 (ar), 132.0 (ar), 129.7 (ar), 129.0 (ar), 128.5 (ar), 128.2 (ar), 125.7 (ar), 124.4 (ar), 124.1 (ar), 123.8 (ar), 121.6 (ar), 108.9 (ar), 108.5 (ar), 64.9 (NCH_2), 56.1 ($CH(CH_3)_2$), 20.45 ($CH(CH_3)_2$).
MS [Scan ES+] m/z (A^+X^-, relative intensity): 655.0 ($2A^+X^-$, 16.1), 363.1 (A^+ frag., 45.1), 209.9 (A^+ frag, 100.0).

Preparation of $C_{40}H_{34}N_4$, Compound **2.18**, product of intramolecular reaction:
In a 250 ml round bottom flask was added 10 ml of chlorobenzene and $LiN(SiMe_3)_2$ (0.26 g, 1.37 mmol). Over a period of 30 min, a suspension of **2.17** (0.50 g, 0.685 mmol) in 10 ml of chlorobenzene was added to the base and subsequently allowed to stir for 18 hours at room temperature. The chlorobenzene was removed by vacuum and the remaining solid was filtered through a frit with celite in toluene. The toluene was removed by vacuum to leave a white solid which was crystallized from chlorobenzene (0.30 g, 76%).
^{1}H NMR (C_6D_6, *200 MHz):* δ 7.10 (m, 18H, C*H*), 5.65 (s, 2H, CH_2), 4.54 (s, 2H, CH_2), 3.77 (m, 2H, $CH(CH_3)_2$), 1.48 (d, 6H, $CH(CH_3)_2$), 0.83 (d, 6H, $CH(CH_3)_2$).
^{13}C NMR (C_6D_6, 500 MHz): δ 143.4 (ar), 143.4 (ar),137.5 (ar), 136.0 (ar), 135.4(ar), 128.9 (ar), 128.5 (ar), 128.5 (ar), 126.1 (ar), 125.9 (ar), 125.4 (ar), 125.3 (ar), 121.7 (ar), 118.3 (ar), 116.5 (ar), 103.3 (ar), 77.5, 57.3, 47.3, 27.3, 21.3, 21.1.

Preparation of $\{C_{10}H_6N(^iPrN)(CH_3OC_6H_4COCH_2)CH\}\{Br\}$, Compound **2.19:**
In a 250 ml round bottom flask was added 2.16 (2.24 g, 10.6 mmol) and 2-bromo-1-(4-methoxy-phenyl)-ethanone (2.44 g, 10.6 mmol) in 100 ml RG acetone. The mixture was allowed to stir for 2 days at room temperature. The bright yellow product was filtered

and washed with ether (50 ml). After drying by vacuo, 3.00 g of powder were recovered (64%).

^{1}H NMR ($CHCl_3$, *200 MHz): δ* 9.84 (s, 1H, N_2CH), 8.09 (d, 2H, C*H*), 7.42 (m, 2H, C*H*), 7.26 (m, 2H, C*H*), 6.95 (m, 3H, C*H*), 6.50 (d, 1H, C*H*), 6.36 (s, 2H, CH_2), 4.52 (sept, 1H, $CH(CH_3)_2$), 3.85 (s, 3H, OCH_3), 1.79 (d, 6H, $CH(CH_3)_2$).

MS [Scan ES+] m/z (A^+X^-, relative intensity): 1677.5 ($4A^+3X^-$, 1.14), 1238.1 ($3A^+2X^-$, 9.90), 798.7 ($2A^+X^-$, 99.6), 359.4 (A^+, 100.0), 210.0 (A^+ frag, 20.0).

Crystal Structure Determination

A suitable crystal was selected, mounted on a glass fiber with viscous oil and cooled to the desired data collection temperature. Data were collected on a Bruker AX SMART 1k CCD diffractometer using one of the following scan sequences: for triclinic unit cells, 4 sets of 650 frames (0.3 deg in ω) at 0, 90, 180, 270 degrees in Φ; all other cells (which are not triclinic) - 3 sets of 650 frames (0.3 deg in ω) at 0, 120, 240 degrees in Φ. Unit-cell parameters were determined from 60 data frames collected at different sections of the Ewald sphere. Semi-empirical absorption corrections based on equivalent reflection were applied (Blessing, R., *Acta Cryst.*, **1995**, A51, 33-38).

To solve the structures, the software package ShelXTL 6.14 was used. The Structure was solved by direct methods, completed with difference Fourier synthesis and refined with full-matrix least-squares procedures based on F^2. All non-hydrogen atoms were refined with anisotropic displacement parameters. All hydrogen atoms were treated as idealized contributions. All scattering factors are contained in the SHEXTL 5.10 program library (Sheldrick, G. M., Bruker AXS, Madison, WI, 1997). Any minor disorders were omitted from the final structure.

IV. Figures and Tables

Figure 2.1. Thermal ellipsoid plot showing the molecular structure and atom numbering scheme for ligand **2.5**. Hydrogen atoms have been omitted for clarity. Thermal ellipsoids are drawn at 30% probability.

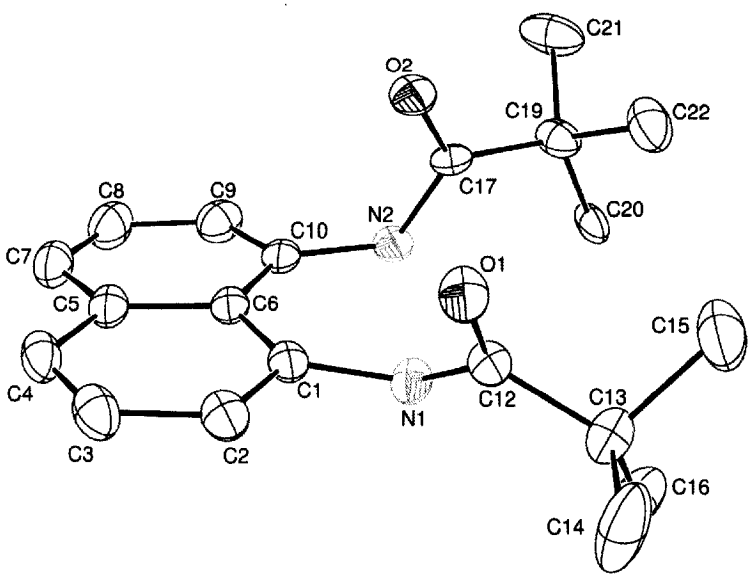

Figure 2.2. Thermal ellipsoid plot showing the molecular structure and atom numbering scheme for ligand **2.6**. Hydrogen atoms have been omitted for clarity. Thermal ellipsoids are drawn at 30% probability.

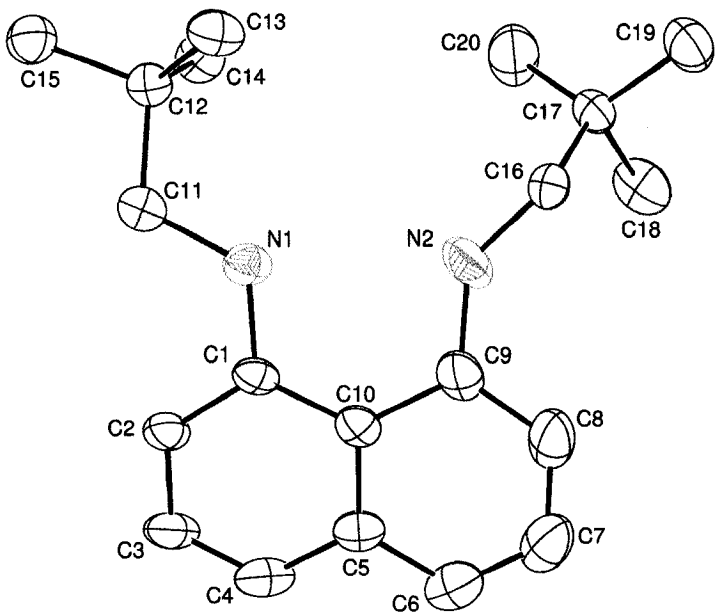

Figure 2.3. Thermal ellipsoid plot showing the molecular structure and atom numbering scheme for perimidinium cation **2.8**. Hydrogen atoms have been omitted for clarity. Thermal ellipsoids are drawn at 30% probability. One solvent molecule (CH_2Cl_2) and tosylate anion removed for clarity.

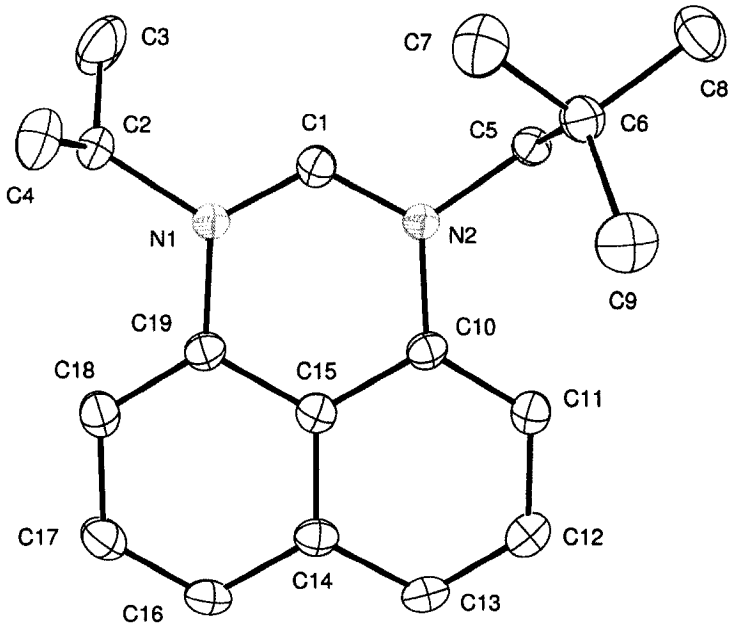

Figure 2.4. Thermal ellipsoid plot showing the molecular structure and atom numbering scheme for carbene **2.11**. Hydrogen atoms have been omitted for clarity. Thermal ellipsoids are drawn at 30% probability.

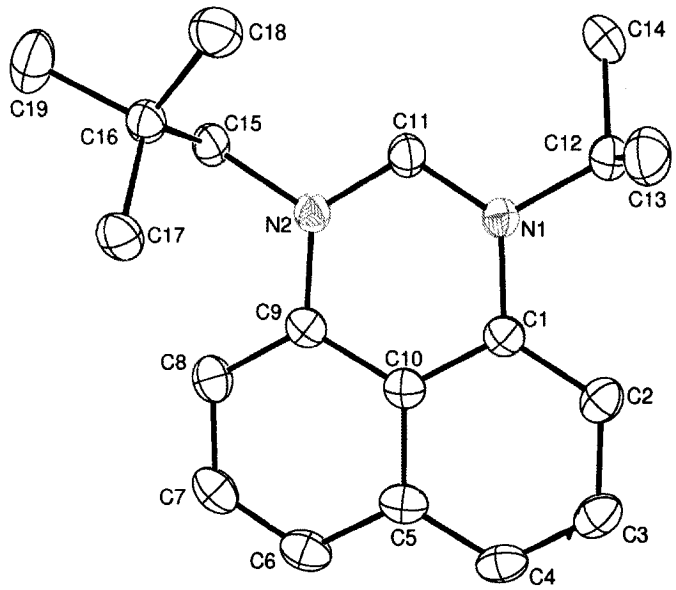

Figure 2.5. Thermal ellipsoid plot showing the molecular structure and atom numbering scheme for product **2.13**. Hydrogen atoms have been omitted for clarity. Thermal ellipsoids are drawn at 30% probability. Shown is one of four molecules present in the asymmetric unit.

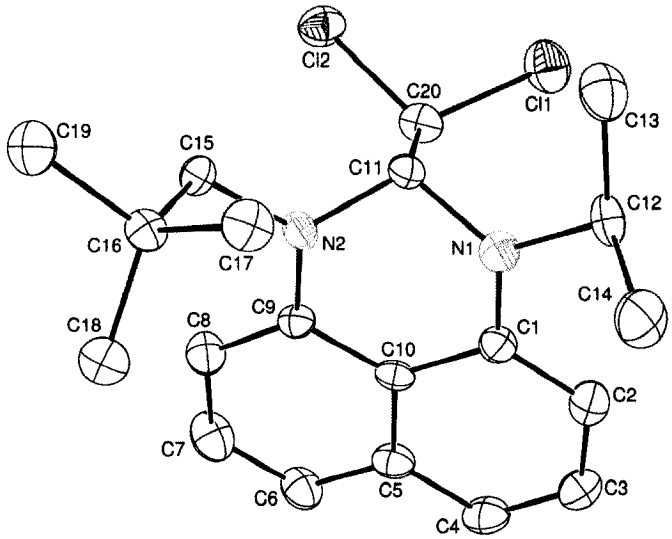

Figure 2.6. Thermal ellipsoid plot showing the molecular structure and atom numbering scheme for product **2.14**. Hydrogen atoms have been omitted for clarity. Thermal ellipsoids are drawn at 30% probability. Two symmetric units are shown. The unique atoms are labeled.

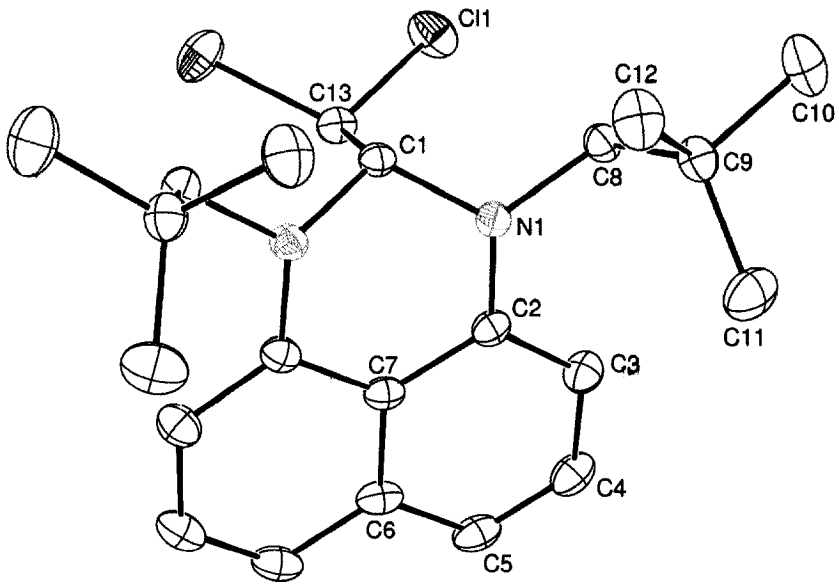

Figure 2.7. Thermal ellipsoid plot showing the molecular structure and atom numbering scheme for product **2.15**. Hydrogen atoms have been omitted for clarity. Thermal ellipsoids are drawn at 10% probability due to complexity of three-dimensional structure.

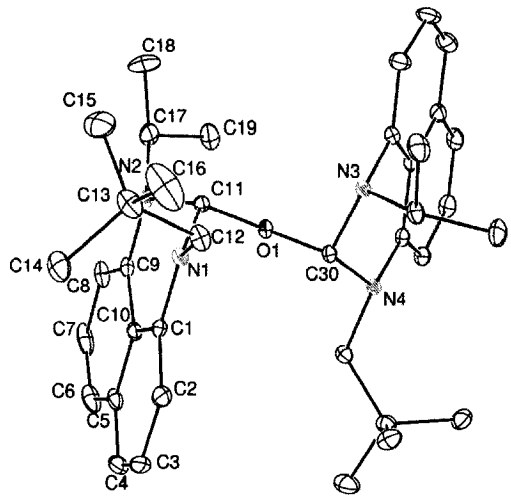

Figure 2.8. Thermal ellipsoid plot showing the molecular structure and atom numbering scheme for product **2.18**. Hydrogen atoms have been omitted for clarity. Thermal ellipsoids drawn at 30% probability. One solvent molecule (toluene) removed for clarity.

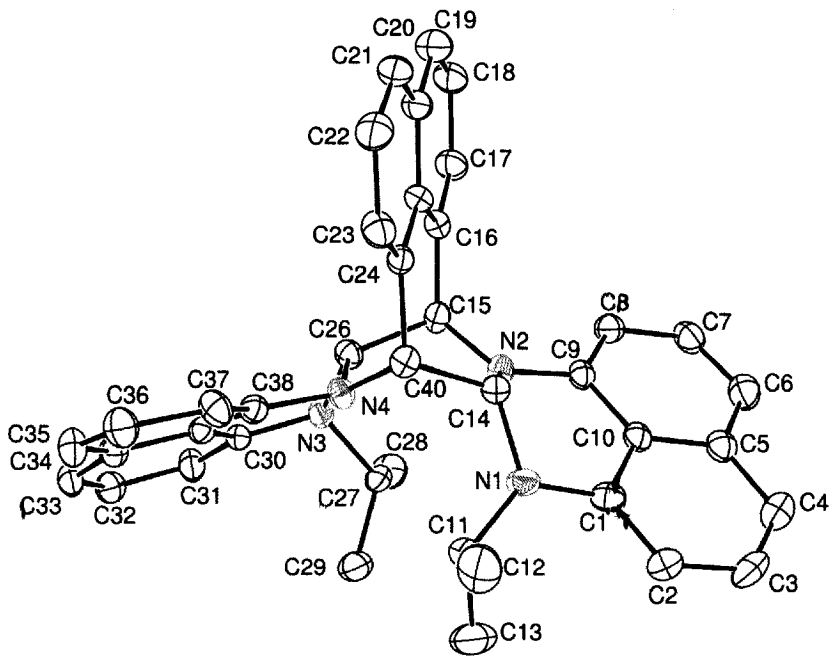

Figure 2.9. Thermal ellipsoid plot showing the molecular structure and atom numbering scheme for complex **2.20**. Hydrogen atoms have been omitted for clarity. Thermal ellipsoids are drawn at 30% probability. Two symmetric units are shown. Only symmetry unique atoms have been labeled.

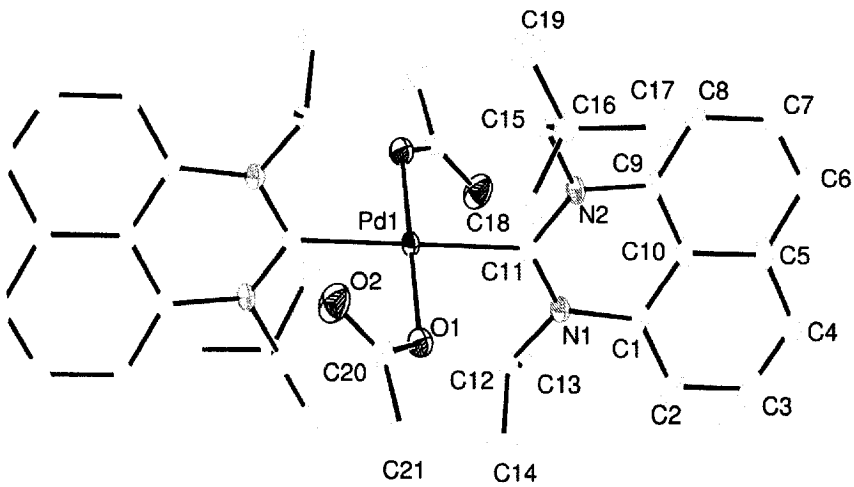

Table 2.1. Selected Crystal Data and Data Collection Parameters for **2.5**, **2.6**, **2.8**, **2.11**, **2.13**, **2.14**, **2.15**, **2.18**, **and 2.20**.

	2.5	**2.6**	**2.8**	**2.11**
empirical formula	$C_{20}H_{26}N_2O_2$	$C_{20}H_{30}N_2$	$C_{27}H_{33}Cl_2N_2O_3S$	$C_{19}H_{24}N_2$
formula weight	326.43	298.46	536.51	280.4
T (K)	203(2)	200(2)	207(2)	200(2)
wavelength (Å)	0.71073	0.71073	0.71073	0.71073
crystal system	Monoclinic	Monoclinic	Monoclinic	Orthorhombic
space group	P2(1)/n	C2/c	P2(1)/n	Pca2(1)
a (Å)	11.791(2)	24.708(7)	10.087(6)	11.1938(15)
b (Å)	9.4097(18)	13.480(4)	16.617(9)	13.9491(19)
c (Å)	17.008(3)	12.258(4)	16.919(9)	10.5219(14)
α (deg)	90	90	90	90
β (deg)	93.221(3)	116.890(5)	101.374(10)	90
γ (deg)	90	90	90	90
V (Å3)	1884.1(6)	3641.1(18)	2780(3)	1642.9(4)
Z	4	8	4	4
abs coeff (mm^{-1})	0.074	0.063	0.339	0.066
final R indeces	R1 = 0.0552	R1 = 0.0678	R1 = 0.0604	R1 = 0.0371
	wR2 = 0.1265	wR2 = 0.1492	wR2 = 0.1446	wR2 = 0.0828

Table 2.1. (continued)

	2.13	**2.14**	**2.15**	**2.18**
empirical formula	$C_{32}H_{41.6}Cl_{3.20}N_{3.2}$	$C_{22}H_{30}Cl_2N_2$	$C_{38}H_{50}N_4O$	$C_{43.50}H_{40}N_4$
formula weight	584.52	393.38	578.82	618.79
T (K)	213(2)	208(2)	207(2)	200(2)
wavelength (Å)	0.71073	0.71073	0.71073	0.71073
crystal system	Triclinic	Orthorhombic	Monoclinic	Monoclinic
space group	P-1	Pnma	P2(1)/c	P2/n
a (Å)	14.389(3)	14.399(7)	16.780(3)	10.209(3)
b (Å)	15.533(3)	18.582(9)	10.662(2)	11.085(3)
c (Å)	17.324(4)	7.863(4)	19.831(4)	29.034(7)
α (deg)	87.661(4)	90	90	90
β (deg)	89.595(4)	90	106.518(4)	93.918(5)
γ (deg)	81.538(4)	90	90	90
V (Å3)	3826.4(14)	2103.9(18)	3401.4(11)	3278.2(14)
Z	5	4	4	4
abs coeff (mm^{-1})	0.343	0.317	0.068	0.074
final R indeces	R1 = 0.0616	R1 = 0.0384	R1 = 0.0718	R1 = 0.0525
	wR2 = 0.1049	wR2 = 0.1021	wR2 = 0.1635	wR2 = 0.1054

Table 2.1. (continued)	
	2.20
empirical formula	$C_{21}H_{27}N_2O_2Pd_{0.50}$
formula weight	392.65
T (K)	207(2)
wavelength (Å)	0.71073
crystal system	Monoclinic
space group	P2(1)/c
a (Å)	12.549(8)
b (Å)	10.574(7)
c (Å)	17.614(12)
α (deg)	90
β (deg)	125.68(4)
γ (deg)	90
V (Å3)	1898(2)
Z	4
abs coeff (mm^{-1})	0.536
final R indeces	R1 = 0.0508
	wR2 = 0.1277

Table 2.2. Selected Bond Lengths and Angles for **2.5**.			
	Bond Lengths (Å)		
N(1)-C(12)	1.357(3)	O(1)-C(12)	1.237(3)
N(1)-C(1)	1.428(3)	O(2)-C(17)	1.233(3)
N(2)-C(17)	1.347(3)	C(1)-C(2)	1.370(4)
N(2)-C(10)	1.423(3)	C(9)-C(10)	1.363(4)
	Bond Angles (deg)		
C(12)-N(1)-C(1)	123.4(2)	C(17)-N(2)-C(10)	122.78(19)
C(2)-C(1)-N(1)	116.5(3)	C(9)-C(10)-N(2)	117.2(3)
O(1)-C(12)-N(1)	121.2(2)	O(2)-C(17)-N(2)	120.0(2)
N(1)-C(12)-C(13)	118.1(2)	N(2)-C(17)-C(19)	118.1(2)
O(1)-C(12)-C(13)	120.5(2)	O(2)-C(17)-C(19)	121.8(2)

Table 2.3. Selected Bond Lengths and Angles for **2.6**.			
	Bond Lengths (Å)		
N(1)-C(1)	1.415(3)	N(2)-C(16)	1.484(6)
N(1)-C(11)	1.460(3)	C(1)-C(2)	1.374(4)
N(2)-C(9)	1.377(4)	C(8)-C(9)	1.390(5)
	Bond Angles (deg)		
C(1)-N(1)-C(11)	119.5(2)	C(2)-C(1)-N(1)	120.2(3)
C(9)-N(2)-C(16)	135.8(3)	N(2)-C(9)-C(8)	120.6(3)
N(1)-C(1)-C(10)	120.6(2)	N(2)-C(9)-C(10)	120.9(3)
N(1)-C(11)-C(12)	113.6(2)	N(2)-C(16)-C(17)	111.3(4)

Table 2.4. Selected Bond Lengths and Angles for **2.8**.

	Bond Lengths (Å)		
N(1)-C(1)	1.328(4)	N(2)-C(1)	1.321(4)
N(1)-C(19)	1.432(4)	N(2)-C(10)	1.431(4)
N(1)-C(2)	1.514(4)	N(2)-C(5)	1.487(4)
	Bond Angles (deg)		
C(1)-N(1)-C(19)	120.8(2)	C(10)-N(2)-C(5)	121.9(2)
C(1)-N(1)-C(2)	119.1(3)	Sum at N(2)	360.1
C(19)-N(1)-C(2)	120.0(2)	N(2)-C(1)-N(1)	124.3(3)
Sum at N(1)	359.9	C(11)-C(10)-N(2)	123.4(3)
C(1)-N(2)-C(10)	120.9(2)	C(18)-C(19)-N(1)	123.1(3)
C(1)-N(2)-C(5)	117.3(2)		

Table 2.5. Selected Bond Lengths and Angles for **2.11**.

	Bond Lengths (Å)		
N(1)-C(11)	1.354(3)	N(2)-C(9)	1.420(3)
N(1)-C(1)	1.417(3)	N(2)-C(15)	1.473(2)
N(1)-C(12)	1.487(3)	C(1)-C(2)	1.387(3)
N(2)-C(11)	1.357(3)	C(8)-C(9)	1.385(3)
	Bond Angles (deg)		
C(11)-N(1)-C(1)	125.16(18)	C(9)-N(2)-C(15)	119.90(16)
C(11)-N(1)-C(12)	116.92(17)	Sum at N(2)	359.99
C(1)-N(1)-C(12)	117.77(16)	N(1)-C(11)-N(2)	115.55(19)
Sum at N(1)	359.85	C(2)-C(1)-N(1)	123.49(19)
C(11)-N(2)-C(9)	125.46(17)	C(8)-C(9)-N(2)	123.83(19)
C(11)-N(2)-C(15)	114.63(17)		

Table 2.6. Selected Bond Lengths and Angles for **2.13**.

	Bond Lengths (Å)		
N(1)-C(1)	1.402(6)	N(2)-C(15)	1.458(6)
N(1)-C(11)	1.467(6)	Cl(1)-C(20)	1.765(5)
N(1)-C(12)	1.469(6)	Cl(2)-C(20)	1.769(5)
N(2)-C(9)	1.403(6)	C(11)-C(20)	1.549(7)
N(2)-C(11)	1.443(6)		
	Bond Angles (deg)		
C(1)-N(1)-C(11)	113.4(4)	N(2)-C(11)-C(20)	108.9(4)
C(1)-N(1)-C(12)	120.3(5)	N(1)-C(11)-C(20)	111.4(4)
C(11)-N(1)-C(12)	123.7(4)	Sum at C(11)	330
Sum at N(1)	357.4	C(11)-C(20)-Cl(2)	109.6(4)
C(9)-N(2)-C(11)	114.7(4)	C(11)-C(20)-Cl(1)	113.4(4)
C(9)-N(2)-C(15)	124.2(4)	Cl(2)-C(20)-Cl(1)	110.4(3)
C(11)-N(2)-C(15)	119.7(4)	Sum at C(20)	333.4
Sum at N(2)	358.6	C(2)-C(1)-N(1)	124.0(5)
N(2)-C(11)-N(1)	109.7(4)	C(8)-C(9)-N(2)	123.6(5)

Table 2.7. Selected Bond Lengths and Angles for **2.14**.

	Bond Lengths (Å)		
Cl(1)-C(13)	1.7811(17)	N(1)-C(8)	1.475(2)
N(1)-C(2)	1.398(3)	C(1)-C(13)	1.562(4)
N(1)-C(1)	1.457(2)	C(2)-C(3)	1.384(3)
	Bond Angles (deg)		
C(1)-C(13)-Cl(1)#1	112.55(12)	Sum at N(1)	354.94
C(1)-C(13)-Cl(1)	112.55(12)	N(1)-C(1)-C(13)	110.28(14)
Cl(1)#1-C(13)-Cl(1)	108.00(15)	N(1)#1-C(1)-C(13)	110.28(14)
Sum at C(13)	333.1	N(1)#1-C(1)-N(1)	109.8(2)
C(2)-N(1)-C(1)	114.88(16)	Sum at C(1)	330.36
C(2)-N(1)-C(8)	121.37(15)	C(3)-C(2)-N(1)	124.11(17)
C(1)-N(1)-C(8)	118.69(16)		

Table 2.8. Selected Bond Lengths and Angles for **2.15**.

	Bond Lengths (Å)		
O(1)-C(30)	1.427(3)	N(2)-C(17)	1.477(4)
O(1)-C(11)	1.444(4)	N(3)-C(20)	1.434(4)
N(1)-C(1)	1.393(4)	N(3)-C(30)	1.445(4)
N(1)-C(11)	1.435(4)	N(3)-C(36)	1.483(4)
N(1)-C(12)	1.442(4)	N(4)-C(28)	1.411(4)
N(2)-C(9)	1.408(4)	N(4)-C(30)	1.438(4)
N(2)-C(11)	1.425(4)	N(4)-C(31)	1.474(4)
	Bond Angles (deg)		
C(30)-O(1)-C(11)	118.5(2)	C(28)-N(4)-C(30)	114.0(3)
C(1)-N(1)-C(11)	115.3(2)	C(28)-N(4)-C(31)	120.0(3)
C(1)-N(1)-C(12)	124.0(3)	C(30)-N(4)-C(31)	112.9(2)
C(11)-N(1)-C(12)	118.8(3)	Sum at (N4)	346.9
Sum at (N1)	358.1	N(2)-C(11)-N(1)	111.0(3)
C(9)-N(2)-C(11)	113.1(3)	N(4)-C(30)-N(3)	115.5(3)
C(9)-N(2)-C(17)	119.1(3)	N(2)-C(11)-O(1)	105.8(2)
C(11)-N(2)-C(17)	116.7(3)	N(1)-C(11)-O(1)	112.4(2)
Sum at (N2)	348.9	Sum at (C11)	336.7
C(20)-N(3)-C(30)	111.5(2)	O(1)-C(30)-N(4)	105.6(2)
C(20)-N(3)-C(36)	116.8(3)	O(1)-C(30)-N(3)	110.1(2)
C(30)-N(3)-C(36)	113.6(3)	Sum at (C30)	334.2
Sum at (N3)	341.9		

Table 2.9. Selected Bond Lengths and Angles for **2.18**.

	Bond Lengths (Å)		
N(1)-C(1)	1.391(5)	N(3)-C(27)	1.488(5)
N(1)-C(14)	1.452(5)	N(4)-C(38)	1.399(5)
N(1)-C(11)	1.471(5)	N(4)-C(40)	1.453(5)
N(2)-C(9)	1.389(5)	N(4)-C(26)	1.480(5)
N(2)-C(14)	1.449(5)	C(14)-C(40)	1.524(5)
N(2)-C(15)	1.451(5)	C(15)-C(16)	1.529(6)
N(3)-C(30)	1.422(5)	C(24)-C(40)	1.522(5)
N(3)-C(26)	1.456(5)	C(15)-C(26)	1.545(5)
	Bond Angles (deg)		
C(1)-N(1)-C(14)	112.0(4)	N(1)-C(14)-C(40)	117.1(4)
C(1)-N(1)-C(11)	124.5(4)	N(2)-C(15)-C(16)	114.3(3)
C(14)-N(1)-C(11)	123.5(4)	N(2)-C(15)-C(26)	110.4(3)
C(9)-N(2)-C(14)	112.4(4)	C(16)-C(15)-C(26)	108.6(3)
C(9)-N(2)-C(15)	122.9(4)	N(3)-C(26)-N(4)	110.7(3)
C(14)-N(2)-C(15)	118.4(3)	N(3)-C(26)-C(15)	116.6(3)
C(30)-N(3)-C(26)	109.4(3)	N(4)-C(26)-C(15)	109.6(3)
C(30)-N(3)-C(27)	118.2(3)	N(4)-C(40)-C(14)	108.6(3)
C(26)-N(3)-C(27)	118.3(3)	N(4)-C(40)-C(24)	114.8(3)
C(38)-N(4)-C(40)	121.9(3)	C(14)-C(40)-C(24)	111.0(3)
C(38)-N(4)-C(26)	110.9(3)	C(2)-C(1)-N(1)	124.2(4)
C(40)-N(4)-C(26)	115.8(3)	C(8)-C(9)-N(2)	125.1(4)
N(2)-C(14)-N(1)	108.6(3)	C(31)-C(30)-N(3)	121.1(4)
N(2)-C(14)-C(40)	109.9(3)	C(37)-C(38)-N(4)	124.7(4)

Table 2.10. Selected Bond Lengths and Angles for **2.20**.

	Bond Lengths (Å)		
Pd(1)-O(1)	2.032(4)	N(1)-C(12)	1.503(7)
Pd(1)-C(11)	2.085(5)	N(2)-C(11)	1.357(6)
N(1)-C(11)	1.353(6)	N(2)-C(9)	1.435(7)
N(1)-C(1)	1.429(6)	N(2)-C(15)	1.473(7)
	Bond Angles (deg)		
O(1)-Pd(1)-C(11)	87.97(18)	Sum at N(2)	359.9
C(11)-N(1)-C(1)	122.9(4)	N(1)-C(11)-Pd(1)	120.8(3)
C(11)-N(1)-C(12)	117.5(4)	N(2)-C(11)-Pd(1)	121.3(4)
C(1)-N(1)-C(12)	119.3(4)	N(1)-C(11)-N(2)	117.9(4)
Sum at N(1)	359.7	Sum at C(11)	360
C(11)-N(2)-C(9)	122.0(4)	C(2)-C(1)-N(1)	123.6(5)
C(11)-N(2)-C(15)	119.2(4)	C(8)-C(9)-N(2)	122.6(5)
C(9)-N(2)-C(15)	118.7(4)		

V. References

1. Bourissou, D.; Guerret, O.; Gabbai, F. P.; Bertrand, G., *Chemical Reviews* **2000,** 100, 39-91.
2. Gleiter, R.; Hoffmann, R., *Journal of the American Chemical Society* **1986,** 90, 1475.
3. Crabtree, R. H., *Journal of Organometallic Chemistry* **2005,** 690, 5451-5457.
4. Arduengo III, A. J.; Harlow, R. L.; Kline, M., *Journal of the American Chemical Society* **1991,** 113, 361-363.
5. Arduengo III, A. J.; Dias, H. V. R.; Harlow, R. L.; Kline, M., *Journal of the American Chemical Society* **1992,** 114, 5530-5534.
6. Xu, G.; Gilbertson, R., *Organic Letters* **2005,** 7, (21), 4605-4608.
7. Herrmann, W. A.; Bohm, V. P. W.; Gstottmayr, C. W. K.; Grosche, M.; Reisinger, C.-P.; Weskamp, T., *Journal of Organometallic Chemistry* **2001,** 617-618, 616-628.
8. Waltman, A. W.; Grubbs, R. H., *Organometallics* **2004,** 23, 3105-3107.
9. Tolman, C. A., *Chemical Reviews* **1977,** 77, 313.
10. Herrmann, W. A.; Schutz, J.; Frey, G. D.; Herdtweck, E., *Organometallics* **2006,** 25, 2437.
11. Lavallo, V.; Canac, Y.; Prasang, C.; Donnadieu, B.; Bertrand, G., *Angewandte Chemie International Edition* **2005,** 44, 5705.
12. Dible, B. R.; Sigman, M. S., *Inorganic Chemistry* **2006,** 45, 8430.
13. Magill, A. M.; Cavell, K. J.; Yates, B. F., *Journal of the American Chemical Society* **2004,** 126, 8717.
14. Amyes, T. L.; Driver, S. T.; Richard, J. P.; Rivas, F. M.; Toth, K., *Journal of the American Chemical Society* 126, 4366.
15. Mercs, L.; Labat, G.; Neels, A.; Ehlers, A.; Albrecht, M., *Organometallics* **2006,** 25, 5648-5656.
16. Alder, R. W.; Blake, M. E.; Chaker, L.; Harvey, J. N.; Paolini, F.; Schutz, J., *Angewandte Chemie International Edition* **2004,** 43, 5896-5911.
17. Bazinet, P.; Yap, G. P. A.; Richeson, D. S., *Journal of the American Chemical Society* **2003,** 125, 13314-13315.
18. Doyle, M. P.; Forbes, D. C., *Chemical Reviews* **1998,** 98, (2), 911-935.
19. Arduengo III, A. J., Rasika Dias, H. V., Calabrese, J. C., Davison, F., *Inorganic Chemistry* **1993,** 32, 1541-1542.
20. Daniele, S., Drost, C., Gehrius, B., Hawkins, S. M., Hitchcock, P. B., Lappert, M. F., Merle, P. G., Bott, S. G., *Journal of the Chemical Society, Dalton Transactions* **2001**, 3179-3188.
21. Chamizo, J. A., Hitchcock, P. B., Jasim, H. A., Lappert, M. F., *Journal of Organometallic Chemistry* **1993,** 451, 89-96.
22. Rohrbach, W. D., Gerson, F., Mockel, R., Boekelheide, V., *Journal of Organic Chemistry* **1984,** 49, 4128-4132.

Chapter 3 —
1,8-Diaminonaphthalene Stabilized Group 13 and 14 Complexes

I. Introduction

A. Germylenes

Expanding the coordination chemistry of the diaminonaphthalene (DAN) ligand beyond carbon to that of similar (isoelectronic or neighbouring) elements of the main group presents the possibility of generating novel organic substrates for oxidation, addition, and insertion reactions,[1] as well as opening up the fundamental chemistry of these elements[2] with this particular ligand system. Drawing inspiration from the previously isolated stable, acyclic germylene, $Ge(N(SiMe_3)_2)_2$,[3] a precedent for successful, nitrogen-based ligands was set. The divalent state of the group 14 main group elements, silicon and germanium, can be stabilized by the σ-acceptor capability of the nitrogen centres.

Molecular structures with delocalized, heterocyclic π-systems increase the stability of divalent germanium compounds, as discussed by theoretical and experimental

results.[4] Many different ligand scaffolds which incorporate the three requirements above, namely nitrogen-based attachment sites, σ-acceptor capability, and heterocyclic π-

Scheme 3.1

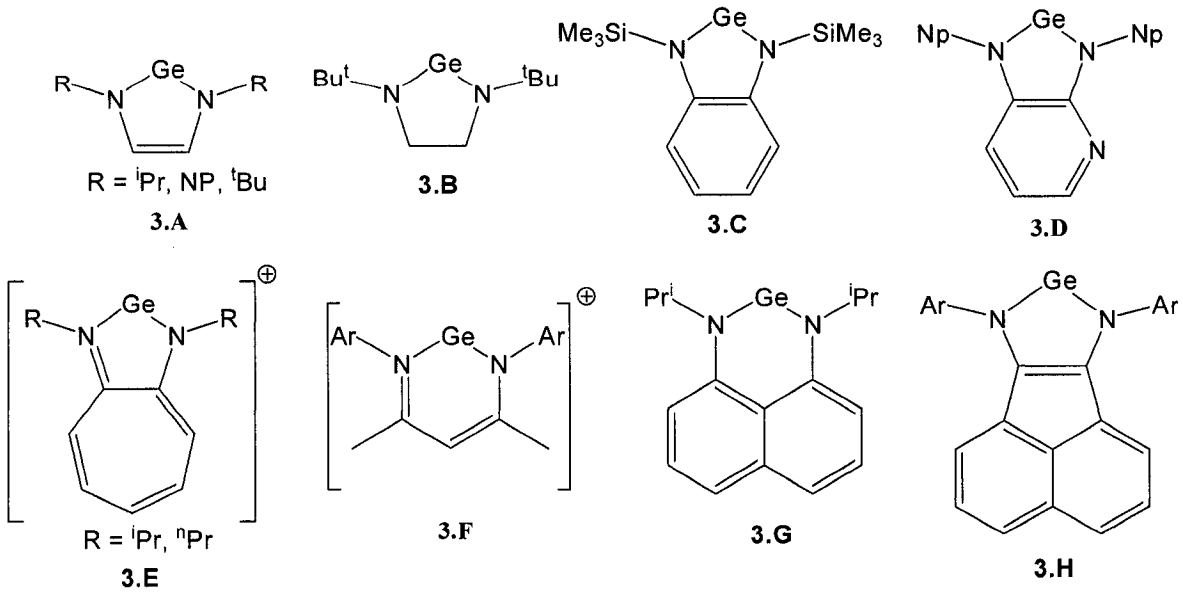

systems, are found in the literature. With the exception of **3.B**, the germylene compounds presented in Scheme 3.1 satisfy these design requirements. The addition of the DAN-based germylene **3.G**,[5] expands the previous scaffolds, namely imidazogermoline-2-ylidine, **3.A**,[6] and its unsaturated, **3.B**,[6] benzo-, **3.C**,[7] and pyrido-, **3.D**,[8] analogues. Cationic species, the aminotroponimidate, **3.E**, and the ketoiminate, **3.F**,[9] have also been isolated. Germylene **3.H** was recently reported based on a 1,2-bis-(arylimino)acenaphthene ligand,[10] an example of a five membered germylene with an extended heterocyclic backbone. It should be noted that until the synthesis of **3.G** was reported, the germylenes presented in the literature were dominated by five-membered or cationic, heterocyclic ligand-stabilized systems.

Among the known literature procedures towards synthesis of germylenes, the most common is the metathetical reaction of the dilithiated ligand with $GeCl_2(dioxane)_2$. Other less common routes include the transamination between the diimine ligand and $Ge(N(SiMe_3)_2)_2$ [5] or reduction of $GeCl_4$ with a suspension of a sodium-ligand amalgam.[10]

B. Silylenes

Silylenes, similar to germylenes, are divalent, dicoordinate silicon species, which are important as reaction intermediates in silicon chemistry and were, until recently, only stable at low temperatures.[11] Shortly after the report of the first stable NHC was published, *vide supra*, the first stable N-heterocyclic silylene was discovered.[12] This species experiences electronic stabilization from the amino groups and steric protection from the pendant groups. At the present time, silylene synthesis is much less developed than that of other group 14 analogues.

Since the first isolation of a thermally stable silylene, several other ligand systems have been discovered which usually, like their germylene analogues, possess a diamino ligand with a π-system. Those without this aromaticity, experience reduced thermal

Scheme 3.2

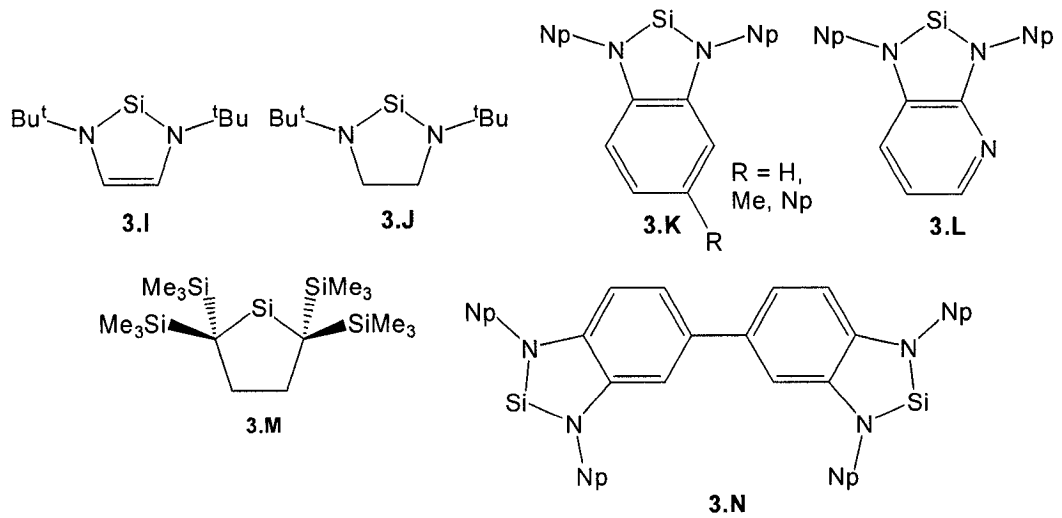

stability. Analogous silylenes to the germylenes previously presented are shown by **3.I** to **3.L**, Scheme 3.2. The first isolable dialkylsilylene, **3.M**,[13] as well as the first disilylene, **3.N**,[14] were recently synthesized.

The importance of steric protection of the silicon centre over that of the electronic stabilization is demonstrated by two examples. The first is from the stability of **3.M**. Although not as thermally stable as **3.I**, **3.K** and **3.L** at elevated temperatures, **3.M** is isolable and characterizable at room temperature, something that could not be accomplished before the pioneering work of West, *et al.*[11] The second is a study performed by Hehrhus,[15] where the pendant groups of **3.K** were changed to ethyl groups. The attempt to generate the silylene from the tetracoordinate dichloride resulted in the

isolation of a stable cyclotetrasilane rather than the free silylene. From these two studies, the great importance of steric protection is uncovered, where the minimum required is tert-butyl or neo-pentyl groups.

Silylene chemistry is still dominated by five-membered ring systems. The only study with a six-membered ring system containing a silylene is a theoretical study of **3.O**, Scheme 3.3.[16] The stability was found to be higher than that of benzene using an isodesmic reaction[‡] in comparison, and was found to have a comparable stability to **3.I.H**.

Scheme 3.3

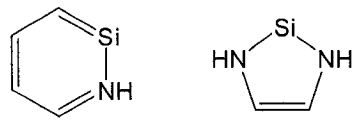

3.O **3.I.H**

Synthesis of N-heterocyclic silylenes follows the same procedure throughout. The dilithiated diamino ligand is combined with $SiCl_4$ to produce the dichloride silylene precursor. This is followed by treatment with a strong reducing agent such as potassium metal, or a sodium/potassium alloy to produce the desired free silylene product.

The inert pair effect exists most strongly for the heavier elements of group 14. As the divalent analogues become lighter when the group is ascended, the stability of these species in this valency decreases. This can be used to explain the synthetic challenges associated with isolating silylenes versus germylenes with an identical ligand structure.

Silylenes and germylenes, the isoelectronic and isolobal equivalent to carbenes, possess the same electronic states. Although silylenes usually exist in the ground state, $^1A_1$, there are two low-lying excited states $^1B_1$ and $^3B_1$, Scheme 3.4. The $^1A_1$ state exists as a singlet whereas the latter two states exist as triplet 1,1-diradicals. These electronic states, as those for the carbene, affect the reactivity of these species.

Scheme 3.4

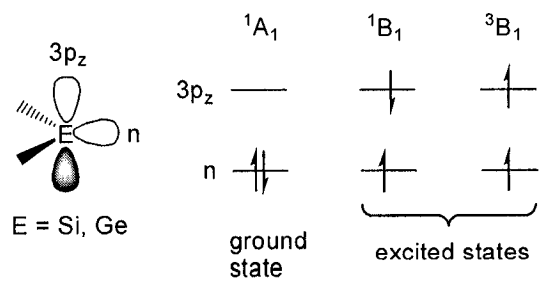

C. Boranes

Fundamental research centered on the main group element boron is much sparser than its group 14 neighbours. Boron is an apt element to study after silicon, since the diagonal relationship between the two elements gives them similar electronic properties and the ability to build isoelectronic compounds. Two studies in the literature target fundamental research towards hydroboranes, **3.P**,[17] and anionic borenes, **3.Q**,[18] Scheme 3.5. Five-membered diamino ligands were chosen to stabilize these boron sites, since the boron atom in both species possesses only six valence electrons, and so needs electronic stabilization which can be provided by the two adjacent nitrogen lone pairs. This ligand

Scheme 3.5

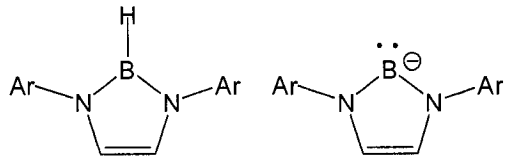

3.P **3.Q**

system also lends aromaticity to the boron-containing ring. A strong parallel can be made between the structures of hydroboranes and the imidazolium salts of the carbene precursors, as well as the anionic borenes with singlet carbenes, silylenes, and germylenes.

The method of choice to generate these complexes involves reduction of the diimine ligand with magnesium metal, followed by reaction with BBr_3. Reduction of the resultant haloborane with $LiAlH_4$ gives the desired hydroborane. The haloborane can be treated with Li(naphthalene) to give the anionic borene.

II. Results and Discussion

Due to the unique properties of the DAN ligand, namely the rigid N-heterocyclic ring system with delocalized π-electrons and the geometric arguments that give the N-substituents a larger steric impact than those on their five-membered analogues, the synthesis of boron, silicon, and germanium complexes stabilized by this ligand were undertaken.

A. Group 14 - DAN compounds

Following the successful synthesis and isolation of carbenes with the DAN ligand providing stabilization, expansion to the synthesis of fundamentally relevant compounds such as silylenes and germylenes was attempted. Following the most successful known literature preparation for silylenes supported by five-membered ring ligand systems, the same procedure was applied to the DAN ligand. Double deprotonation of the diamine ligand with a standard alkyllithium base followed by treatment with $SiCl_4$ at different temperatures ranging from -78 to 110°C in solvents with different polarities ranging from moderate to high, unfortunately did not lead to the successful isolation of the dichloride silylene precursor. Although observations indicated successful deprotonation, the incorporation of the silicon into the heterocyclic ring system at the desired location proved to be exceedingly difficult. Reasons for this can be speculated to be a lower nucleophilicity of our ligand compared to the five-membered variety, or increased steric hindrance from more prominent pendant groups.

Continuing this exploratory effort into the main group chemistry of group 14, the germylene compound stabilized by the dineopentyl DAN ligand was attempted. It was hypothesized that, since the inert pair effect becomes more prominent as group 14 is descended, that the divalent, dicoordinate germanium compound would be more easily accessible than the silylene equivalent. A reliable procedure was employed which was successful in producing germylene complexes as published in the literature. In two separate experiments, the dineopentyl DAN ligand was treated with first two and then three equivalents of *n*-butyllithium, followed by reaction with $GeCl_2(dioxane)_2$.

Although two X-ray quality crystal samples were obtained from these two procedures with identical unit cells, only one structure is shown in Figure 3.1. The common product obtained from these experiments is the protonated germanium chloride complex, **3.1**, shown in Scheme 3.6. The signal for the protonated amine site in the ^1H NMR is present at 5.35 ppm as a broadened singlet. The methylene protons of the neopentyl group on the ligand opposite the NH site are shifted downfield relative to the free ligand, appearing at 3.43 ppm, most likely due to the increased induction from the GeCl unit through the sigma-framework. A second methylene signal is seen as a doublet at 2.81 ppm originating from those protons on the neopentyl group attached to the NH

site. The splitting of this signal is due to the adjacent NH proton, compared to the lack of splitting, concomitant with the lack of this proton at the opposite amine site. The evidence for inequivalent methylene peaks on the ligand suggests no proton exchange occurs on the NMR timescale between the two amine sites of the ligand.

Scheme 3.6

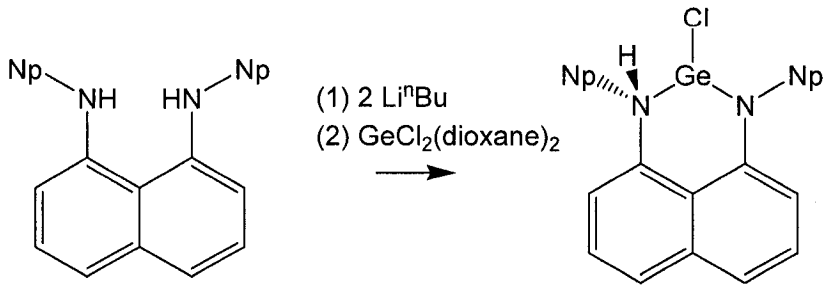

2.6 **3.1** (36%)

This spectroscopic observation is in agreement with the solid state X-ray diffraction data presented. The sums of the three angles at both nitrogen sites are drastically different. The protonated site, N(2), is clearly highly pyramidalized (332.9°), whereas the neutral amine site, N(1), is nearly planar (355.8°). The germanium site is also quite pyramidalized with an angle sum of 279.1°.

B. Group 13 - DAN Compounds

As presented above, the similar electronic properties of silicon and boron, as well as the structural parallels between hydroboranes and perimidinium carbene precursors, generated an interest in building DAN-stabilized, borane complexes. Direct reaction of either the mixed isopropyl-neopentyl DAN or the dineopentyl DAN ligands with the ligand stabilized boron reagent $BH_3{\cdot}S(CH_3)_2$, upon heating generates the desired hydroboranes, Scheme 3.7. A notable shift of the methylene peak in the ^{1}H NMR

Scheme 3.7

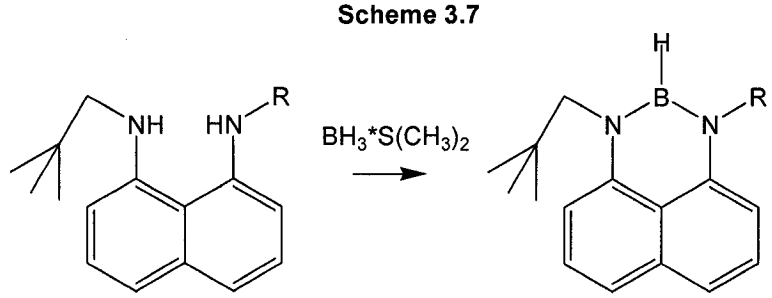

R = ^{i}Pr, **2.4**
R = Np, **2.6**

R = ^{i}Pr, **3.2** (90%)
R = Np, **3.3** (93%)

spectrum belonging to the dineopentyl-DAN stabilized boron complex compared to that of the corresponding perimidinium cation, Scheme 3.8, is observed. The signal appears at 4.13 ppm for cation **2.8**, whereas an upfield shift to 3.31 ppm is observed for the hydroboranes **3.3**. This observation can be explained by the higher electronegativity, and thus sigma induction, of carbon compared to its isoelectronic boron complex equivalent.

Scheme 3.8

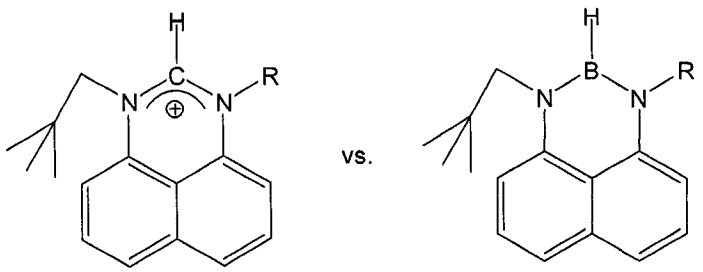

R = ^{i}Pr, **2.8**
R = Np, **2.9**

R = ^{i}Pr, **3.2**
R = Np, **3.3**

Crystals suitable for single crystal X-ray diffraction studies were obtained for both compounds, **3.2** and **3.3**, Figures 3.2 and 3.3. Interestingly, the central angles for both complexes **2.8** (the N-C-N angle) and for **3.2** (the N-B-N angle), are very similar, with values of 124.3(3)° and 121.3(2)° respectively. The small difference in these angles can be justified by the radius contraction across period 2, especially prominent for the cationic carbon centre. These values are considerably larger than those measured for five-membered hydroboranes, having values near 105°.[17] All four carbon centres as shown in Scheme 3.8 have angle sums of 359.9(2)° to 360.1(2)°, showing exceptional planarity. The central N-B bonds, which display an average distance of 1.41 Å, are longer than the corresponding, partially π-conjugated N-C bonds, which display an average distance of 1.32 Å. Finally, the N-$C_{naphthalene}$ bonds are very similar for both **2.8** and **3.2**, displaying average lengths of 1.43 and 1.41 Å respectively, revealing a comparable amount of stabilization required due to π-conjugation from the N-heterocyclic ring.

III. Experimental Section

Preparation of $C_{20}H_{28}ClGeN_2$, protonated germanium chloride complex, Compound **3.1:**

The diamine **2.6** (0.26 g, 0.80 mmol) was deprotonated with $LiCH_3$ (1.05 ml of 1.6 M in ether, 1.6 mmol) in 20 ml of ether and stirred for 1 h. Without workup, $GeCl_2(dioxane)_2$ (0.27 g, 0.80 mmol) was added, creating a red/brown cloudy mixture which was allowed to stir for 18 h. All volatiles were removed before dissolving the remaining solid in hexane. The suspension was filtered through a medium-pore filter frit with celite. The filtrate was concentrated and the red product crystallized at -25°C from hexane (0.11 g, 36%).

^1H NMR (C_6D_6): δ 7.16 (m, 4H, C*H*), 6.69 (m, 2H, C*H*), 5.35 (s br, 1H, N*H*), 3.43 (s, 2H, CH_2), 2.81 (d, 2H, CH_2), 0.86 (s, 18H, CH_3).

Preparation of $C_{20}H_{20}BN_2$, isopropyl neopentyl hydroborane, Compound **3.2:**

The diamine **2.6** (0.500 g, 1.85 mmol) was dissolved in 30 ml of toluene in a Teflon screw cap Schlenk flask. To this was added $BH_3{\cdot}SMe_2$ (0.93 ml, 0.140 g, 1.85 mmol) as a 2 M solution in toluene. The mixture was heated at 70°C for 18 h. The volatiles were removed by vacuum, and the crude, bright orange mixture was crystallized from hexane to give colourless crystals of **3.2** (0.46 g, 90 %), which were dried under vacuum.

Preparation of $C_{20}H_{29}BN_2$, dineopentyl hydroborane, Compound **3.3:**

The diamine **2.4** (0.500 g, 1.67 mmol) was dissolved in 30 ml of toluene in a Teflon screw cap Schlenk flask. To this was added $BH_3{\cdot}SMe_2$ (0.84 ml, 0.127 g, 1.67 mmol) as a 2 M solution in toluene. The mixture was heated at 70°C for 18 h. The volatiles were removed by vacuum, and the crude, bright orange mixture was crystallized from hexane to give colourless crystals of **3.3** (0.48 g, 93%), which were dried under vacuum.

^1H NMR (C_6D_6): without ^{11}B decoupling δ 7.24 (m, 2H, C*H*), 6.62 (m, 1H, C*H*), 3.31 (s, 2H, CH_2), 0.95 (s, 9H, CH_3), the BH peak is not observed.

^{13}C NMR (C_6D_6): δ 143.4 (*C*), 137.6 (*C*), 128.3 (*C*), 126.9 (*C*H), 118.6 (*C*H), 105.2 (*C*H), 58.4, (*C*H_2), 34.1 (*C*), 28.9 (*C*H_3).

Figure 3.1. The molecular structure and atom numbering scheme for compound **3.1.** Hydrogen atoms omitted for clarity. Thermal ellipsoids drawn at 30 % probability.

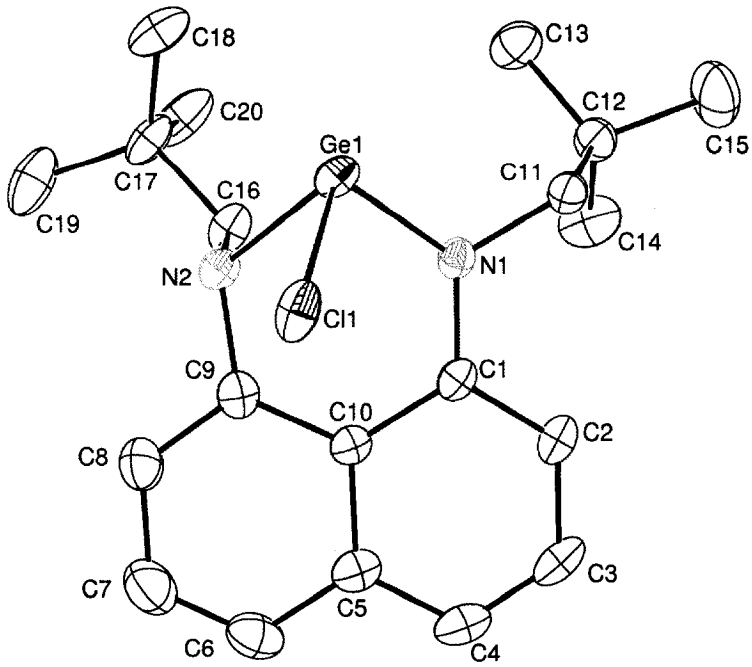

Figure 3.2. The molecular structure and atom numbering scheme for compound **3.2.** Hydrogen atoms not attached to boron omitted for clarity. Thermal ellipsoids drawn at 30 % probability.

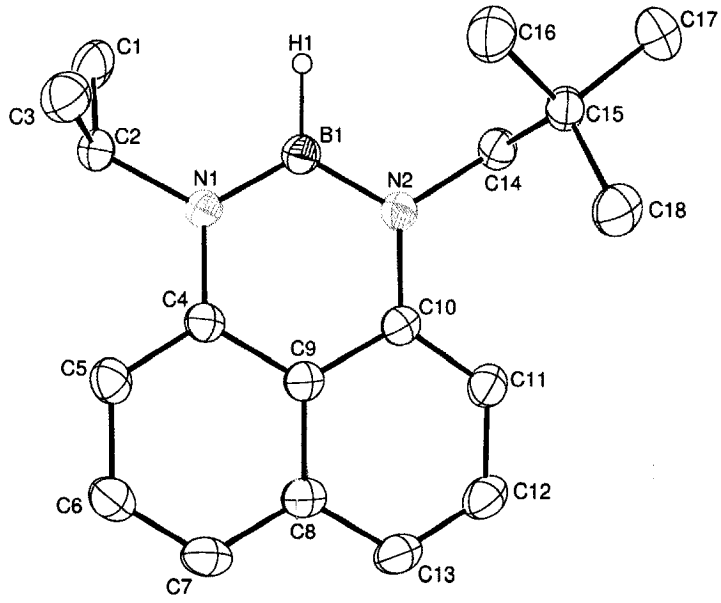

Figure 3.3. The molecular structure and atom numbering scheme for compound **3.3**. Hydrogen atoms not attached to boron omitted for clarity. Thermal ellipsoids drawn at 30 % probability.

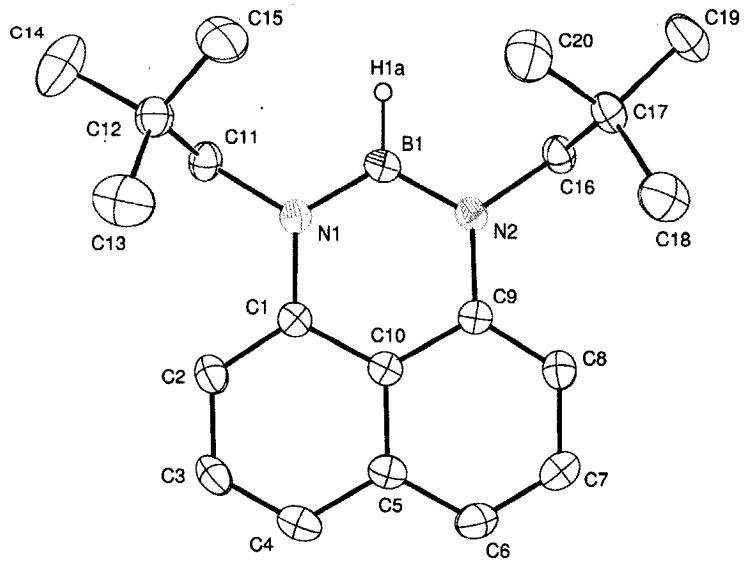

Table 3.1. Selected Crystal Data and Data Collection Parameters for **3.1**, **3.2**, and **3.3**.

	3.1	**3.2**	**3.3**
empirical formula	$C_{20}H_{28}ClGeN_2$	$C_{20}H_{20}BN_2$	$C_{20}H_{29}BN_2$
formula weight	404.48	299.19	308.26
T (K)	200(2)	213(2)	207(2)
wavelength (Å)	0.71073	0.71073	0.71073
crystal system	Triclinic	Monoclinic	Triclinic
space group	P-1	P2(1)/n	P-1
a (Å)	9.4417(13)	8.22(2)	9.510(8)
b (Å)	10.3774(14)	22.91(6)	9.594(8)
c (Å)	12.2495(16)	9.56(2)	11.284(9)
α (deg)	68.435(2)	90	82.104(11)
β (deg)	70.029(2)	114.46(4)	67.101(10)
γ (deg)	74.639(2)	90	78.567(11)
V (Å3)	1035.7(2)	1639(7)	927.6(13)
Z	2	4	2
abs coeff (mm^{-1})	1.611	0.07	0.063
final R indices	R1 = 0.0453	R1 = 0.0424	R1 = 0.0607
	wR2 = 0.0979	wR2 = 0.1024	wR2 = 0.1478

Table 3.2. Selected Bond Distances and Angles for **3.1**.

	bond lengths (Å)		
Ge(1)-N(1)	1.888(4)	N(1)-C(11)	1.479(6)
Ge(1)-N(2)	2.093(4)	N(2)-C(9)	1.455(7)
Ge(1)-Cl(1)	2.3332(15)	N(2)-C(16)	1.511(6)
N(1)-C(1)	1.408(6)		
	bond anges (deg)		
N(1)-Ge(1)-N(2)	87.26(17)	Sum at N(1)	355.8
N(1)-Ge(1)-Cl(1)	101.11(13)	C(9)-N(2)-C(16)	109.5(4)
N(2)-Ge(1)-Cl(1)	90.75(12)	C(9)-N(2)-Ge(1)	112.5(3)
Sum at Ge(1)	279.12	C(16)-N(2)-Ge(1)	110.9(3)
C(1)-N(1)-C(11)	119.7(4)	Sum at N(2)	332.9
C(1)-N(1)-Ge(1)	124.6(3)	C(2)-C(1)-N(1)	121.7(5)
C(11)-N(1)-Ge(1)	111.5(3)	C(8)-C(9)-N(2)	116.2(5)

Table 3.3. Selected Bond Distances and Angles for **3.2**.

	bond lengths (Å)		
B(1)-N(2)	1.406(3)	N(1)-C(2)	1.483(3)
B(1)-N(1)	1.411(4)	N(2)-C(10)	1.408(4)
N(1)-C(4)	1.406(4)	N(2)-C(14)	1.472(3)
	bond anges (deg)		
N(2)-B(1)-N(1)	121.3(2)	B(1)-N(2)-C(14)	118.9(2)
C(4)-N(1)-B(1)	120.16(16)	C(10)-N(2)-C(14)	121.38(15)
C(4)-N(1)-C(2)	117.3(2)	Sum at N(2)	359.98
B(1)-N(1)-C(2)	122.4(2)	C(5)-C(4)-N(1)	123.07(17)
Sum at N(1)	359.89	C(11)-C(10)-N(2)	123.2(2)
B(1)-N(2)-C(10)	119.7(2)		

Table 3.4. Selected Bond Distances and Angles for **3.3**.

	bond lengths (Å)		
B(1)-N(1)	1.410(4)	N(1)-C(11)	1.472(3)
B(1)-N(2)	1.412(4)	N(2)-C(9)	1.403(3)
N(1)-C(1)	1.409(3)	N(2)-C(16)	1.475(3)
	bond angles (deg)		
N(1)-B(1)-N(2)	121.7(3)	B(1)-N(2)-C(16)	118.1(2)
C(1)-N(1)-B(1)	119.9(2)	Sum at N(2)	359.9
C(1)-N(1)-C(11)	120.6(2)	C(2)-C(1)-N(1)	123.3(3)
B(1)-N(1)-C(11)	119.3(2)	N(1)-C(1)-C(10)	117.6(2)
Sum at N(1)	359.8	C(8)-C(9)-N(2)	123.5(2)
C(9)-N(2)-B(1)	120.2(2)	N(2)-C(9)-C(10)	117.4(2)
C(9)-N(2)-C(16)	121.6(2)		

V. References

1. Barrau, J., Escudi, J., Stage, J., *Chemical Reviews* **1990,** 90, 283.
2. Lappert, M. F., *Main group Materials Chemistry* **1994,** 17, 183.
3. Harris, D. H., Lappert, M. F., *Journal of the Chemical Society, Chemical Communications* **1974**, 895.
4. Driess, M., Grutzmacher, H., *Angewandte Chemie International Edition* **1996,** 35, 828.
5. Bazinet, P., Yap, G. P. A., Richeson, D. S., *Journal of the American Chemical Society* **2001,** 123, 11162-11167.
6. Herrmann, W. A., Denk. M., Behm, J., Scherer, W., Kilngan, F. R., Bock, H., Solouki, B., Wagner, M., *Angewandte Chemie, International Edition* **1992,** 31, 1485.
7. Pfeiffer, F., Maringgele, W., Noltemeyer, M., Meller, A., *Chem. Ber.* **1988,** 122, 245.
8. Kuh, O., Lonnecke, P., Heinike, J., *Polyhedron* **2001,** 20, 2215.
9. Ayers, A. E., Klapotke, T. M., Dias, H. V. H., *Inorganic Chemistry* **2001,** 40, 1000.
10. Fedushkin, I. L., Skatova, A. A., Chukakova, V. A., Khvoinova, N. M., Baurin A. Y., *Organometallics* **2004,** 23, 3714-3718.
11. Haaf, M., Schmedake, T. A., West, R., *Accounts of Chemical Research* **2000,** 33, 704-714.
12. Denk, M., Lennon, R., Hayashi, R., West, R., Haaland, A., Belyakov, H., Verne, P., Wagner, M., Metzler, N., *Journal of the American Chemical Society* **1994,** 116, 2691-2692.
13. Kira, M., Iwamoto, T., Ishida, S., *Bull. Chem. Soc Jpn.* **2007,** 80, (2), 258-275.
14. Hill, N. J., West, R., *Journal Of Organometallic Chemistry* **2004,** 689, 4165-4183.
15. Gehrus, B., Hitchcock, P., Zhang, L., *Angewandte Chemie International Edition* **2004,** 43, 1124.
16. Veszpremi, T., Nyulaszi, L., Karpati, T., *Journal of Physical Chemistry A* **1996,** 100, 6262.
17. Segwa, Y., Yamashita, M., Nozake, K., *Science* **2006,** 314, 112-115.
18. Weber, L., Schnieder, M., Lonnecke, P., *Journal of the Chemical Society, Dalton Transactions* **2001**, 3459-3464.

‡Isodesmic Reaction: A reaction (actual or hypothetical) in which the types of bonds that are made in forming the products are the same as those which are broken in the reactants. [Taken from the IUPAC Compendium of Chemical Terminology, 2nd Edition, 1997.]

Chapter 4 — Guanidines and Propiolamidines, Catalytic Synthesis and Characterization

I. Introduction

Guanidines are an attractive target for biological, medicinal and organic chemists due to their nitrogen-rich nature and fundamental prevalence in biological and pharmaceutical compounds.[1, 2] Alkylguanidines are protonated in aqueous solution due to their strong basicity ($pK_a = 13$). This protonated form, though soluble in water, is not so in organic solvents, presenting a synthetic hurdle. Typically, the reaction of an amine with an electrophilic guanylating reagent is the common synthetic route.[3-5] A common class of substrates has been discovered to work well for these syntheses, which incorporate the displacement of a leaving group from a protected carbodiimide-equivalent. Widespread leaving groups are *t*-butylcarbamate (Boc) and carboxybenzylcarbamate (Cbz), Scheme 4.1. Beyond their expected function, these

carbamate-protecting groups activate the reagent to reaction with amine, thus allowing direct synthesis of protected guanidines. Despite this, the need for a protecting group restricts the guanidine products to mono- or N,N-disubstituted guanidines. Because of these synthetic factors, alternate, more efficient, and catalytic methods for creating guanidines from the large variety of amines commercially available is invaluable.

Scheme 4.1

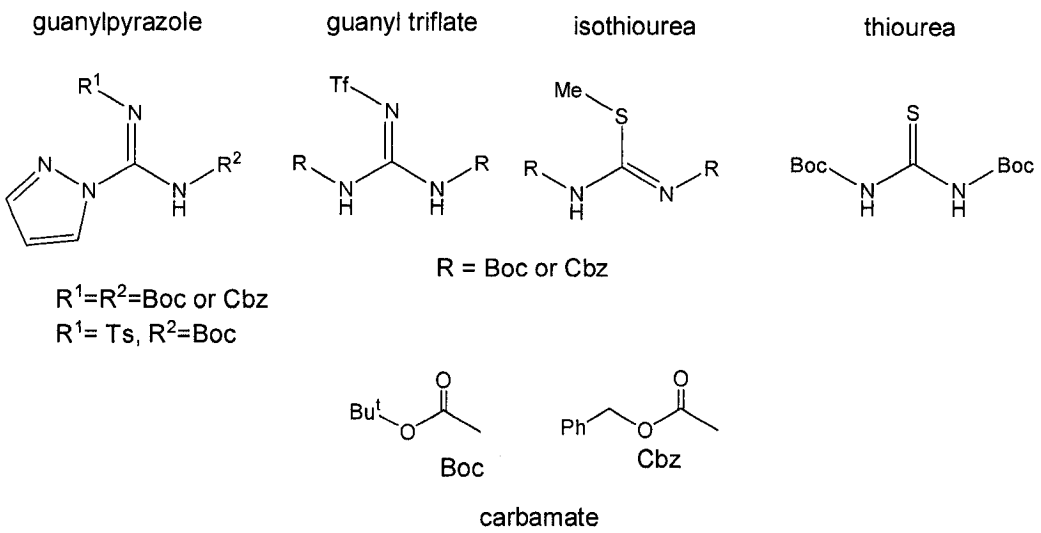

In their anionic form, guanidines and amidines are growing to become a versatile group of ligands in main group and transition metal chemistry. Their simplicity as organic molecules and their tunability in terms of their steric and electronic features make them an attractive class of ligands.[6] These species exhibit a high degree of resonance, Scheme 4.2. More specifically, for the deprotonated guanidinate molecule, three major resonance contributions apply and can be used to describe its reactivity. Amidinates are similar in structure, but have one less nitrogen bonded to the central carbon, thus reducing the number of resonance structures. Phophaguanidinates possess three resonance structures, though only one has a minor contribution due to weak C-P π-overlap.

Although many possible binding modes exist between guanidinates and group 1 metals, three of the ones most commonly seen in the literature are described in Scheme 4.3. Common features among them include a metal to guanidine ratio of 1:1, as dictated by a parallel charge ratio, rather than steric restrictions, and the presence of basic ligands. In the case of lithium, the presence of basic ligands is extremely common since they are

Scheme 4.2

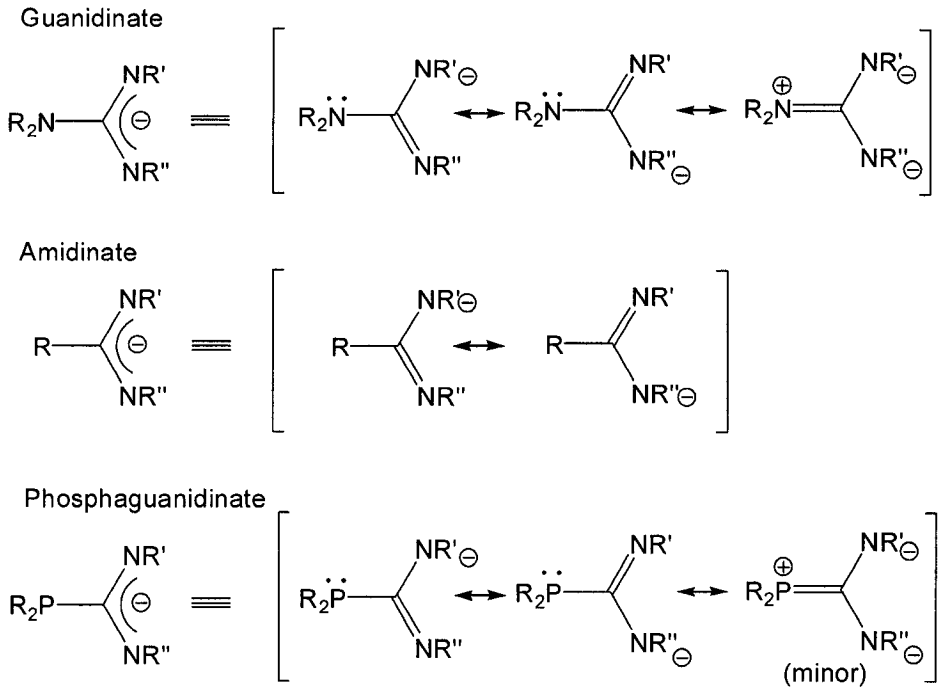

necessary to satisfy the hard Lewis acidity and unsaturated coordination sphere of the metal centre. In the case of **4.A** and **4.C**, the guanidine ligand is coordinated in a bidentate κ^2-*N*-mode to one metal centre, whereas for **4.B**, each guanidine is coordinated in a μ,κ^1,κ^1-mode to two metal centres.

Scheme 4.3

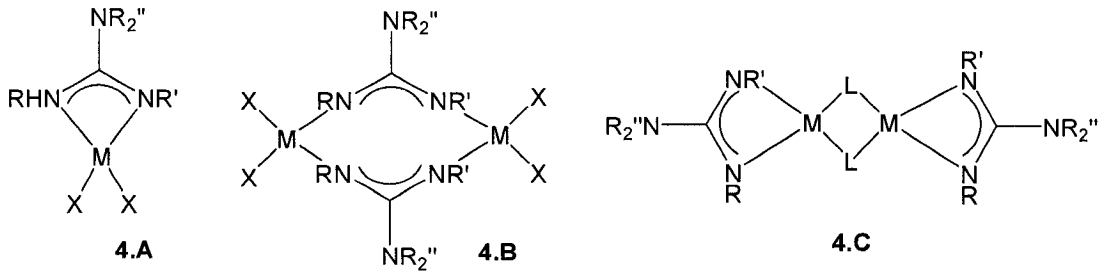

4.A **4.B** **4.C**

X = monodentate, basic ligand
L = bidentate, basic ligand
M = Group 1 metal

Synthesis of guanidines as ligands was first reported for a group of complexes of tetramethylguanidine at divalent Co, Cu, Zn, Pd, Ni, and trivalent Cr centres.[7] Since this initial publication, the general synthetic approach to synthesizing neutral guanidines has been through the non-catalytic reaction of lithium-amide with carbodiimide, which is

quenched by a proton source.[6] This route is a successful way to produce tri- and tetra-substituted guanidines.

In chelating to any metal, guanidines bind preferentially by the imine site with the strongest electron withdrawing group. The reason for this is that it creates a strongly nucleophilic site, which is more likely to bind a strong Lewis acid than a weaker site would. Pendent groups which fit this description include nitro groups, aromatic groups, and aromatic groups with σ-withdrawing substituents in the ortho or para positions, among other σ-withdrawing groups.

Amidines which are non-symmetric depend on the positioning of the double bond and substituents relative to each other. The strength of an amidine-metal interaction can be influenced by these different forms. The methods of interconversion between each form is either C-N bond rotation or C=N isomerisation, Scheme 4.4.

Scheme 4.4

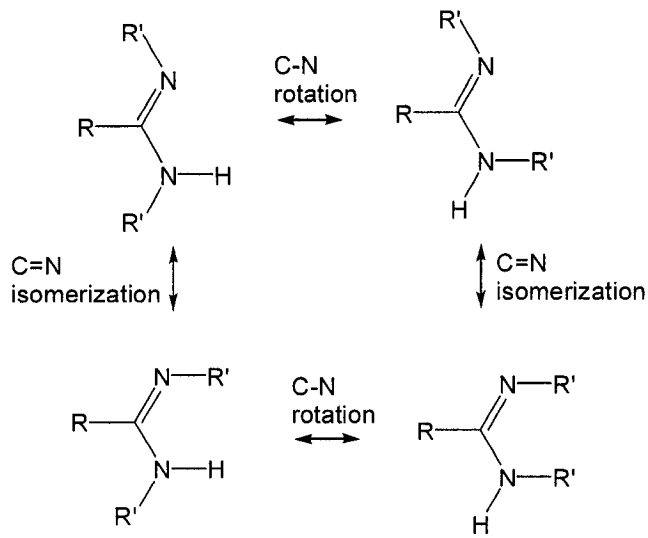

Two historically relevant routes in synthesizing amidines include one with and one without a silyl migration pathway. The first involves a reaction between benzonitriles and lithium bis(trimethylsilyl)amide. During this reaction a trimethylsilyl group migrates between two nitrogen centers and generates a more symmetrical N,N'-disilylated benzamidinate lithium intermediate. The final step towards the product involves quenching the lithio-salt with water to give the neutral amidine product.[8] The second method proceeds through a lithium-alkyl or -aryl reagent and carbodiimide

reaction. This reaction is not catalytic, and has the option of synthesizing amidines with extremely bulky terphenyl pendant groups.[9]

Formation of amidines and guanidines at metal centres is relatively rare in comparison to the lithiated organic synthesis. The reactions occur on chemically varied metal centres, including hard Co(III), soft Pt(II), and intermediate Os(III) centres, Scheme 4.5.[10] To form the amidine-metal complex, reaction of a metal-nitrile complex with an amine through a metal arginine interaction occurs. N-N cleavage with migration of the metal centre from carbon to nitrogen is the proposed mechanism. The analogous reaction occurs with metal-cyanamide complexes to yield the guanidine complex.

Scheme 4.5

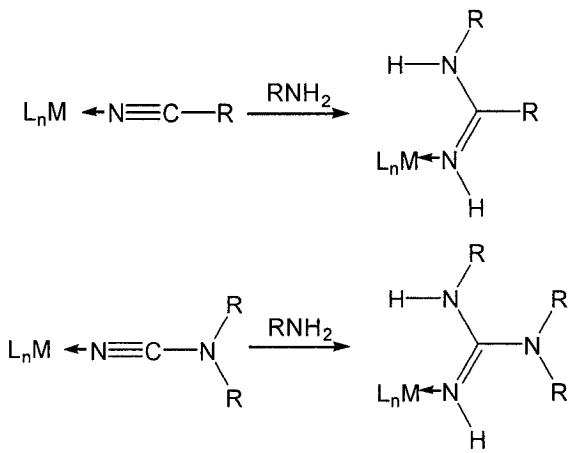

Historically, IR spectroscopy was the most common technique used to determine if a guanidine or amidine was present. For example, diarylacetamidines, $R_2NC(Me)=NR$, have absorptions in the ranges 3100-3300 cm^{-1} and 1620 cm^{-1} for υ(N-H) and υ(C=N), respectively. ^{13}C NMR spectroscopy is used to characterize the presence of a CN_2 core in amidines in the range of 140-150 ppm or a CN_3 core for guanidines in the range of 150-160 ppm. Single crystal X-ray diffraction data can be used to characterize the organic ligand species or metal-ligand complex. Changes in bond lengths and geometries upon coordination to a metal can be examined. The C=N imine bond can be distinguished from the C-N amine bond of a complexed guanidine since they have bond lengths of approximately 1.28 and 1.38 Å respectively. The degree of delocalization of the C=N π-bond within guanidines and amidines can be assessed by finding the Δ_{CN} value from the solid state structure, where Δ_{CN} = d(C-N) – d(C=N).[6] A fully delocalized system would give a value of 0 Å, whereas a localized system has a value up to 0.1 Å.

It is proposed that amidines are stronger electron donors to metals than their guanidine cousins. Since donation to the metal occurs through the sigma framework of the ligand, one with more electron density available will be able to donate more strongly to a metal. Because of the electron withdrawal from the nitrogen situated in the backbone of the guanidine ligand, amidines should have a slightly higher capacity for electron donation relative to guanidine ligands.

The only known example of lithium catalysis for the purpose of assembling guanidine and amidine ligands was recently published by our group.[11] The method used parallels that were accomplished by much more complex catalysts such as half-sandwich yttrium alkyl complexes[12, 13] or Ti- and V-imido catalysts.[12, 14] In this chapter, an efficient method for the guanylation of aromatic and heterocyclic amines with carbodiimides is presented which uses the catalyst precursor lithium hexamethyldisilazide, a commercially available compound. This method can be extended to the realm of C-C bond formation by adding terminal alkynes to carbodiimides to form propiolamidines. For both of these syntheses, a common intermediate is proposed which contains a rare staircase structure containing the main group metal, lithium.

II. Results and Discussion

Although aliphatic amines will react directly with carbodiimides to give guanidines, even with prolonged heating at 140°C, without a catalyst, aromatic amines will not react with diisopropylcarbodiimide in an amount detectable by ^{1}H NMR. Previous studies by our group in the pursuit of a commercially applicable catalyst for the guanylation of aromatic amines with carbodiimides produced a Ti-imido complex, $[\{(Me_2N)C(N^iPr)_2\}_2Ti{=}N(2,6\text{-}Me_2C_6H_3)]$.[14] These reactions typically required temperatures in excess of 100°C to achieve good guanidine yields.

The commercially available base, $LiN(Si(CH_3)_3)_2$, when added to a reaction mixture of aromatic amines with various carbodiimides in a catalytic amount is also able to stimulate guanylation. The amount of lithium catalyst required ranges from 2 mol % in most cases, to 5 mol % in some. Most products are isolated in 18 h at room temperature, in contrast with the much higher temperature required (100°C) for the Ti-

imido catalyst described previously. Isolation of the pure guanidine product in good yield is achieved simply by crystallization.

The results for the guanylation reactions of aromatic amines with carbodiimides at room temperature are presented and summarized in Table 4.1 and Scheme 4.5. For entries with a basic, nucleophilic amine with negligible steric hindrance, entries 1-4, guanidines **4.1-4.4**, quantitative yields were obtained with 2 mol % catalyst in 18 h or less at room temperature. These examples all contain neutral or σ-electron withdrawing substituents in the *ortho-* or *para*-positions, which act to reduce the pK_a of the amine, increasing its nucleophilicity as well as its reactivity towards the carbodiimide centre. Direct contrast between *ortho-* and *para*-substituted amines is provided by entries 4 and 5 using methoxyanilines. Evidence of the effect of steric hindrance of the amine toward the yield can be measured directly, as the ortho substituted amine requires heating to 100°C to achieve a quantitative yield, guanidines **4.4** and **4.5**.

Scheme 4.5

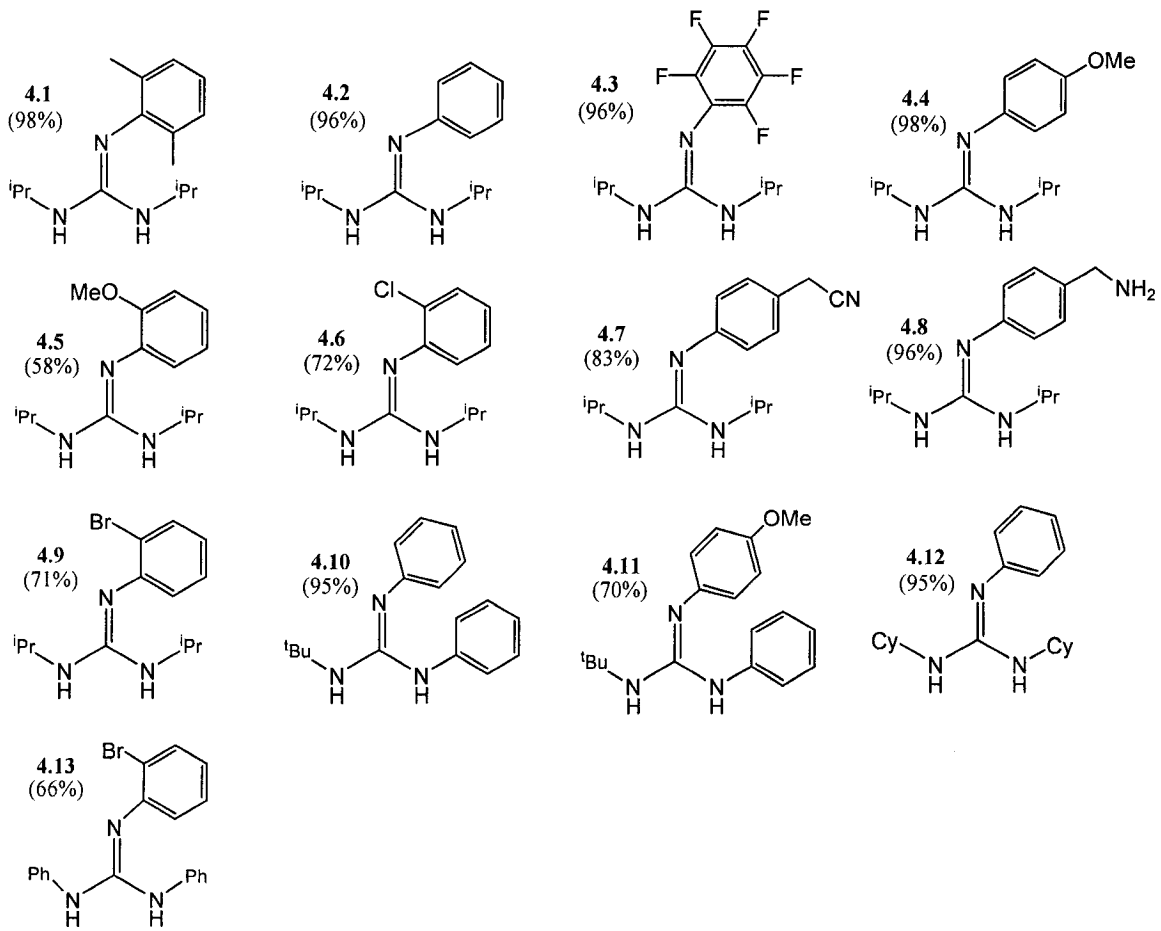

Applying a halogen substitution in the ortho position of the aniline substrate, entries 6 and 9, provides an opportunity to study their effect on this guanylation reaction. Though both reactions were resistant to providing quantitative yields under initial conditions, elevating the catalyst loading to 5 mol % or elevating the temperature to 100°C produced moderately good yields for both cases, producing guanidines **4.6** and **4.9**. The stronger acidity of the chloro-substituted aniline substrate is a likely explanation for why this substrate did not require a temperature elevation, whereas the bromo-substituted substrate did. Relatively neutral para-benzyl substituted aniline substrates, entries 7 and 8, guanidines **4.7** and **4.8**, produced high to quantitative yields, likely for similar reasons as the first 4 entries: lack of steric hindrance around the basic site of the substrate combined with strong nucleophilicity of the deprotonated aniline site. Despite the fact that the substrate for entry 8 contains two amine sites, one aryl and one benzyl, it achieves high chemoselectivity with a quantitative guanylation at the aryl-amine site, the more strongly nucleophilic site. The results discussed here show the potential of alkali metal catalyzed guanylation with mild conditions.

Table 4.1. Room-Temperature Guanylation of Aromatic Amines with Carbodiimide Using $LiN(Si(CH_3)_3)_2$.

Entry	$Ar'NH_2$	RNCNR'	product	yield (%)[a,c]
1	$2,6\text{-}Me_2C_6H_3NH_2$	^{i}PrNCN^{i}Pr	**4.1**	98[b] (90)
2	$C_6H_5NH_2$	^{i}PrNCN^{i}Pr	**4.2**	96
3	$C_6F_5NH_2$	^{i}PrNCN^{i}Pr	**4.3**	96
4	$p\text{-}MeOC_6H_4NH_2$	^{i}PrNCN^{i}Pr	**4.4**	98
5	$o\text{-}MeOC_6H_4NH_2$	^{i}PrNCN^{i}Pr	**4.5**	58; (96)[d]
6	$o\text{-}ClC_6H_4NH_2$	^{i}PrNCN^{i}Pr	**4.6**	(72)[e]
7	$p\text{-}NCCH_2C_6H_4NH_2$	^{i}PrNCN^{i}Pr	**4.7**	83
8	$p\text{-}H_2NCH_2C_6H_4NH_2$	^{i}PrNCN^{i}Pr	**4.8**[f]	96 (90)
9	$o\text{-}BrC_6H_4NH_2$	^{i}PrNCN^{i}Pr	**4.9**	(71.2)[d]
10	$p\text{-}MeOC_6H_4NH_2$	^{t}BuNCNPh	**4.10**	0;95[e,g] (90)[e,g]
11	$C_6H_5NH_2$	^{t}BuNCNPh	**4.11**	70[e,g] (62.0)[e,g]
12	$p\text{-}MeOC_6H_4NH_2$	CyNCNCy	**4.12**	(95)[e]
13	$o\text{-}BrC_6H_4NH_2$	PhNCNPh	**4.13**	(66)[d]

[a] All reactions were run for 18 h with 2 mol % catalyst unless otherwise specified. Yields determined by integration of ^{1}H NMR relative to the internal standard of $1,3\text{-}(MeO)_2C_6H_4$. [b] Quantitative yield was obtained after 5 h. [c] Isolated yields given in parentheses. [d] Yield for reaction at 100°C. [e] Reaction run with 5 % catalyst loading. [f] Product is $H_2NCH_2(C_6H_4)N{=}C(^i PrNH)_2$. [g] Reaction run with addition of 10 mol % TMEDA.

For each case of guanylation mentioned for entries 1-9, the applied diisopropylcarbodiimide has moderate steric protection and relatively neutral induction from its pendant groups. This was shown to have little effect on the yield of guanylation reactions compared to the sterics and electronics of the aniline substrate. For the last four entries of Table 4.1, the substitution of the carbodiimide is varied to explore its affect on the catalytic guanylation reaction.

Asymmetric carbodiimides can introduce a higher level of specialization to the resulting guanidine. In contrast to the symmetric diisopropylcarbodiimide employed previously, the *t*-butyl-phenylcarbodiimide applied in entries 10 and 11 provides the opportunity to generate a guanidine with three unique pendant groups, guanidines **4.10** and **4.11**. However, the electrophilicity of the central carbodiimide carbon is decreased due to the phenyl group, making it necessary to increase the catalyst loading and reactivity. Tetramethylethylenediamine (TMEDA), added to the reaction in 10 mol % is proposed to break up clustering, modulating the coordination sphere of the alkali metal, which is commonly seen with lithium compounds, and to increase the separation of the lithium and its anionic base, thus increasing the Lewis acidity of the main group centre. This effect is prominently seen in entry 10 with a para-methoxy substituted aniline substrate: under initial conditions, no observable product is obtained, however a near-quantitative yield is obtained with the application of higher catalyst loading and TMEDA. Applying the same conditions to entry 11, a simple aniline substrate, generates a noticeably lower guanylation yield, likely due to the somewhat lower nucleophilicity of the deprotonated amine site in comparison to that employed in the previous entry. The final two entries, 12 and 13, producing guanidines **4.12** and **4.13**, describe reactions that use a dicyclohexylcarbodiimide and its aromatic analogue, diphenylcarbodiimide. Both entries 12 and 13 show decreased electrophilicity in direct comparison with their diisopropylcarbodiimide analogues, entries 4 and 9 respectively, through their need for increased catalyst loading or increased reaction temperature to obtain quantitative or moderate yields.

It should be noted that the π-bond of the CN_3 core of the guanidine is always represented along the C-N bond adjacent to the most electron withdrawing pendant group. This is due to the increased acidity of this nitrogen centre, which corresponds to

an increased electrophilicity. Because of this, the extra electron density available resides preferentially at this site. However, due to the high mobility of protons, especially in a polar solvent, some resonance of the π-bond in the CN_3 core is proposed to exist.

Spectral characterization by NMR and mass spectroscopy provides evidence for the product structures as shown in Scheme 4.5. Guanidines synthesized from symmetric, aliphatic carbodiimides, **4.1**-**4.9** and **4.12**, produce one broad, singlet peak for the two NH signals in a very small range of chemical shifts in the ^{1}H NMR, namely 3.5-3.6 ppm. The broadness of the peak suggests a certain amount of proton exchange within the molecule, and the lack of two signals implies a plane of symmetry, consistent with the placement of the C-N double bond as discussed previously.

Guanidines synthesized from a mixed aliphatic-aromatic carbodiimide, **4.10** and **4.11**, produce two broad peaks, each integrating for one proton relative to other peaks in the ^{1}H NMR. These peaks are shifted downfield relative to those mentioned previously, showing expression in the range of 3.6 to 5.5 ppm, likely due to the increased nucleophilicity of the nitrogen centres on which they reside. The existence of two signals is expected, as no plane of symmetry can be proposed. Consistent with other guanidines previously characterized by ^{13}C NMR in the literature, the central guanidine carbon, a relatively deshielded, electrophilic, sp^2-hybridized centre produces a strongly shifted signal in the range of 146 to 154 ppm for compounds **4.1**-**4.12**.

Guanidine **4.13**, synthesized from a symmetric aromatic carbodiimide, presents an exception to the above series, by possessing three aromatic substituents. This has a noticeable effect on the ^{1}H NMR shift of the NH peaks, producing one broad signal at 6.00 ppm. Similar to those guanidines with two aromatic pendant groups, a third aromatic group further increases the nucleophilicity of the nitrogen centres, causing the corresponding NH peak to migrate further downfield. A parallel shift is observed for the core carbon in the ^{13}C NMR, which resonates at 158 ppm.

Expanding the scope of the amine substrates to heterocyclic amines and amides was done to further understand the substrate tolerance of this catalysis, and to broaden the functionality of the resulting guanidines for enhanced applicability. Scheme 4.6 describes the synthesis of guanidines **4.14** from a heterocyclic amine, 2,3-dimethylindole,

and guanidine **4.15** from an aliphatic amide, acetamide. Both guanylations required the addition of TMEDA to enhance the reactivity of the alkali metal catalyst.

Scheme 4.6

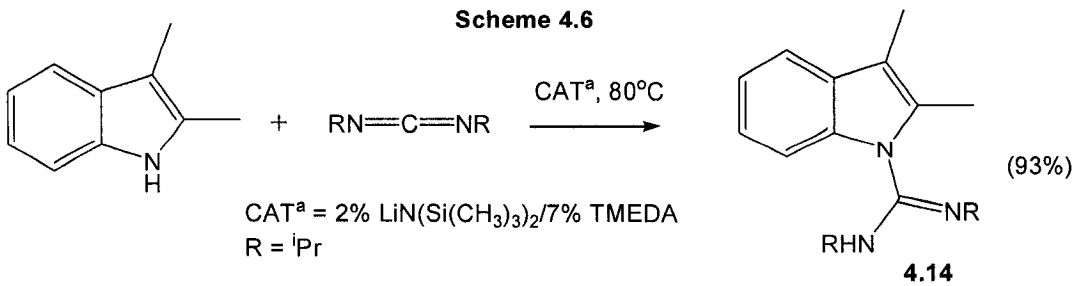

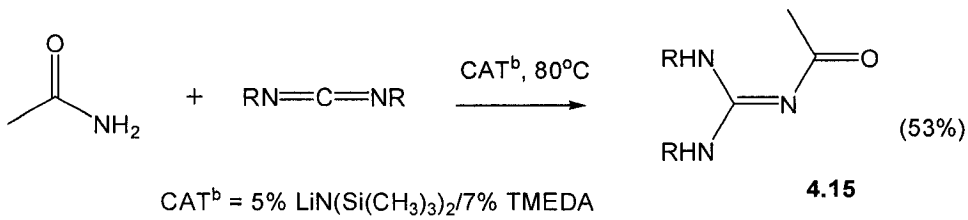

An amine functionality within a heterocyclic ring produces a near quantitative yield of the desired guanidine product. Due to the reactivity of the indole ring at the 2- and 3-positions, a substrate with protection at those sites was necessary. The resulting guanidine, **4.14**, possesses two noteworthy signals by ^{1}H and ^{13}C NMR: one signal for the NH species, which is sharpened in comparison to those for guanidines **4.1-4.13**, and one signal for the core carbon at 141.4 ppm. The signal for the NH proton is sharpened, likely due to restricted π-delocalization. The reduced nucleophilicity of the heterocyclic amine substrate, as well as the presence of two other aliphatic pendant groups, causes a lessening of the downfield shift of the core carbon. The application of an amide functionality as a substrate, one that possesses π-conjugation next to the amine site, reducing its nucleophilicity, is tolerated by this catalysis, producing guanidine **4.15**. Although the catalyst loading is increased, the yield is low in comparison to aromatic substrates, due to the reduced substrate nucleophilicity. No signal is observed in the ^{1}H NMR for the NH protons because of an extremely high degree of exchange. Interestingly, at 156.7 ppm, the central CN_3 core carbon is not the most strongly downfield shifted carbon in the ^{13}C NMR due to strong π-delocalization and resonance through the α-carbonyl function.

An analogous reaction which applies a terminal alkyne rather than an amine or amide as the substrate should follow a similar route to form a related compound, a

Scheme 4.7

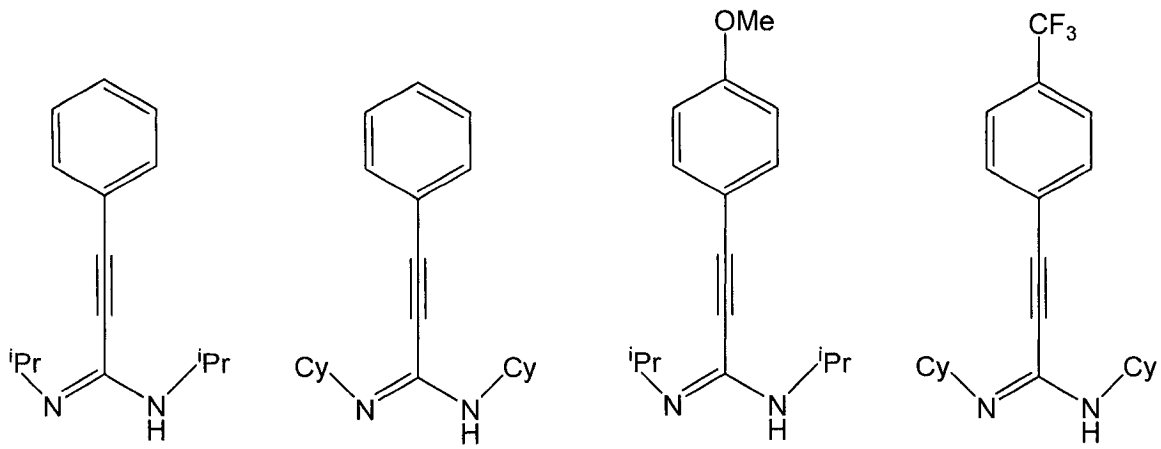

4.16 (98%) **4.17** (95%) **4.18** (96%) **4.19** (96%)

propiolamidine. It is proposed that a catalytic C-C bond formation process will function in a similar fashion to the C-N bond formation. Reaction of symmetric, aliphatic carbodiimides with different terminal alkyne substrates was performed at 80°C and the minimum time to reach a quantitative yield was determined, Scheme 4.7, Table 4.2.

Table 4.2. Catalytic Formation of Propiolamidines by Addition of Alkyne to Carbodiimide at 80°C Using 5 mol % $LiN(Si(CH_3)_3)_2$.

entry	carbodiimide	alkyne	product (time)[a]	yield (%)[b]
1	^{i}PrNCN^{i}Pr	HCCPh	**4.16** (120)	95
2	CyNCNCy	HCCPh	**4.17** (90)	95
3	^{i}PrNCN^{i}Pr	HCC(*p*-C_6H_4OMe)	**4.18** (90)	93
4	CyNCNCy	HCC(*p*-$C_6H_4CF_3$)	**4.19** (75)	95

[a] Reaction time in minutes is given in parentheses. [b] Yields determined by integration of 1H NMR relative to internal standard of 1,3-$(MeO)_2C_6H_4$.

A mechanism for the guanylation and propiolamination reactions discussed above is proposed in Scheme 4.8. During the guanylation mechanism, deprotonation of the aromatic amine, heterocyclic amine, or amide by the alkali metal acid generates a lithium amide. This species undergoes carbodiimide insertion to give a κ^2-chelating lithium guanidinate complex. Transfer protonation between the lithium guanidinate and a remaining amine or amide produces the guanidine product and regenerates the lithium

Scheme 4.8

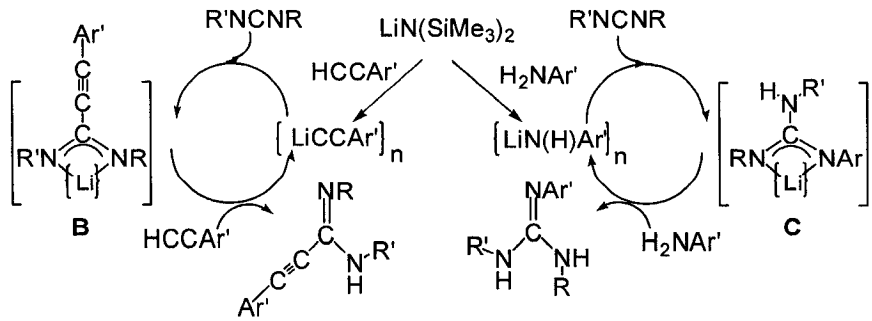

amide catalytically active species. The transfer protonation step is driven by the stronger basicity of the guanidine in comparison to the amide anion. A parallel mechanism can be drawn for the production of propiolamidines from terminal alkynes. Deprotonation of the terminal alkyne by the alkali metal acid generates the active catalyst species, a terminal acetylide, which undergoes carbodiimide insertion to give the κ^2-chelating lithium propiolamidinate complex. This is followed by a transfer protonation step, which produces the propiolamidine product and regenerates the active lithium acetylide catalyst species.

Evidence to support this mechanism is shown through trapped intermediates in the synthesis of products **4.2** and **4.5**, Scheme 4.9, and their single crystal X-ray

Scheme 4.9

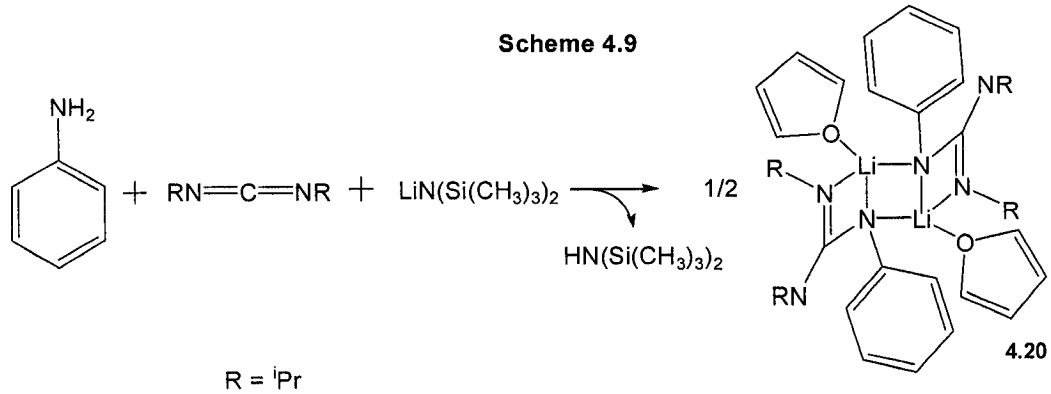

structures in Figures 4.3 and 4.4. Selected bond lengths and angles are given in Tables 4.3 and 4.4. These figures represent the first known structures of their kind stabilized by traditional, non-heterocyclic, guanidinate ligands. Both **4.20** and **4.21** show proof of carbodiimide insertion into the amidolithium species $C_6H_5(H)NLi$ and *o*-$MeOC_6H_4(H)NLi$, respectively. Both of these intermediates show three fused, four-membered rings in a folded-ladder arrangement. This fused ring system possesses a *cis*-arrangement around the Li_2N_2 metallacyclic core. Both structures have a common coordination geometry, displaying a μ-η^1,η^2-bridging mode for each guanidinate species across the dimeric core. Trapped, dimeric intermediate **4.20** has two basic ligands, THF molecules, included in the structure to quench the strong Lewis acidity of the lithium centres. The strategic orientation of the methoxy group in the ortho position relative to the amine in intermediate **4.21** provides a chelating interaction to satisfy the Lewis acidity of the lithium centres of this dimeric molecule, removing the need to trap solvent molecules for this purpose.

Two staircase structures presented recently by Coles, *et al*,[15, 16] show a dimeric structure for lithium guanidinate-derivative complexes characterized by X-ray crystallography in the solid state, which contain a central Li_2N_2 core. The first structure, $Li(Ph_2PC\{N^iPr\}_2)(THF)_2$, in addition to the two lithium phosphaguanidinate complexes joined together to form the dimeric structure, two coordinated THF molecules are included, and are necessary to satisfy the Lewis acidity of the lithium centres, Figure 4.1. Phosphorous, due to its weaker π-overlap with elements from the second row caused by size and energy differences, creates a phosphaguanidinate ligand with weaker resonance interactions. This in turn can cause the phosphaguanidinate to be a weaker donating ligand than its corresponding guanidinate, creating the need for additional basic coordination ligands. The central staircase structure of this molecule, composed of three fused, four-membered rings, embodies a centrosymmetric dimer. The phosphaguanidinate ligand is bound as a μ-κ^1-N,κ^2-N-bridge between two lithium centres.

An interesting point to note is the choice of coordination site made by the phosphaguanidines when coordinating to the lithium centre. Although with guanidines, the most basic site, which is normally bound to one or more aromatic group, is

coordinated to the metal centre, this is not the case with this structure. The diaryl stubstituted phosphine site is not the most basic, rather it is the aliphatic substituted nitrogen site. Finally, this complex was isolated as an intermediate in the formation of phosphaguanidines, as well as monomeric lithium and aluminium phosphaguanidinate complexes.

Figure 4.1. A lithium phosphaguanidinate dimer complex, $Li(Ph_2PC\{N^iPr\}_2)(THF)_2$.[15]

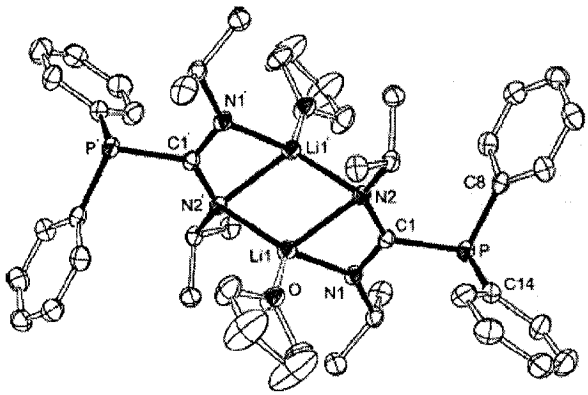

The second structure which contains a central Li_2N_2 core stabilized by guanidinate-derived ligands is $[Li(hpp)(hppH)]_2$, where hpp describes 1,3,4,6,7,8-hexahydro-2H-pyrimido[1,2-a]pyrimidine and hppH describes the protonated version, 2H-pyrimido[1,2a]pyrimidine. The heterocyclic backbone of the guanidinate ligands provides both structural rigidity and an extended π-system. The orientation of the three fused, four-membered rings, which make up the staircase core possess a different orientation than the structure presented previously: the staircase is oriented in a trans-configuration across the Li_2N_2 core. This is likely directed by the extra hppH ligands, orienting themselves to act as both a base to quench the Lewis acidity of the lithium centre through an η^1-connection to the backbone, and to offer an intramolecular hydrogen bond across the Li_2N_2 core. This compound was also isolated as an intermediate in assembling a lithium framework to encapsulate a peroxide dianion.

Figure 4.2. A Li_2N_2 core is stabilized by guanidinate-derived ligands $[Li(hpp)(hppH)]_2$, where hpp is 1,3,4,6,7,8-hexahydro-2H-pyrimido[1,2-a]pyrimidine and hppH is 2H-pyrimido[1,2a]pyrimidine.[16]

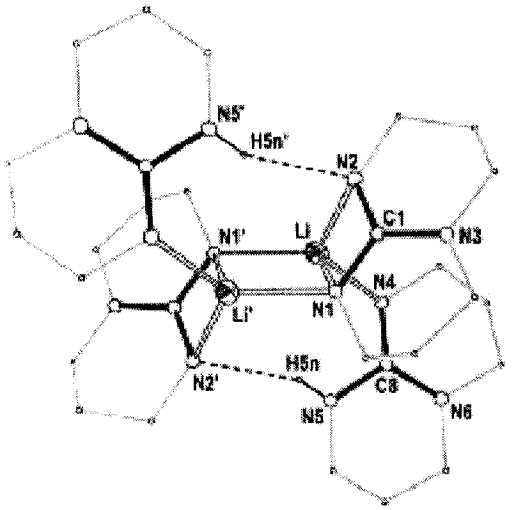

A wide variety of amines were employed to demonstrate the scope of electronic and steric features of the nucleophiles which can be tolerated by the reaction system. Combining these organic bases with a Lewis acid main group centre will induce activation of the amine substrate. The resulting species can then be coupled with carbodiimides to produce guanidines. Employing this route to guanidines creates a facile method to generate specific, substituted guanidines. This route can also be extended to the production of propiolamidines by changing the substrate from an amine to a terminal alkyne. This creates an atom-economical route to both of these species.

III. Experimental Section

General: Unless otherwise noted, all manipulations were carried out in either a nitrogen filled glovebox or under nitrogen using standard Schlenk techniques. Reaction solvents were sparged with nitrogen then dried by passage through column of activated alumina using an apparatus purchased from Anhydrous Engineering. Deuterated benzene, and dichloromethane were purchased from Aldrich Chemical Company. Deuterated benzene and dichloromethane were dried over activated molecular sieves for 3 days. $LiN(SiMe_3)_2$ was purchased from Aldrich Chemical Company and purified by crystallization from cold hexane. The following chemicals were purchased from Aldrich Chemical Company and used without further purification: 1,8-diaminonaphthalene, $LiAlH_4$, triethylamine,

pivaloylchloride, sodium sulfate, triethyl orthoformate, formic acid, NaOH, NaCl, p-toluenesulfonic acid, anhydrous chlorobenzene, 1,8-naphthalic anhydride, lithium bromide, and phosphorous (III) bromide. Celite 545 was purchased from Aldrich Chemical Company and dried at 110°C for 3 days. Molecular sievers (4Å, beads, 4-8 mesh) were purchased from Aldrich Chemical Company and activated by drying under vacuum at 120°C for 5-6 hours. ^{1}H and ^{13}C NMR spectra were run on either a Varian Gemini 200 MHz, a Bruker Advance 300 MHz, a Varian Inova 500 MHz or a Bruker Advance 500 MHz spectrometer using the residual protons of the deuterated solvent for reference. Elemental analyses were performed by Guelph Chemical Laboratories Ltd., Guelph, ON or in the Department of Chemistry at the University of Ottawa on a Perkin-Elmer PE CHN 4000 elemental analysis system.

General procedure for the guanylation of aromatic amines with diisopropylcarbodiimide to yield compounds 4.1-4.9 using $LiN(SiMe_3)_2$. A vial was loaded with 0.1 equiv $LiN(SiMe_3)$, 40 equiv carbodiimide, 40 equiv arylamine, 10 equiv 1,3-dimethoxybenzene or $(Me_3Si)_2O$ as a internal standard, and approximately 0.5 mL C_6D_6. The solution was subsequently transferred to a sealed-NMR tube and single pulse ^{1}H NMR spectrum was obtained. The tube was left at room temperature until all the aniline was consumed. The conversion and yield were determined by comparison of the integration of the internal standard and a well-resolved signal for the product guanidine. The identity of the guanidine product was further confirmed by GC-MS.

Preparation of N-2,6-dimethylphenyl,N',N''-diisopropylguanidine, Compound **4.1:**
Yield: 98%; Isolated yield 90%. This compound has been reported previously.

N-phenyl,N',N''-diisopropylguanidine, Compound **4.2:**
Yield: 96%. This compound has been reported previously.

N-pentafluorophenyl,N',N''-diisopropylguanidine, Compound **4.3:**
Yield: 96%. This compound has been reported previously.

N-*p*-methoxyphenyl,N',N''-diisopropylguanidine, Compound **4.4:**

Yield: 98%. This compound has been reported previously.

N-*o*-methoxyphenyl,N',N''-diisopropylguanidine, Compound **4.5:**

Yield: 58% (25 °C); Isolated yield: 96% (100 °C). This compound has been reported previously.

N-*o*-chlorophenyl,N',N''-diisopropylguanidine, Compound **4.6:**

A solution of 2-chloroaniline (1.184 g, 9.281 mmol), diisopropylcarbodiimide (1.169 g, 9.281 mmol) and $LiN(SiMe_3)_2$ (78 mg, 0.464 mmol) in 40 mL of toluene was allowed to stir at room temperature for a period of 18 hours. The volatiles were removed *in vacuo* to afford a white solid, which was further purified by 10 mL of ether washing. Yield: 1.818 g (72.3%).

^{1}H NMR ($CDCl_3$): 1.17 (d, 12H, CH_3), 3.56 (br, 2H, NH), 3.76 (sept, 2H, CH), 6.89 (d, 2H, C_6H_4), 7.12 (t, 1H, C_6H_4), 7.32(d, 1H, C_6H_4).

^{13}C NMR ($CDCl_3$): 23.3 (CH_3), 43.4 (*C*H), 122.6, 125.2, 127.5, 129.9, 128.3, 137.0 (C_6H_4), 150.0 (CN_3).

HRMS ESI (*m/z*): calcd for $C_{13}H_{18}N_3Cl$, 253.1346; found 253.1326.

N-*p*-cyanomethylphenyl-N',N''-diisopropylguanidine, Compound **4.7:**

Yield: 83.3%. This compound has been reported previously.

N-*p*-aminomethylphenyl-N',N''-diisopropylguanidine, Compound **4.8:**

Yield: 96%; Isolated yield: 90%.

^{1}H NMR ($CDCl_3$): 1.12 (d, 12H, CH_3), 1.34 (br, 2H, CH_2), 3.55 (br, 2H, CH), 3.70 (br, 2H, NH), 3.75(br, 2H, NH), 6.78 (d, 2H, C_6H_4), 7.09 (d, 2H, C_6H_4).

^{13}C NMR ($CDCl_3$): 23.3 (CH_3), 43.2 (*C*H), 46.1 (CH_2), 123.5, 128.8, 136.1, 148.8 (C_6H_4), 150.2 (CN_3).

HRMS ESI (*m/z*): calcd for $C_{14}H_{24}N_4$, 248.2001; found 248.2023.

N-*o*-bromophenyl-N',N''-diisopropylguanidine, Compound **4.9:**

Isolated yield: 71.2% (100°C). This compound has been reported previously.

N-*t*-butyl, N'-*p*-methoxyphenyl,N"-phenylguanidine, Compound **4.10:**

A solution of p-anisidine (0.042 g, 0.344 mmol), 1,3-*t*-butyl-phenylcarbodiimide (0.050 g, 0.287 mmol), $LiN(SiMe_3)_2$ (~2 mg, 0.014 mmol) and TMEDA (~ 7 mg, 0.057 mmol) in 0.5 mL of C_6D_6 was loaded into an NMR tube at room temperature and allowed to react for 18 hours. Yield of the reaction was determined to be 95.0 % by comparison of the integration of the internal standard and a well-resolved signal for the product guanidine. The product was further purified by removing the solvent *in vacuo* to afford a white solid. The solid was redissolved in 2 mL of ether and hexane (50:50 by volume) and was cooled to –30 °C to afford a white solid, which was isolated by filtration (isolated yield: 90 %).

^{1}H NMR ($CDCl_3$): 1.42 (s, 9H, *t*-Bu), 3.77 (s, 3H, OCH_3), 3.97 (br, 1H, NH), 5.50 (br, 1H, NH), 6.85 (br, 3H), 6.95 (br, 4H), 7.25 (br, 2H).

^{13}C NMR ($CDCl_3$): 29.4 (CH_3), 51.0 (CMe_3), 55.4 (OCH_3), 114.6, 121.4, 121.8, 123.1, 123.6, 125.6, 129.3, 147.3 (aromatic carbon), 150.2 (CN_3).

HRMS ESI (*m/z*): calcd for $C_{18}H_{23}N_3O$, 297.1841; found 297.1857.

Preparation of N,N'-diphenyl-N"-*t*-butylguanidine, Compound **4.11:**

A solution of aniline (0.055 g, 0.597 mmol), 1,3-*t*-butyl-phenylcarbodiimide (0.096 g, 0.551 mmol), $LiN(SiMe_3)_2$ (~5 mg, 0.0300 mmol) and TMEDA (0.010 g, 0.0862 mmol) in 0.5 mL of C_6D_6 was loaded into an NMR tube at room temperature and allowed to react for 18 hours. Yield of the reaction was determined to be 70.0 % by comparison of the integration of the internal standard and a well-resolved signal for the product guanidine. The product was further purified by removing the solvent *in vacuo* to afford a white solid. The solid was redissolved in 2 mL of ether and hexane (50:50 by volume) and was cooled to –30 °C to afford a white solid, which was isolated by filtration (isolated yield : 62 %).

^{1}H NMR ($CDCl_3$): 1.46 (s, 9H, *t*-Bu), 3.98 (br, 1H, NH), 3.59 (br, 1H, NH), 6.90-7.40 (m, 10H, C_6H_5).

^{13}C NMR ($CDCl_3$): 29.4 (CH_3), 51.1 (CMe_3), 121.6, 122.9, 123.4, 129.3 (C_6H_5), 146 (CN_3).

HRMS ESI (*m/z*): calcd for $C_{17}H_{21}N_3$, 267.1735; found 267.1853.

N-*p*-methoxyphenyl-N',N''-dicyclohexylguanidine, Compound **4.12:**

A solution of *p*-anisidine (0.370 g, 2.99 mmol), dicyclohexylcarbodiimide (0.615 g, 2.99 mmol) and $LiN(SiMe_3)_2$ (~25 mg, 0.15 mmol) in 15 mL of toluene was allowed to stir at room temperature. A white cloudy solution was observed after 18 hour of the reaction time. The reaction mixture was dried *in vacuo* to afford a white solid, which was washed with 10 mL ether. Yield: 0.934g (95%).

^{1}H NMR ($CDCl_3$): 0.95-1.45 (m, 10H, CH_2 of cyclohexyl), 1.60 (m, 6H, CH_2 of cyclohexyl), 1.97 (m, 4H, CH_2 of cyclohexyl), 3.37 (br, 2H, CH of cyclohexyl), 3.59 (br, 2H, NH), 3.73(s, 3H, OCH_3), 6.75(d, 4H, C_6H_4).

^{13}C NMR ($CDCl_3$): 24.9 (CH_2), 25.6 (CH_2), 33.8 (CH_2), 50.1 (*C*H), 114.5, 124.3, 143.2, 150.5 (C_6H_4), 154.4 (CN_3).

HRMS ESI (*m/z*): calcd for $C_{20}H_{32}H_4$, 329.2467; found, 329.2484.

N-*o*-bromophenyl-N,N''-diphenylguanidine, Compound **4.13:**

A solution of 2-bromoaniline (0.886 g, 5.149 mmol), 1,3-diphenylcarbodiimide (1.000 g, 5.149 mmol) and $LiN(SiMe_3)_2$ (0.062 g, 0.257 mmol) in 40 mL of toluene was heated in a thick-walled glass vessel with a Teflon stopcock at 100 °C for 18 hours. The resulting brown cloudy solution was dried *in vacuo* to afford a brown oil. The brown oil was triturated with 20 mL of hexane and was stirred for 2 days. The volatiles were removed *in vacuo* and the residue was dissolved in 10 mL of ether. The saturated solution was cooled to -30 °C to afford a white solid, which was isolated by filtration. Yield: 1.240 g (65.7%).

^{1}H NMR ($CDCl_3$): 6.0 (br, 2H, NH), 6.85 (m, 1H, aromatic H), 7.05 (m, 2H, aromatic H), 7.31 (m, 10H, aromatic H), 7.56 (m, 1H, aromatic H).

^{13}C NMR ($CDCl_3$): 121.4, 122.2, 123.0, 123.7, 128.3, 129.3, 129.5, 132.7, 132.8, 144.8 (aromatic carbon), 158.0 (CN_3).

HRMS ESI (*m/z*): calcd for $C_{19}H_{16}BrN_3$, 365.0317; found, 365.0536.

Preparation of guanidine 4.14 from 2,3-dimethylindole:

A solution of 2,3-dimethylindole (0.050 g, 0.34 mmol), diisopropylcarbodiimide (0.036 g, 0.29 mmol), $LiN(SiMe_3)_2$ (~2 mg, 0.01 mmol) and TMEDA (~10 mg, 0.02 mmol) in 0.5 mL of C_6D_6 was loaded into an NMR tube at room temperature and allowed to react for 18 hours. Yield of the reaction was determined to be 92.7 % by comparison of the integration of the internal standard and a well-resolved signal for the product guanidine. The product was further purified by removing the solvent *in vacuo* to afford a white solid. The solid was redissolved in 2 mL of ether and hexane (50:50 by volume) and was cooled to –30 °C to afford a white solid, which was isolated by filtration (Isolated yield: 70.0 %).

^{1}H NMR ($CDCl_3$): 0.85 (d, 3H, CH_3), 0.95 (d, 3H, CH_3), 1.05 (d, 3H, CH_3), 1.15 (d, 3H, CH_3), 2.12 (s, 3H, CH_3), 2.20 (s, 3H, CH_3), 3.08 (br, 2H, CH), (4.10, 1H, NH), 7.19 (d, 1H, C_6H_4), 7.21 (d, 1H, C_6H_4), 7.33 (m, 1H, C_6H_4), 7.56 (m, 1H, C_6H_4).

^{13}C NMR ($CDCl_3$): 8.6 (CH_3), 10.1 (CH_3), 23.7 (CH_3, broad), 24.4 (CH_3, broad), 45.1 (*C*H, broad), 47.6 (*C*H, broad), 107.8, 109.6, 118.0, 120.0, 121.5, 128.4, 130.7, 135.1 (*C* on indole ring), 141.4(CN_3).

HRMS ESI (*m/z*): calcd for $C_{17}H_{25}N_3$, 271.2048; found, 271.2083.

Preparation of 4.15 from acetamide and diisopropylcarbodiimide:

A solution of acetamide (0.500 g, 9.08 mmol), diisopropylcarbodiimide (1.430 g, 11.35 mmol), $LiN(SiMe_3)_2$ (~76 mg, 0.454 mmol) and TMEDA (0.263 g, 2.270 mmol) in 45 mL of toluene was loaded into a sealed Schlenk flask and heated at 80 °C for 18 hours. The product was further purified by removing the solvent *in vacuo* to afford a white solid. The solid was redissolved in 10 mL of ether and was cooled to –30 °C to afford a white solid, which was isolated by filtration. Yield of the reaction was determined to be 53.0 % (0.850g).

^{1}H NMR ($CDCl_3$): 1.14 (d, 12H, CH_3), 1.99 (s, 3H, $COCH_3$), 3.80 (br, 2H, CH).

^{13}C NMR ($CDCl_3$): 21.9 (CH_3), 27.3 ($COCH_3$), 41.5 (*C*H), 156.7 (CN_3), 183.1 ($COCH_3$).

HRMS ESI (*m/z*):calcd: $C_9H_{19}N_3O$, 185.1528; found 185.1522

General procedure for the catalytic addition of terminal alkyne to carbodiimide to yield compounds 4.16-4.19 using $LiN(SiMe_3)_2$. A vial was loaded with 1 equiv $LiN(SiMe_3)_2$ (5 mg, 0.030 mmol) 20 equiv 1,3-diisopropylcarbodiimide (75 mg, 0.598 mmol), 20 equiv alkyne, 10 equiv 1,3-dimethoxybenzene or toluene as a internal standard and approximately 0.5 mL C_6D_6. The solution was subsequently transferred to a sealed-NMR tube and single pulse ^1H NMR spectrum was obtained. The tube was left at 80 °C until all the substrates were consumed. The conversion and yield were determined by comparison of the integration of the internal standard and a well-resolved signal for the product propiolamidines. The identity of the propiolamidines **4.16-4.19** were further confirmed by GC-MS. Compounds **4.16-4.19** have been reported previously in Zhang, W.-X.; Nishiura, M.; Hou, Z. *J. Am. Chem. Soc.* **2005,** *127*, 16788.

Crystal Structure Determination

A suitable crystal was selected, mounted on a glass fiber with viscous oil and cooled to the desired data collection temperature. Data were collected on a Bruker AX SMART 1k CCD diffractometer using one of the following scan sequences: for triclinic unit cells, 4 sets of 650 frames (0.3 deg in ω) at 0, 90, 180, 270 degrees in Φ; all other cells (which are not triclinic) - 3 sets of 650 frames (0.3 deg in ω) at 0, 120, 240 degrees in Φ. Unit-cell parameters were determined from 60 data frames collected at different sections of the Ewald sphere. Semi-empirical absorption corrections based on equivalent reflection were applied (Blessing, R., *Acta Cryst.*, **1995**, A51, 33-38).

To solve the structures, the software package ShelXTL 6.14 was used. The Structure was solved by direct methods, completed with difference Fourier synthesis and refined with full-matrix least-squares procedures based on F^2. All non-hydrogen atoms were refined with anisotropic displacement parameters. All hydrogen atoms were treated as idealized contributions. All scattering factors are contained in the SHEXTL 5.10 program library (Sheldrick, G. M., Bruker AXS, Madison, WI, 1997). Any minor disorders were omitted from the final structure.

IV. Figures and Tables

Figure 4.3. Molecular structures and partial atom-numbering scheme for $[Li(^{i}PrNC(HN^{i}Pr)N(C_6H_5)(THF)]_2$, **4.20**. Thermal ellipsoids are shown at 30 % probability. Hydrogen atoms have been omitted for clarity. Two symmetric units are shown.

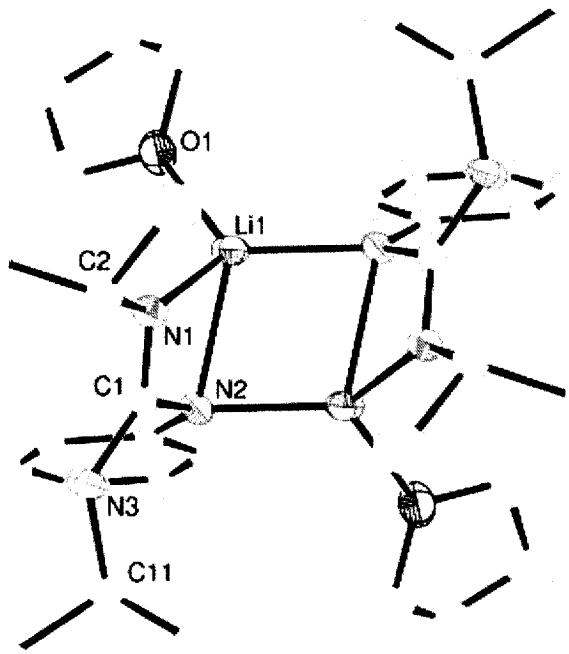

Figure 4.4. Molecular structures and partial atom-numbering scheme for $[Li(^{i}PrNC(HN^{i}PR)N(C_6H_4OMe)]_2$, **4.21**. Thermal ellipsoids are shown at 30 % probability. Hydrogen atoms have been omitted for clarity.

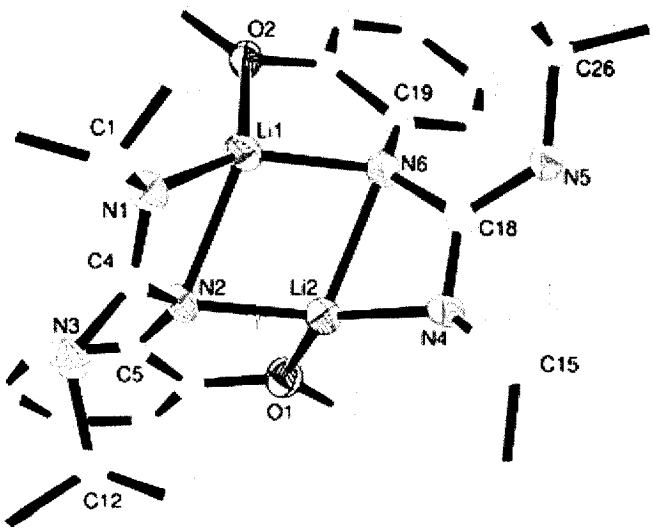

Table 4.3. Selected bond lengths and angles for **4.20**.

	Bond Lengths (Å)		
Li(1)-O(1)	1.919(6)	N(1)-C(1)	1.307(4)
Li(1)-N(1)	2.016(6)	N(2)-C(1)	1.388(4)
Li(1)-N(2A)	2.031(6)	N(3)-C(1)	1.369(4)
Li(1)-N(2)	2.204(6)		
	Bond Angles (deg)		
O(1)-Li(1)-N(1)	111.7(3)	C(1)-N(2)-C(5)	119.5(3)
O(1)-Li(1)-N(2A)	116.8(3)	C(1)-N(2)-Li(1A)	111.3(3)
N(1)-Li(1)-N(2A)	127.4(3)	C(5)-N(2)-Li(1A)	127.8(3)
O(1)-Li(1)-N(2)	121.8(3)	C(1)-N(2)-Li(1)	84.1(2)
N(1)-Li(1)-N(2)	65.39(19)	C(5)-N(2)-Li(1)	119.3(2)
C(1)-N(1)-C(2)	120.6(3)	N(1)-C(1)-N(3)	124.6(3)
C(1)-N(1)-Li(1)	94.2(3)	N(1)-C(1)-N(2)	115.9(3)
C(2)-N(1)-Li(1)	145.1(3)	N(3)-C(1)-N(2)	119.5(3)

Table 4.4. Selected bond lengths and angles for **4.21**.

	Bond Lengths (Å)		
Li(1)-O(2)	1.952(7)	Li(2)-N(6)	2.159(8)
Li(1)-N(1)	1.982(8)	N(1)-C(4)	1.298(5)
Li(1)-N(6)	1.993(8)	N(2)-C(4)	1.374(5)
Li(1)-N(2)	2.189(8)	N(3)-C(4)	1.390(5)
Li(2)-O(1)	1.928(8)	N(4)-C(18)	1.299(5)
Li(2)-N(4)	1.947(8)	N(5)-C(18)	1.379(5)
Li(2)-N(2)	1.974(8)	N(6)-C(18)	1.390(5)
	Bond Angles (deg)		
O(2)-Li(1)-N(1)	137.6(4)	C(4)-N(2)-C(5)	121.3(3)
O(2)-Li(1)-N(6)	83.3(3)	C(4)-N(2)-Li(2)	125.5(4)
N(1)-Li(1)-N(6)	137.1(4)	C(5)-N(2)-Li(2)	109.9(3)
O(2)-Li(1)-N(2)	124.9(4)	C(4)-N(2)-Li(1)	83.2(3)
N(1)-Li(1)-N(2)	65.9(2)	C(5)-N(2)-Li(1)	133.7(3)
N(6)-Li(1)-N(2)	104.9(3)	Li(2)-N(2)-Li(1)	73.8(3)
C(4)-N(1)-C(1)	120.6(4)	N(1)-C(4)-N(2)	116.9(4)
C(4)-N(1)-Li(1)	94.0(3)	N(1)-C(4)-N(3)	123.4(4)
C(1)-N(1)-Li(1)	143.6(4)	N(2)-C(4)-N(3)	119.7(4)

V. References

1. Mori, A., Cohen, B. D., Lowenthal, A., Guanidines: Historical, Biological, Biochemical and Clinical Aspects of the Naturally Occurring Guanidino Compounds. **1985**.
2. Mori, A., Cohen, B. D., Koide, H, Eds., Guanidines 2: Further Explorations of the Biological and Clinical Significance of Guanidino Compounds. **1987**.
3. Yu, Y., Ostresh, J. M., Houghten, R. A., *Journal of Organic Chemistry* **2002,** 67, 3138.
4. Linton, B. R., Carr, A. J., Orner, B. P., Hamilton, A. D., *Journal of Organic Chemistry* **2000,** 65, 1566.
5. Tamaki, M., Han, G., Hruby, V. J., *Journal of Organic Chemistry* **2001,** 66, 1038.
6. Coles, M. P., *Journal of the Chemical Society, Dalton Transactions* **2006**, 985-1001.
7. Longhi, R., Drago, R. S., *Inorganic Chemistry* **1965,** 4, 11.
8. Sanger, A. R., *Inorg. Nucl. Chem. Lett.* **1973,** 9, 351.
9. Schmidt, J. A. R., Arnold, J, *Journal of the Chemical Society, Dalton Transactions* **2002**, 2890.
10. Fairlie, D. P., Jackson, W. G., Skeleton, B. W., Wen, H., White, A. H., Wickramasinghe, W. A., Woon, T. C., *Inorganic Chemistry* **1997,** 36, 1020.
11. Ong, T.-G., O'Brien, J. S., Korobkov, I., Richeson, D. S., *Organometallics* **2006,** 25, 4728-4730.
12. Montilla, F., Pastor, A., Galindo, A., *Journal of Organometallic Chemistry* **2004,** 689, 993.
13. Zhang, W.-X., Nishiura, M., Hou. Z., *Synletters* **2006**, 1213.
14. Ong, T. G., Yap. G. P. A., Richeson. D. S., *Journal of the American Chemical Society* **2003,** 125, 8100.
15. Coles, M. P., Hitchcock, P. B., *Chemical Communications* **2005**, 3165-3167.
16. Mansfield, N. E., Coles M. P., Hitchcock, P. B., *Dalton Transactions* **2005**, 2833-2841.

Chapter 5 — Conclusions

The first large portion of this work employed 1,8-diaminonaphthalene as a stabilizing ligand for main group elements. The unusual six-membered ring containing the main group element possesses the important geometrical characteristic, which places the N-substituents in a position to impart a significant steric impact. The conjugated π-system of the naphthalene ring, coupled with the two nitrogen centres, creates an opportunity to provide a noteworthy amount of electronic stabilization towards coordinatively or electronically unsaturated centres.

After exploring the design features of aliphatic N-substituents to generate symmetric and asymmetric ligands, the ability of these ligands to stabilize a divalent, 6-electron carbon centre was demonstrated. The carbon centre is stabilized through

donation of π-electrons from the nitrogen lone pairs to a certain extent. Two interesting reactions involving the carbene centre and a nucleophile were also presented.

Continuing the effort to stabilize interesting main group compounds, synthesis of Si(II), Ge(II), and B(III) compounds was undertaken. Although the desired precursor for the silylene product could not be reached, an interesting germanium compound was crystallized. The partially π-stabilized germanium chloride compound was isolated from the anionic 1,8-DAN ligand. Following this, the stable borane compounds, both symmetric and asymmetric, were produced from the dianionic 1,8-DAN ligand.

The second large portion of this work involved the development of a catalytic route to guanidines and propiolamidines. These biologically relevant molecules can be constructed from their respective carbodiimides, amines, or terminal alkynes. A lithium amide catalyst, industrially relevant due to its commercial availability, is required, since these substrates do not combine to any measurable amount, even after applying high heat. The conditions required and yields obtained can easily be related to the sterics and electronics of the substrates required for designing each product.

The scope of this catalytic reaction was expanded by varying the amine substrate to heterocyclic amines and amides, namely 2,3-dimethylindole and acetamide respectively. Moderate yields could be obtained, compared to the quantitative yields generated previously with primary, aromatic amines. The chelating molecule tetramethylethylenediamine (TMEDA) was required, though, to break up clustering of the lithium amide catalyst, thus increasing its reactivity.

A glimpse into the mechanistic pathway for this catalytic process was obtained through crystal structures of dimeric reaction intermediates, which display a Li_2N_2 core and a ladder-like central geometric configuration.

Diaminonaphthalene and guanidine molecules present several synthetic challenges, but ultimately prevail as useful N-based ligands. As the search for new materials, catalytic pathways, and efficient methods towards enantiopure products continues, the need for ligands with specific design characteristics will continue to march forward. The need for the design of new catalysts will certainly rival that of the products themselves. Finally, considering the thought that everything is made of something once

developed by a chemist, the quest for new technology will likely never end, ensuring its continued expanding its role in science.